


Spring 2007

# Growth and behavior of chondrocytes on nano engineered surfaces and construction of micropatterned co-culture platforms using layer-by-layer platforms using layer -by -layer assembly lift-off method

Jameel Shaik  
*Louisiana Tech University*

Follow this and additional works at: <https://digitalcommons.latech.edu/dissertations>

 Part of the [Biomedical Engineering and Bioengineering Commons](#), and the [Materials Science and Engineering Commons](#)

---

## Recommended Citation

Shaik, Jameel, "" (2007). *Dissertation*. 553.  
<https://digitalcommons.latech.edu/dissertations/553>

This Dissertation is brought to you for free and open access by the Graduate School at Louisiana Tech Digital Commons. It has been accepted for inclusion in Doctoral Dissertations by an authorized administrator of Louisiana Tech Digital Commons. For more information, please contact [digitalcommons@latech.edu](mailto:digitalcommons@latech.edu).

GROWTH AND BEHAVIOR OF CHONDROCYTES ON NANO  
ENGINEERED SURFACES AND CONSTRUCTION OF  
MICROPATTERNED CO-CULTURE PLATFORMS  
USING LAYER-BY-LAYER ASSEMBLY  
LIFT-OFF METHOD

by

Jameel Shaik, B.H.M.S.

A Dissertation Presented in Partial Fulfillment  
of the Requirement for the Degree  
Doctor of Philosophy

COLLEGE OF ENGINEERING AND SCIENCE  
LOUISIANA TECH UNIVERSITY

May 2007

UMI Number: 3268112

### INFORMATION TO USERS

The quality of this reproduction is dependent upon the quality of the copy submitted. Broken or indistinct print, colored or poor quality illustrations and photographs, print bleed-through, substandard margins, and improper alignment can adversely affect reproduction.

In the unlikely event that the author did not send a complete manuscript and there are missing pages, these will be noted. Also, if unauthorized copyright material had to be removed, a note will indicate the deletion.

**UMI**<sup>®</sup>

---

UMI Microform 3268112

Copyright 2007 by ProQuest Information and Learning Company.

All rights reserved. This microform edition is protected against unauthorized copying under Title 17, United States Code.

ProQuest Information and Learning Company  
300 North Zeeb Road  
P.O. Box 1346  
Ann Arbor, MI 48106-1346

LOUISIANA TECH UNIVERSITY

THE GRADUATE SCHOOL

5-2-2007

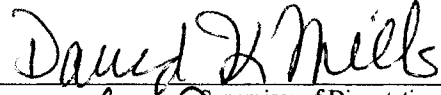
Date

We hereby recommend that the dissertation prepared under our supervision  
by Jameel Shaik

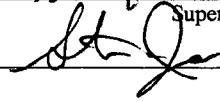
entitled Growth and Behavior of Chondrocytes on Nanoengineered Surfaces and Construction

of Co-culture Platforms using Layer-by-Layer Assembly Lift-Off Method

be accepted in partial fulfillment of the requirements for the Degree of  
Doctor of Philosophy



Supervisor of Dissertation Research

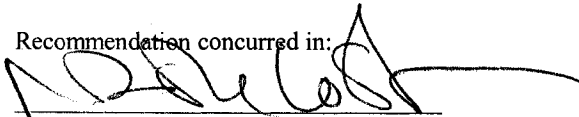


Head of Department

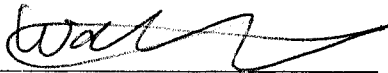
Biomedical Engineering

Department

Recommendation concurred in:



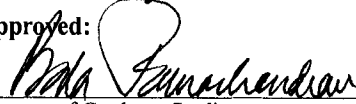
Yuri Lvov



Advisory Committee

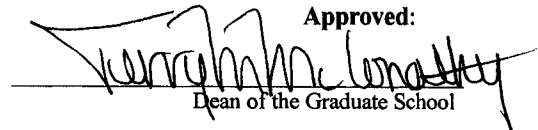


Approved:




Director of Graduate Studies

Approved:



Dean of the Graduate School



Dean of the College

GS Form 13  
(5/03)

## ABSTRACT

Several approaches such as self-assembled monolayers and layer-by-layer assembled multilayer films are being used as tools to study the interactions of cells with biomaterials *in vitro*. In this study, the layer-by-layer assembly approach was used to create monolayer, bilayer, trilayer, five, ten and twenty-bilayer beds of eleven different biomaterials. The various biomaterials used were poly(styrene-sulfonate), fibronectin, poly-L-lysine, poly-D-lysine, laminin, bovine serum albumin, chondroitin sulfate, poly(ethyleneimine), polyethylene glycol amine, collagen and poly(dimethyldiallyl-ammonium chloride) with unmodified tissue-culture polystyrene as standard control. Three different cell lines – primary bovine articular chondrocytes, and two secondary cell lines, human chondrosarcoma cells and canine chondrocytes were used in these studies. Chondrocyte morphology and attachment, viability, proliferation, and functionality were determined using bright field microscopy, the Live/Dead viability assay, MTT assay, and immunocytochemistry, respectively.

Atomic force microscopy of the nanofilms indicated an increase in surface roughness with increasing number of layers. The most important observations from the studies on primary bovine articular chondrocytes were that these cells exhibited increasing viability and cell metabolic activity with increasing number of bilayers. The increase in viability was more pronounced than the increase in cell metabolic activity. Also, bovine chondrocytes on bilayers of poly(dimethyldiallyl-ammonium chloride, poly-

L-lysine, poly(styrene-sulfonate), and bovine serum albumin were substantially bigger in size and well-attached when compared to the cells grown on monolayer and trilayers. Lactate dehydrogenase assay performed on chondrosarcoma cells grown on 5- and 10-bilayer multilayer beds indicated that the 10-bilayer beds had reduced cytotoxicity compared to the 5-bilayer beds. MTT assay performed on canine chondrocytes grown on 5-, 10-, and 20-bilayer nanofilm beds revealed increasing cell metabolic activity for BSA with increasing bilayers.

Micropatterned multilayer beds having poly-L-lysine, poly-D-lysine, laminin poly(dimethyldiallyl-ammonium chloride) and poly(ethyleneimine) as the terminating layers were fabricated using the Layer-by-layer Lift-off (LbL-LO) method that combines photolithography and LbL self-assembly. Most importantly, micropatterned co-culture platforms consisting of anti-CD 44 rat monoclonal and anti-rat osteopontin (MPIIB10<sub>1</sub>) antibodies were constructed using the LbL-LO method for the first time. These co-culture platforms have several applications especially for studies of stem and progenitor cells. Co-culture platforms exhibiting spatiotemporal-based differentiation can be built with LbL-LO for the differentiation of stem cells into the desired cell lineage.

## APPROVAL FOR SCHOLARLY DISSEMINATION

The author grants to the Prescott Memorial Library of Louisiana Tech University the right to reproduce, by appropriate methods, upon request, any or all portions of this Dissertation. It is understood that "proper request" consists of the agreement, on the part of the requesting party, that said reproduction is for his personal use and that subsequent reproduction will not occur without written approval of the author of this Dissertation. Further, any portions of the Dissertation used in books, papers, and other works must be appropriately referenced to this Dissertation.

Finally, the author of this Dissertation reserves the right to publish freely, in the literature, at any time, any or all portions of this Dissertation.

Author 

Date 05-10-2007

## **DEDICATION**

This dissertation is dedicated to the Almighty.



## TABLE OF CONTENTS

ABSTRACT.....	iii
DEDICATION.....	vi
TABLE OF CONTENTS .....	vii
LIST OF TABLES .....	xi
LIST OF FIGURES .....	xii
ACKNOWLEDGMENTS .....	xvi
CHAPTER 1 INTRODUCTION.....	1
1.1 Physico-Chemical Influences.....	2
1.1.1 Mechanical Influences .....	3
1.1.2 Chemical Influences.....	4
1.1.3 Influence of Stiffness .....	4
1.1.4 Influence of Roughness.....	5
1.1.5 Influence of Elasticity.....	5
1.1.6 Stem Cells .....	5
1.1.7 Importance of Cell Shape.....	6
1.2 Research Need.....	8
1.3 Objectives and Novel Aspects .....	10
1.4 Organization of Chapters .....	12
CHAPTER 2 BACKGROUND.....	14
2.1 Cell Culture Substrates .....	18
2.1.1 Coated Substrates-Substrates Coated with ECM Proteins .....	19
2.1.2 SAMs .....	19
2.1.3 LbL Self-Assembly .....	20
2.2 Micropatterned Substrates.....	22
2.3 Two-Dimensional (2-D) vs. Three-Dimensional (3-D) Substrates.....	23
2.4 Cell Adhesion.....	24
2.4.1 Cell Adhesion and Cell Culture .....	24
2.4.2 Cell Adhesion and 2D, 3D, and Coated Culture Substrates .....	25
2.5 Cartilage and Chondrocytes.....	26
2.6 Chondrocyte Cytoskeleton, Morphology, and Phenotype .....	27

2.6.1 Chondrocyte Cytoskeleton.....	27
2.6.2 Focal Adhesion Plaques.....	28
2.6.3 Integrins .....	29
2.7 Patterned Self-Assembled Films.....	29
2.7.1 Soft Lithography.....	29
2.7.2 Photolithography.....	30
CHAPTER 3 EXPERIMENTAL DESIGN .....	32
3.1 Layer-by-Layer Assembly .....	32
3.1.1 Multilayer Architectures .....	32
CHAPTER 4 MATERIALS AND METHODS .....	35
4.1 Chondrocytes .....	35
4.1.1 Cell Culture.....	35
4.1.1.1 PBAC .....	35
4.1.1.2 Human Chondrosarcoma Cells .....	35
4.1.1.3 Canine Chondrocytes .....	36
4.1.2 Substrates .....	36
4.1.3 Biomaterials (Polyelectrolyte and Polypeptide) Preparation.....	36
4.1.4 Fabrication Techniques.....	37
4.1.5 Characterization Techniques.....	37
4.1.5.1 AFM.....	37
4.1.5.2 Ellipsometry.....	38
4.1.6 MTT Assay.....	38
4.1.7 Live-Dead Assay.....	38
4.1.8 Statistical Analyses .....	39
4.2 Micropatterned Surfaces .....	39
4.2.1 Substrates .....	39
4.2.2 Chemicals.....	39
4.2.3 Preparation of Polyelectrolyte and Polypeptide Solutions.....	39
4.2.4 Mask Design .....	39
4.2.5 Fabrication .....	40
4.2.6 Substrate Pretreatment .....	40
4.2.7 Photolithography.....	40
4.2.8 LbL Self-Assembly.....	40
4.2.9 Lift-Off.....	41
4.2.10 Characterization.....	41
4.3 Micropatterned Co-Culture Platforms .....	41
4.3.1 Substrates .....	41
4.3.2 Chemicals.....	41
4.3.3 Mask Design .....	42
4.3.4 Instrumentation .....	42
4.3.5 Fabrication .....	42
4.3.6 Substrate Pretreatment, Photolithography, LbL Assembly, and Lift-Off.....	43
4.3.7 Characterization.....	43

CHAPTER 5 RESULTS AND DISCUSSION.....	44
5.1 <i>In Vitro</i> Evaluation of Chondrocytes on Layer-by-Layer Assembled Nanofilms.....	44
5.1.1 PBAC on TCPS.....	44
5.1.2 Functionality – PBAC.....	44
5.1.3 AFM – Monolayer, Bilayers and Trilayers.....	46
5.1.4 Morphological Observations – PBAC on Different Biomaterials.....	49
5.1.4.1 PBAC on TCPS.....	49
5.1.4.2 PBAC on PEG-NH <sub>2</sub> .....	50
5.1.4.3 PBAC on PDDA.....	51
5.1.4.4 PBAC on BSA.....	52
5.1.4.5 PBAC on PDL.....	53
5.1.4.6 PBAC on CS.....	54
5.1.4.7 PBAC on PEI.....	55
5.1.4.8 PBAC on Collagen.....	56
5.1.4.9 PBAC on PLL.....	57
5.1.4.10 PBAC on Fibronectin.....	58
5.1.4.11 PBAC on PSS.....	59
5.1.4.12 PBAC on Laminin.....	60
5.1.5 Results from Viability Studies on PBAC.....	61
5.1.5.1 PBAC on TCPS.....	62
5.1.5.2 PBAC on PEG-NH <sub>2</sub> .....	62
5.1.5.3 PBAC on PDDA.....	63
5.1.5.4 PBAC on BSA.....	64
5.1.5.5 PBAC on PDL.....	65
5.1.5.6 PBAC on CS.....	66
5.1.5.7 PBAC on PEI.....	67
5.1.5.8 PBAC on Collagen.....	68
5.1.5.9 PBAC on PLL.....	69
5.1.5.10 PBAC on Fibronectin.....	70
5.1.5.11 PBAC on PSS.....	71
5.1.5.12 PBAC on Laminin.....	72
5.1.6 Live/Dead Data.....	74
5.1.6.1 Cell Density One (5000 cells/ml).....	75
5.1.6.2 Cell Density Two (15000 cells/ml).....	75
5.1.6.3 Cell Density Three (25000 cells/ml).....	76
5.1.7 Live/Dead Image Analysis.....	78
5.1.7.1 Cell Density One (5000 cells/ml).....	80
5.1.7.2 Cell Density Two (15000 cells/ml).....	80
5.1.7.3 Cell Density Three (25000 cells/ml).....	80
5.1.8 MTT Data.....	81
5.1.8.1 Cell Density A (500 cells/ml).....	82
5.1.8.2 Cell Density B (1000 cells/ml).....	82
5.1.8.3 Cell Density C (1500 cells/ml).....	83
5.1.9 Statistical Analyses.....	84

5.1.9.1 Live-Dead Assay.....	84
5.1.9.2 MTT Assay .....	84
5.1.10 Biomaterial Thickness Profiles .....	85
5.1.11 Roughness Profiles of the Biomaterials .....	86
5.1.12 LDH-L Assay–Chondrosarcoma Cells .....	88
5.1.13 Canine Chondrocytes–MTT Assay.....	89
5.1.14 Roughness vs. Canine Chondrocyte Cell Metabolic Activity Profiles.	91
5.1.14.1 PEG-NH <sub>2</sub> .....	95
5.1.14.2 Chondroitin Sulfate.....	95
5.1.14.3 PDDA.....	96
5.1.14.4 PEI.....	96
5.1.14.5 Fibronectin .....	96
5.1.14.6 Laminin .....	96
5.1.14.7 Collagen .....	96
5.1.14.8 PDL .....	97
5.1.14.9 PLL .....	97
5.1.14.10 BSA.....	97
5.1.14.11 PSS.....	98
5.1.15 Statistical Analyses .....	98
5.1.15.1 MTT Assay – Canine Chondrocytes.....	98
5.1.15.2 LDH-L Assay – Chondrosarcoma Cells .....	99
5.2 Micropatterned Surfaces .....	99
5.2.1 Phase Contrast Images of Micropatterned Substrates.....	100
5.2.1.1 Micropatterned Substrates with PDDA as the Outermost Layer.....	101
5.2.1.2 Micropatterned Substrates with CS as the Outermost Layer ....	102
5.2.1.3 Micropatterned Substrates with PEI as the Outermost Layer...103	
5.2.1.4 Micropatterned Substrates with Collagen as the Outermost Layer .....	104
5.2.1.5 Micropatterned Substrates with PSS as the Outermost Layer ..105	
5.3 Micropatterned Co-Culture Platforms .....	106
5.3.1 Phase Contrast Microscopy.....	107
5.3.2 AFM Analysis.....	108
 CHAPTER 6 CONCLUSIONS AND FUTURE WORK.....	 110
6.1 Conclusions.....	110
6.2 Future Work.....	113
 REFERENCES .....	 115

## LIST OF TABLES

Table 3.1	Molecular weights, pH, charges, LbL architectures and concentrations of the different biomaterials used in this study.....	33
Table 3.2	LbL architectures of the different biomaterials used in this study .....	34
Table 5.1	Average roughnesses of the monolayer, bilayer, and trilayer nanofilms of the different biomaterials [Mean $\pm$ Standard Deviation) ( $n=3$ )].....	46
Table 5.2	Summary of morphological observations of phenotypes exhibited by PBAC on monolayer, bilayers, and trilayers (Cell density 1 – 5000 cells/ml) .....	61
Table 5.3	Summary of morphological observations of phenotypes exhibited by PBAC after Live-Dead Analysis on monolayer, bilayers, and trilayers (Cell density 1 – 5000 cells/ml) .....	73
Table 5.4	Highest viabilities exhibited by PBAC on the different biomaterials .....	76
Table 5.5	Highest cell metabolic activities exhibited by PBAC on the different biomaterials .....	83
Table 5.6	Statistical analysis results of Live-Dead Assay on PBAC .....	84
Table 5.7	Statistical analysis results of MTT Assay on PBAC .....	84
Table 5.8	Thickness profiles of 5-, 10-, and 20-bilayers of the biomaterials [(Mean $\pm$ Standard Deviation ( $n=3$ )] .....	85
Table 5.9	Roughness profiles of 5-, 10-, and 20-bilayers of the biomaterials [(Mean $\pm$ Standard Deviation) ( $n=3$ )] .....	86
Table 5.10	Statistical outputs for the canine chondrocytes' cell metabolic activity.....	98
Table 5.11	Statistical analysis results of LDH-L Assay conducted on PBAC .....	99

## LIST OF FIGURES

Figure 3.1	LbL assembly.....	32
Figure 5.1	(a), (b) Passage Three PBAC grown on TCPS .....	44
Figure 5.2	(a) Anti-type II collagen, (b) Anti-aggrecan immunocytochemistry of PBAC; Controls for (c) Anti-type II Collagen and (d) Anti-aggrecan immunocytochemistry of PBAC [arrows indicate chondrocytes] .....	45
Figure 5.3	AFM images of (a) PSS/PDL, (b) (PSS/PDL) <sub>2</sub> , (c) (PSS/PDL) <sub>3</sub> .....	47
Figure 5.4	AFM images of (a) (CS/PEI)/CS, (b) (CS/PEI) <sub>2</sub> /CS, and (c) (CS/PEI) <sub>3</sub> /CS .....	48
Figure 5.5	PBAC on TCPS: (a) After 34 hours; (b), (c) After 72 hours .....	49
Figure 5.6	PBAC on PEG- NH <sub>2</sub> : After 34 hours – (a) On monolayer, (b) On bilayers, (c) On trilayers; after 72 hours –(d) On monolayer, (e) On bilayers, (f) On trilayers.....	50
Figure 5.7	PBAC on PDDA: After 34 hours – (a) On bilayers; after 72 hours – (b) On bilayers, (c) On trilayers.....	51
Figure 5.8	PBAC on BSA: After 72 hours – (a) On monolayer, (b) On bilayers, (c) On trilayers .....	52
Figure 5.9	PBAC on PDL: After 34 hours – (a) On bilayers, (b) On trilayers; after 72 hours - (c) On monolayer, (d) On bilayers, (e) On trilayers.....	53
Figure 5.10	PBAC on CS: After 34 hours – (a) On bilayers, (b) On trilayers; after 72 hours – (c) On trilayers .....	54
Figure 5.11	PBAC on PEI: After 34 hours – (a) On monolayer, (b) On bilayers; after 72 hours – (c) On trilayers.....	55
Figure 5.12	PBAC on collagen: After 34 hours – (a) On trilayers; after 72 hours– (b) On monolayer, (c) On bilayers, (d) On trilayers .....	56
Figure 5.13	PBAC on PLL: After 34 hours – (a) On monolayer, (b) On bilayers, (c) On trilayers; after 72 hours – (d) On trilayers .....	57
Figure 5.14	PBAC on fibronectin: After 34 hours – (a) On monolayer, (b) On bilayers, (c) On trilayers; after 72 hours – (d) On monolayer, (e) On bilayers .....	58

Figure 5.15	PBAC on PSS: After 34 hours – (a) On monolayers(b) On bilayers, (c) On trilayers; after 72 hours – (d) On bilayers, (e) On trilayers .....	59
Figure 5.16	PBAC on Laminin: After 34 hours – (a) On monolayer, (b) On bilayers, (c) On trilayers; after 72 hours – (d) On bilayers.....	60
Figure 5.17	(a), (b) Live PBAC on TCPS .....	62
Figure 5.18	Live PBAC on PEG-amine: (a) monolayer, (b) bilayers, (c) trilayers.....	62
Figure 5.19	Live PBAC on PDDA: (a) monolayer), (b) bilayers, (c) trilayers .....	63
Figure 5.20	Live PBAC on BSA: (a) monolayer, (b) bilayers, (c) trilayers .....	64
Figure 5.21	Live PBAC on PDL: (a) monolayer, (b) bilayers, (c) trilayers.....	65
Figure 5.22	Live PBAC on CS: (a) monolayer, (b) bilayers, (c) trilayers .....	66
Figure 5.23	Live PBAC on PEI: (a) monolayer, (b) bilayers, (c) trilayers .....	67
Figure 5.24	Live PBAC on Collagen: (a) monolayer, (b) bilayers, (c) trilayers .....	68
Figure 5.25	Live PBAC on PLL: (a) monolayer, (b) bilayers, (c) trilayers .....	69
Figure 5.26	Live PBAC on Fibronectin: (a) monolayer, (b) bilayers, (c) trilayers .....	70
Figure 5.27	Live PBAC on PSS: (a) monolayer, (b) bilayers, (c) trilayers.....	71
Figure 5.28	Live PBAC on laminin: (a) monolayer, (b) bilayers; dead PBAC on laminin: (c) trilayers.....	72
Figure 5.29	Viability exhibited by PBAC on different biomaterials at Cell Density 1 (5000 cells/ml) .....	74
Figure 5.30	Viability exhibited by PBAC on different biomaterials at Cell Density 2 (15000 cells/ml) .....	74
Figure 5.31	Viability exhibited by PBAC on different biomaterials at Cell Density 3 (25000 cells/ml) .....	75
Figure 5.32	Live-Dead Image Analysis results of PBAC on different biomaterials: Cell Density 1 (5000 cells/ml) .....	78
Figure 5.33	Live-Dead Image Analysis results of PBAC on different biomaterials: Cell Density 2 (15000 cells/ml) .....	79
Figure 5.34	Live-Dead Image Analysis results of PBAC on different biomaterials: Cell Density 3 (25000 cells/ml) .....	79
Figure 5.35	Cell metabolic activity exhibited by PBAC on different biomaterials at Cell Density A (500 cells/ml) .....	81
Figure 5.36	Cell metabolic activity exhibited by PBAC on different biomaterials at Cell Density B (1000 cells/ml) .....	81

Figure 5.37	Cell metabolic activity exhibited by PBAC on different biomaterials at Cell Density C (1500 cells/ml) .....	82
Figure 5.38	AFM images of (a) (PSS/Collagen) <sub>5</sub> , (b) (PSS/Collagen) <sub>10</sub> , and (c) (PSS/Collagen) <sub>20</sub> .....	87
Figure 5.39	AFM images of (a) (PSS/PDL) <sub>5</sub> , (b) (PSS/PDL) <sub>10</sub> , and (c) (PSS/PDL) <sub>20</sub> ....	87
Figure 5.40	LDH-L assay profile of chondrosarcoma cells (a) Cell Density 1 –5000 cells/ml, (b) Cell Density 2 – 25000 cells/ml .....	89
Figure 5.41	MTT assay profile of canine chondrocytes grown on monolayer, 5-,10-, and 20-bilayers .....	90
Figure 5.42	Roughness and normalized MTT activity for monolayer, 5-, 10-, and 20-bilayers of PEG-NH <sub>2</sub> .....	91
Figure 5.43	Roughness and normalized MTT activity for monolayer, 5-, 10-, and 20-bilayers of Chondroitin Sulfate .....	92
Figure 5.44	Roughness and normalized MTT activity for monolayer, 5-, 10-, and 20- bilayers of PDDA.....	92
Figure 5.45	Roughness and normalized MTT activity for monolayer,5-, 10-, and 20- bilayers of PEI.....	92
Figure 5.46	Roughness and NMA for monolayer, 5-, 10-, and 20-bilayers of Fibronectin.....	93
Figure 5.47	Roughness and NMA for monolayer, 5-, 10-, and 20-bilayers of Laminin.....	93
Figure 5.48	Roughness and NMA for monolayer, 5-, 10-, and 20-bilayers of Collagen.....	93
Figure 5.49	Roughness and NMA for monolayer, 5-, 10-,and 20- bilayers of PDL.....	94
Figure 5.50	Roughness and NMA for monolayer, 5-, 10-,and 20-bilayers of PLL .....	94
Figure 5.51	Roughness and NMA for monolayer, 5-, 10-, and 20-bilayers of BSA.....	94
Figure 5.52	Roughness and NMA for monolayer, 5-, 10-, and 20-bilayers of PSS.....	95
Figure 5.53	(a) (PSS/PDDA) <sub>5</sub> –80 μm, (b) (PSS/PDDA) <sub>5</sub> –100 μm, (c) (PSS/PDDA) <sub>10</sub> –80 μm, (d) (PSS/PDDA) <sub>10</sub> –100 μm .....	101
Figure 5.54	(a) (CS/PEI) <sub>5</sub> /CS–80 μm, (b) (CS/PEI) <sub>5</sub> /CS–100 μm, (c) (CS/PEI) <sub>10</sub> /CS–80 μm, (d) (CS/PEI) <sub>10</sub> /CS–100 μm .....	102
Figure 5.55	(a) (PSS/PEI) <sub>5</sub> –80 μm, (b) (PSS/PEI) <sub>5</sub> –100 μm, (c)(PSS/PEI) <sub>10</sub> –80 μm, (d) (PSS/PEI) <sub>10</sub> –100 μm .....	103
Figure 5.56	(a) (PSS/Collagen) <sub>5</sub> –80 μm, (b) (PSS/Collagen) <sub>5</sub> –100 μm, (c) (PSS/Collagen) <sub>10</sub> –80 μm, (d) (PSS/Collagen) <sub>10</sub> –100 μm.....	104



Figure 5.57	(a) (PSS/PEI) <sub>5</sub> /PSS–80 μm, (b) PSS/PEI) <sub>5</sub> /PSS–100 μm, (c) (PSS/PEI) <sub>10</sub> /PSS–80 μm, (d) (PSS/PEI) <sub>10</sub> /PSS–100 μm.....	105
Figure 5.58	(a), (b) – Single-component micropatterns; (c), (d) – double component (checker board) patterns .....	107
Figure 5.59	(a) AFM image of antibody deposited on the co-culture pattern; (b), (c) edges of co-culture pattern tiles .....	108
Figure 5.60	Average roughness and RMS roughness of antibodies deposited on co-culture platforms .....	109

## ACKNOWLEDGMENTS

I would like to express my sincere gratitude to my advisor, Dr. David K. Mills, who has a unique style of giving the freedom and opportunity to students to pursue their research. He taught me several cell-culture techniques taking time out of his “always-busy” schedule. I would like to thank Dr. Michael J. McShane for the research collaboration. I would like to acknowledge support provided by my advisory committee members, Dr. Mark A. DeCoster, Dr. Steven A. Jones, Dr. Yuri M. Lvov and Dr. Walter G. Besio. In addition, I would like to acknowledge the support provided by Dr. Raja Nassar for help with statistics, Lisa White, and all members of biomorph lab, past and present, Mr. James White for helping with facilities in the School of Biological Sciences. I would like to acknowledge Mr. Philip Coane, Mr. Scott Williams, Mr. Donald Tatum, Ms. Deborah Wood, Mr. Ji Fang, and Mr. John McDonald for their assistance in metrology, and for arranging special facilities needs and access. Also I would like to acknowledge Stephanie Tully for help with Atomic Force Microscopic imaging of co-culture patterns. I would like to acknowledge financial support from the College of Engineering & Science.

Finally, I humbly acknowledge the unstinted support of my parents who always gave me the utmost freedom to pursue my life. But my parents also took care that I was always in the right direction. I also acknowledge the support provided by my younger

brother, Javeed Shaikh Mohammed who helped me in innumerable number of ways despite his busy work-schedule, and all my relatives.

## CHAPTER 1

### INTRODUCTION

Nanobiotechnology, a relatively nascent scientific field, is an interdisciplinary one encompassing biotechnology and nanotechnology, and several other related sciences. The *in vivo* environment is entirely different from the *in vitro* one. The fact that the dimensions in biology are in the range of nanometers makes this science a marriage of convenience. Attempts at replicating the *in vivo* environment have been made by researchers for diverse purposes. For example, one of the foremost beneficiaries would be tissue engineering which aims at the recreation of organs to replace diseased organs. A recent success has been the creation of an artificial urinary bladder [1]. The commercial versions of the artificial skin graft and artificial cartilage are Integra<sup>®</sup> and Carticel<sup>®</sup> respectively. The role played by artificial organs cannot be overestimated to any extent. The proportion of aged persons throughout the world is on a steady increase. For aged people and burn victims and patients with debilitating and disfiguring diseases, artificial organs are a boon. Thus, artificial organs generated by tissue engineering help in the alleviation of pain and debility and increase the self-esteem of affected patients, thereby helping in curbing the loss of man-hours and saving a great deal of money. While there have been few successes in tissue engineering such as artificial skin grafts [2-7], artificial cartilage [8-14], there still remain huge obstacles in the creation of artificial organs. This work is focused on developing ideal platforms for chondrocyte culture and co-cultures

of stem cells and progenitor cells. A combination of “bottom-up” nanoscale self-assembly and “top-down” microscale lithography is to be utilized for the development of these platforms [15].

In addition to tissue engineering, such platforms have additional applications in sensors [16], drug-testing [17], and drug-delivery platforms, lab-on-a-chip microsystems, etc.. The developing fields of bionanotechnology and nanobiotechnology envisage the development of microfluidic platforms involving nanoparticles, nanostructures, nanocoatings, nanoactuators, and cells. These microfluidic platforms act as an interface to the macroworld [18].

### **1.1 Physico-Chemical Influences**

It is well-known that cells respond to various spatial signals within their microenvironment in a variety of ways. These may be in the form of soluble molecules within the extracellular medium, present on the surface of the extracellular matrix (ECM) such as the various ECM proteins or membrane receptors [19]. Cell-ECM interactions are important in the structure and function of cells and tissues, morphogenesis of tissues and organs and their maintenance, growth and development and wound healing. Tissue engineering requires the delivery of appropriate signals for cell proliferation and development, protein synthesis and cell functionality. These signals are delivered in the form of growth factors, cell-ECM and cell-cell interactions and from a variety of physicochemical and mechanical stimuli [20]. One of the foremost success stories developed from the ECM family of proteins has been the Small Intestinal Submucosa (SIS), which has resulted in more than 100 products to treat a variety of clinical problems including urinary incontinence, hernias, chronic wounds, etc.. SIS also helps in wound

healing and tissue remodeling [21]. The precise control and engineering of the various physicochemical cues would not only lead to a better understanding of cell biology [22] but also help in the understanding of disease processes *in vivo* by the development of appropriate *in vitro* models.

Because cells are in a constant state of flux in the body, they encounter a variety of signals. Cells are responsive to different factors like elasticity [23, 24], mechanical stress [25-28], surface chemistry and topography [29-31], stiffness [24] and roughness [32-35]. Cell behavior is affected by all of the above-mentioned factors.

Also, cells react to nanoscale features (5-500 nm) and differentiate between symmetries and asymmetries [36] producing changes in different cell characteristics like adhesion [37], morphology [38], and gene expression [39]. There is a possibility that cells use filopodia and microspikes to explore the nanofeatures in the cells' surrounding microenvironment [36]. Differences in cellular behavior seem to stem from subtle differences in surface chemistry while some studies suggest that this is also due to the concomitant difference in surface topography [40-43].

### **1.1.1 Mechanical Influences**

The role played by mechanical forces on cells cannot be underestimated as they are of immense importance for development of many tissues and are linked to the pathologies of many diseases such as atherosclerosis, myopathies and hypertension. It had been suggested that mechanical forces act as extracellular information transmitted to and received by tendon cells during early development [44]. The findings of many *in vitro* experimental models and experiments corroborate to an extent with the *in vivo* findings. For example, in endothelial cells, gene signaling pathways are activated by

mechanical strain that is similar to what endothelial cells undergo upon shear stress induction. But, there are differences in the time course of the responses [45]. Besides gene expression changes in endothelial cells as a response to shear stress, changes are also observed in focal adhesions and cytoskeletal organization [46].

There are differences between cell membrane based receptors and cytoskeletal based receptors sensing the mechanical stiffness of cells. These differences are different for different types of cells and depend on specific receptors establishing the hypothesis that cytoskeletal networks are individualized with a variety of classes of receptors with their own individual mechanical properties [47].

### **1.1.2 Chemical Influences**

It is well-known that the movement of cells is influenced by potentials in several factors including chemicals [48], and light [49]. But cell movement is also regulated by the rigidity of the substrate. 3T3 fibroblasts exhibited a preference for stiffer substrates demonstrating that cell movement at the cell-substrate interface is also a purely physical phenomenon [50].

### **1.1.3 Influence of Stiffness**

Myoblasts cultured on collagen strips demonstrated differential muscle striation formation on gels. Myosin/actin striations were evident only on normal muscle-like gels (passive Young's modulus,  $E \sim 12$  kPa), whereas they were absent in dystrophic muscle-like gels (glass and gels either too soft or too stiff). Thus, striation is clearly dependent on the stiffness of the substrates [24].

#### **1.1.4 Influence of Roughness**

Osteoblasts form an osteogenic microenvironment on surfaces with rough microtopographies when compared with smooth surfaces. On rough surfaces (titanium surfaces with a roughness of 4-7  $\mu\text{m}$ ), osteoblasts exhibited increased differentiation and an enhanced response to growth factors and cytokines. Specifically, osteoblasts formed hydroxyapatite similar to *in vivo* conditions on microrough surfaces when compared to the osteoblasts grown on smooth surfaces. While the differentiation of the cells increased with the increasing roughness of the substrates, the cellular plasticity decreased. These findings suggest that topographical features of the surface have a role in the osteogenesis [33].

#### **1.1.5 Influence of Elasticity**

A recent study showed that elasticity of tissues influences the differentiation of mesenchymal stem cells (MSCs) with different types of elasticity leading to development of different types of tissue. For example, soft brain-like matrices produced neurogenic tissue while stiff muscle-like matrices produced myogenic tissue and rigid collagenous bone-like matrices produced osteogenic tissue. There are concomitant changes in several characteristics like morphology and marker proteins [23].

#### **1.1.6 Stem Cells**

Interest in mesenchymal stem cells has increased tremendously in the recent years specifically due to their immense therapeutic potential. These cells have the ability to develop into cell lines of different lineages such as adipocytes, chondrocytes or osteocytes [51]. However, the difficulty in the maintenance of the phenotype of cells like chondrocytes is well-known. Stem cells can be coaxed to form and maintain the



phenotype of cells with the required specific characteristics. For example, the loss of the specific marker, type II collagen in chondrocytes with successive passages could be replaced by the development of stem cells having the above-mentioned marker.

Also, stem cells are important in the understanding of one of the deadliest diseases, cancer. Tumorigenic cells may originate from the normal stem cells due to the similar signaling pathways between the normal stem cells and the 'rogue' stem cells which may turn out to be tumorigenic [52] leading to an exciting hope for cancer which may lie in the isolation of the 'rogue' tumorigenic stem cells [53].

#### **1.1.7 Importance of Cell Shape**

The maintenance of cell shape, i.e., the phenotype, is very important and especially so in the case of chondrocytes which have a very labile phenotype. Changes in phenotype have also been associated with diseases like sickle cell anemia where decreased deformability of the red blood cell (RBC) is the chief cause [54]. The cardiovascular system responds to mechanical forces by changes in cell shape and gene expression which is dependent on the low molecular weight guanine triphosphatases (GTPases) of the Rho family [55]. Specifically with regard to chondrocytes it has been hypothesized that phenotypic modulation of chondrocytes can be a therapeutic strategy for the treatment of osteoarthritis. The loss of matrix molecules like proteoglycans which are abundant in cartilage [56, 57], one of the chief characteristics of osteoarthritic cartilage is supposed to be caused by an increase in matrix metabolism by most researchers [58-60]. Thus it has been suggested that the stabilization of the chondrocytic phenotype, coupled with redifferentiation of the osteoarthritic chondrocytes is required to help correct matrix anabolism [57].

Human and bovine capillary endothelial cells were grown on micropatterned substrates containing ECM-coated islands of decreasing size to determine a 'switch' of life and death of cells by imposing constraints on cell growth and extension. It was found that cell shape was the determining factor in the cell being either alive or dead without being dependent on the type of ECM protein or anti-integrin antibody used for mediating cell adhesion [61]. The movement of cells across a substrate has been found to be strongly dependent on the biophysical nature like the precise spatial arrangement of the required ligands, for example: RGD sequence, YGRGD (ligand clustering required on the ~50 nm scale) [55], the GRGDSPK peptide and ECM rigidity [62, 63]. Also in smooth muscle cells one of the reasons affecting cell structure and phenotype through integrin-cytoskeleton linkages has been externally applied strain, another example of mechanotransduction [64].

Cells in the body are not isolated. They exist along with other cells. Thus there are always interactions between two and sometimes more than two types of cells necessitating the creation of co-cultures *in vitro* to better understand the situation of two or more types of cells *in vivo*. Co-cultures of murine endothelial cells and neonatal rat cardiomyocytes led to the formation of beating cardiomyocytes along with the expression of cardiac markers. Similarly co-cultures of well-differentiated human umbilical vein endothelial cells and rat cardiomyocytes lead to the formation of cardiomyocytes expressing von Willebrand factor and sarcomeric myosin. But in the case of neural stem cells which differentiate into both skeletal muscle and cardiomyocytes, the rate of differentiation into cardiomyocytes is low [65]. Microfabricated co-cultures of hepatocytes and fibroblasts first established as models of parenchymal/mesenchymal

interactions [66] revealed that fibroblast density regulates hepatocyte function in a dose-dependent manner. Microfabricated co-cultures are a big improvement over 'random' co-cultures as they help in precise spatial localization of two cell types and a better control over cell-cell homotypic interactions and the cell-cell heterotypic interface [67].

## 1.2 Research Need

The studies demonstrating the relationship of cells to physico-chemical stimuli are continually on the increase but some salient points emerge from the above examples. To understand the influences of the various physico-chemical and other kinds of stimuli on cell behavior, there is a need to recreate these stimuli/influences. This need is filled by *in vitro* models which ultimately lead us to a better understanding of the *in vivo* environment. Microfabrication in combination with LbL can act as a means for recreating the stimuli *in vitro*. The *in vitro* models utilize substrates or scaffolds for the growth of cells. Though great strides have been made in the advancement of substrate technology, the quest for an ideal substrate that encourages cell growth and preserves cell functionality still eludes us. A variety of materials are being evaluated for use as biomaterial scaffolds, some of the most common being polyelectrolytes and proteins. Several surface-modification techniques have been utilized towards this end like Langmuir-Blodgett (LB) technique [68, 69], Self-Assembled Monolayers (SAMs) [70-72] and the relatively new LbL assembly technique. The LbL technique has many advantages in that precise control over different characteristics like surface roughness, thickness, etc., can be achieved. The importance of the maintenance of cell shape has been discussed above. Use of LbL films to stabilize the phenotype of chondrocytes and also testing of materials and the number of bilayers of films to achieve maximum

functionality of chondrocytes was to be achieved in this study. Micropatterned surfaces were utilized to better understand cell behavior and select a material which promoted maximum functionality. Cell-cell communication is an important factor in the maintenance of cell phenotype and functions. Co-culture platforms have been created using a variety of techniques like microfabrication, SAMs, and electroactive substrates. However, the LbL-LO technique brings in all the advantages of LbL assembly. The most exciting feature of the LbL-LO technique is the insertion of growth factors and peptides in the multiple layers which can be used to influence cell behavior to the desired levels.

Listed below are some salient advantages arising out of this research. An achievement of rounded phenotype of chondrocytes would help in the creation of better artificial cartilage. The rounded phenotype can be achieved through a better understanding of the influence of multilayers, specifically a greater number of multilayers like 5-, 10- and 20-bilayers. Previous work at Louisiana Tech has demonstrated that smooth muscle cells (SMCs) achieved a more natural morphology on 20-bilayers when compared with one-bilayer [73, 74]. A number of hypotheses arose from this work and formed the base for the hypotheses to be tested in the present study. They were as follows:

- As the number of bilayers in the multilayer films increases, cells grown on the films will adopt a more rounded phenotype, i.e. a more natural morphology.
- There will be an increase in cell metabolic activity, viability and cellular function with an increase in the number of bilayers.

In this study, the methodology adapted to SMCs was applied to chondrocytes which as mentioned earlier have a very labile phenotype. This work can be applied to

other types of cells as well, leading to a better understanding of many diseases. Tissue engineering would be one of the greatest beneficiaries of this work as the achievement of a natural morphology of cells as in the *in vivo* milieu would help in the creation of better artificial organs. The LbL technique is promising in that it can deliver the required growth factors, peptides and other essential items required for the proper growth and behavior of cells. Also, micropatterning, especially the LbL-LO technique, can be used to create unique, instructional platforms for building scaffolds for chondrocyte culture, co-cultures of stem cells and other progenitor cells. For example, platforms that can be used to differentiate stem cells in a spatially controlled manner can be created using the LbL-LO technique. These can be applied to dynamic scaffolds to be used in *in vivo* settings to generate artificial organs or correct diseases which would be a boon to tissue engineering in that it will help alleviate the sufferings of thousands of diseased people.

### **1.3 Objectives and Novel Aspects**

The discussion in the preceding sections points to the necessity of controlling the phenotype of chondrocytes which have a very labile phenotype. Also an optimal biomaterial on which cells exhibit the desired functionality would be of benefit for tissue engineering and disease understanding. A better cell culture system for chondrocytes is yet another benefit accruing from this research. This work was directed towards testing the viability, cell metabolic activity and several other chondrocyte functions on various biomaterials consisting of polyelectrolytes and polypeptides engineered using nanoscale LbL self-assembly.

Micromachining technologies coupled with electrostatic LbL assembly were used to build microfabricated substrates from the materials exhibiting optimal biocompatibility

and cellular behavior. Making use of the microfabricated structures, chondrocytes were grown on a variety of substrates to test and determine the effect of surface characteristics and the nature of cell adhesion on cultured chondrocytes. These technologies will help us in creating new culture methods that may more closely resemble the *in vivo* chondrocyte microenvironment. Some of the other important issues to be addressed were as follows:

What type of substrate would enhance chondrocyte attachment, maximizing cell density, and maintaining differentiation? The preservation of the cell phenotype is one of the major targets to be achieved for creating a better artificial cartilage. The chondrocyte phenotype is very labile. Normally it is round, and the maintenance of this rounded shape was one of the important aims.

The ultimate goal of this project is to develop a better understanding of the microenvironmental conditions that direct chondrocyte growth and alignment. The general significance of this project is as follows:

- A better understanding of the influence of varying multilayer configurations on cellular functions like viability and cell metabolic activity will help in the creation of biomaterials tailored with specific multilayer configurations. The potential benefits of such biomaterials would find applications in the field of cell and tissue engineering.
- Another important significance of this project is the creation of co-culture scaffolds using LbL-LO technology for a better understanding of cell-cell interactions and promoting stem cell differentiation into multiple lineages in a precisely engineered manner. This would help in the realization of instructive nanoengineered platforms with good spatiotemporal control. The benefits arising

from this would be tremendous for tissue engineering and an understanding of diseases associated with specific cell types, especially stem cells.

- Thus, as an added benefit from this project, research in tissue engineering, will assist in promoting the development of the biomaterial industry. This research aims at a better comprehension of the cell behavior *in vitro* by creating biomimetic microenvironment. Biocompatibility is also an important factor to be considered in tissue engineering. The improvement of biocompatibility would help in the speedy evolution of artificial organs and tissues. Current cell culture systems often have problems with cell adhesion, proliferation, and orientation of the cells. Engineering cellular behavior for tissue reconstruction has in general focused on the understanding of a number of critical cell functions mentioned above. The proposed project is expected to derive a better understanding of the various multilayer configurations on chondrocyte cell function.

#### **1.4 Organization of Chapters**

The contents of this dissertation have been organized in a simple and clear way. This is a modest exploration into some aspects of the novel and growing science, nanobiotechnology. Chapter Two deals with a review of the literature and presents a succinct discussion about the different kinds of substrates, patterning techniques and the importance of the cell biology of chondrocytes. Chapter Three deals with the experimental designs followed in this work. Chapter Four elaborates the materials and methods used in this study. Chapter Five details the results and the discussion. This chapter further describes the *in vitro* evaluation of primary bovine articular chondrocytes (PBAC), human chondrosarcoma cells and canine chondrocytes on LbL assembled films.

Chapter Five also describes the building of micropatterned substrates and co-culture scaffolds using LbL-LO techniques. This chapter is a combination of the nanoengineering technique, LbL and various cellular assays performed on nanoengineered surfaces containing chondrocytes. Chapter Six describes the overall conclusions of this work and an outline and proposal for future work.



## CHAPTER 2

### BACKGROUND

Cell culture and tissue engineering require a scaffold for the growth and proliferation of cells. Nanotechnology, besides helping in the creation of biocompatible scaffolds, can impart many unique properties to the resulting scaffolds [75]. Several techniques like LB films [76-78] and SAMs [79-87] have been used in the creation of platforms for cell culture. LbL assembly, a relatively new technique has been utilized for the creation of platforms for cell culture [88-91]. LbL was introduced by Decher in 1991 [92-94]. Each of the surface modification technique mentioned above has its advantages and disadvantages.

A variety of materials like polyelectrolytes and proteins have been used for coating surfaces. Extracellular matrix components and protein molecules are useful in the rendering of an *in vitro* environment *in vivo* and promoting cell adhesion. Tsuchiya et al. used several extracellular components and cell adhesion molecules- type I collagen, type II collagen, fibronectin, vitronectin, poly-L-lysine, laminin, chondroitin-4-sulfate, chondroitin-6-sulfate, aggrecan, and hyaluronic acid to study their effects on the adhesion of chondrocytes, ligament cells and mesenchymal stem cells (MSCs). But these were monolayer coatings. In the above study by Tsuchiya et al., fibronectin

showed the most promise among all the polyelectrolytes tested, but the effects varied with the type of cell. The adhesion of ligament cells was far greater than that of chondrocytes and MSCs [95].

Another important issue has been the various studies made on the interactions between cells and LbL films. LbL films are very versatile having many distinct advantages. The LbL technique is very simple [96-98], cost-effective, and can be performed on a variety of materials and surfaces. Good control over roughness, thickness and other characteristics can be achieved through LbL. Multilayer films and their control by pH [99-101], salt concentration [102, 103], and several other factors have been studied in detail. Also, diverse factors necessary for the growth of cells can be incorporated in successive layers of LbL films. A number of factors like DNA [92, 104-107], enzymes [108-111], antibodies [112, 113], can be inserted into the films making these films unique and tunable platforms. These factors can be delivered to the cells in a controlled manner to influence the growth and behavior of cells. Different types of eukaryotic cells have been grown on LbL films and their interactions tested [73, 89, 112, 114-116]. Various parameters like adhesion [89, 117-122], viability [118, 123-125], morphology [123, 126-128], and proliferation [120, 125, 126], have been tested on multilayer films.

LbL assembly in relation to cell culture has fostered the development of two major hypotheses; the first suggests that only the outermost layer of the assembled nanofilms has an effect on the cells with the underlying layers having no effect at all. The second hypothesis hypothesizes that even the underlying layers too have an effect on the cells. A variety of other factors are also important in the attachment of the cells onto the nanofilms such as presence/absence of serum in cell-culture media, etc. [102, 119, 129].

An examination of the studies on the above-mentioned topic reveals a lack of consensus on this issue. Approaches to grow cells on LbL films have had two major goals – either making cell-adhesive or cell-resistant platforms depending on the application required. For example, Richert et al. demonstrated that primary chondrocyte cell adhesion decreases when the number of bilayers increases to five pairs [102]. This work by Richert et al. was aimed at promoting cell adhesion on the multilayer surfaces. Another work by Elbert et al. was aimed at creating bioinert surfaces. Here human fibroblast cells displayed poor spreading after the addition of the second and remained constant on the subsequent bilayers (up to 15 bilayers) [130]. Similarly, Tryoen-Toth et al. stated that cells could detect the influence of only the outermost layer in a biocompatibility study [118].

However, there has also been sufficient support for the other hypothesis, that cells are influenced by the underlying layers. In a study by Zhu et al., there was no change in the endothelial cell attachment on LbL-modified PLLA compared with unmodified control PLLA. But there were significant changes in the morphology, activity and proliferation of the endothelial cells on the LbL-modified PLLA compared with control PLLA [131, 132]. In another study by a different research group, Zhu et al. reported faster growth of chondrocytes on LbL-modified poly(DL-lactide) (PDL-LA) than on unmodified PDL-LA virgin substrate, better chondrocyte attachment and viability on PEI/gelatin multilayer modified PDL-LA substrates [133, 134]. Smooth muscle cells demonstrated more natural spread morphology when grown on 20 bilayers while demonstrating a less spread morphology on one bilayer [73, 74, 135].

An important aim of surface modification has been the preservation of the cell phenotype. The phenotype of cells is crucial for many cells because it is one of the main characteristics which need to be preserved when building artificial organs. Hydrogels, like agarose and alginate, have been used to stabilize the phenotype of chondrocytes. Several efforts have been aimed at the preservation of the phenotype of chondrocytes, one of the chief among them being by Benya and Shafer. Benya and Shafer demonstrated that chondrocytes regain their rounded morphology when grown on agarose [136]. Phenotype is all the more important in the case of chondrocytes as these cells gradually lose their rounded phenotype with successive passages; i.e., they dedifferentiate. Thus, the chondrocytes attained a fibroblast morphology *in vitro*. Therefore, the achievement of rounded phenotype has been one of the chief goals in chondrocyte culture *ex vivo* and *in vitro*. The focus in this work was directed towards retention of the rounded phenotype. An attempt was also made at obtaining a biomaterial which showed optimum viability and cell metabolic activity to construct scaffolds using LbL-LO method [74]. With the LbL-LO method, scaffolds having the critical third dimension can be added. The third dimension is important in replicating the *in vivo* environment.

Polyelectrolytes and the proteins, before their use as platforms for cell culture and tissue engineering, need to be evaluated for their cytotoxicity which is achieved through different assays like Live-Dead and MTT. In addition to these, morphological analysis using phase-contrast microscopy and immunocytochemical analysis are also used. Once the required materials exhibiting the desired characteristics are identified, the next task is building the scaffolds.

Several methods like contact angle measurement [114, 131], ellipsometry [137], attenuated total reflection (ATR-FTIR) [133], X-ray photoelectron spectroscopy (XPS) [125, 133, 138, 139], and atomic force microscopy (AFM) [125, 140] have been used to investigate the properties of LbL films. In the present study, AFM and ellipsometry were utilized for the characterization of LbL films. The results correspond with the results obtained by other researchers, proteins and polypeptides, did not show any appreciable differences in surface roughness barring a few while polyelectrolytes showed increasing roughness with increasing number of bilayers [102, 141-143].

## 2.1 Cell Culture Substrates

Cells, once they are removed from the *in vivo* environment, require a platform for their attachment and growth. Different surface modification techniques have been adopted for the creation of these platforms, the simplest being protein adsorption which takes advantage of the characteristic property of proteins to adsorb on suitable surfaces. Various other surface modification techniques like nanoscale self-assembly (SAMs and LbL) [74, 90, 91, 138], plasma surface modification [144], etc. have been utilized to generate surfaces for cell culture. Different kinds of base materials have been used based on the requirement and the technique adapted. The most common and ubiquitous material, however, has been tissue culture polystyrene (TCPS) which has long been one of the standard materials used in commercial cell and tissue culture substrates.

### **2.1.1 Coated Substrates- Substrates Coated with ECM Proteins**

Coated substrates using ECM molecules have been used for studying a wide variety of cell functions and biocompatibility assays. Cells can be adherent like chondrocytes, osteoblasts, fibroblasts, etc. or non-adherent like lymphocyte-derived cell lines. Cell-substrate adhesion involves the binding of cell-surface receptors to a secreted ECM molecule immobilized on the substrate. Studies of adherent cells have usually involved glass or polystyrene substrates coated with ECM proteins. ECM proteins like collagen, fibronectin, laminin, proteoglycans, etc., besides providing the necessary support and structure also provide the necessary signals for the attachment and growth of cells. The simple preparation technique of these substrates using protein adsorption has allowed these substrates to be used commonly. One of the most commonly used ECM proteins in commercial TCPS substrates is Type I collagen. ECM protein-coated substrates are preferred due to their ability of mimicking the ECM, but they are unsuitable for mechanistic studies, thus the need for substrates with precise surface ligand chemicals [145].

### **2.1.2 SAMs**

SAMs, studied first by Nuzzo and Allara in 1983 [146], can be spontaneously formed on appropriate substrates by dipping them into solutions of desired composition [147]. Some of the unique qualities of SAMs are their well-defined nature, accessibility, and design flexibility [148]. The most commonly used substrates for SAMs of alkanethiolates have been gold [149] and silver [150] along with several other metals. Most of these metals are costly, and another major disadvantage of silver is its rapid oxidization in air and its toxicity to cells [151]. The best advantage of SAMs is the ability

to incorporate different functional groups or molecules as end groups which can be done either before or after monolayer deposition [145, 152]. According to the IUPAC, a monolayer is a single, closely packed layer of atoms or molecules whereas bilayer is a multilayer two monolayers thick [153].

SAMs have been used in cell culture to produce cell adhesive or cell repellent platforms [79, 154]. Another disadvantage of SAMs is their essentially static nature [155]. Recently, there have been demonstrations of dynamic SAMs substrates utilizing electroactive methods [156, 157]. Electrically activated systems are attractive in that they are non-invasive and have well controlled effects but a drawback is their ability to provide only one type of temporal variation. In biology-related work entailing complex entities like ECM and biological membranes where the spatio-temporal signals are multiple, there is a need for careful orchestration [15].

### **2.1.3 LbL Self-Assembly**

LbL self-assembly, which utilizes the principle of electrostatic adsorption, was first introduced into practice by Decher in 1991 [93, 94]. This is a very versatile method which helps in the deposition of alternately charged polymers or polypeptides from dilute aqueous solutions onto any surface irrespective of its size, shape, or composition [117]. Films in the nanorange scale with highly tunable characteristics and superior control over thickness (~2-10 nm per layer), surface roughness, composition, conformation, porosity and molecular structure can be produced using this technique [15]. Besides electrostatic adsorption, these films have also been built based on van der Waals forces [158], hydrogen bonding [159], etc.. This technique has the scope for development of unique instructive cell culture platforms with the ability to deliver growth factors and other

important requirements necessary for the proper growth and attachment of cells [160]. A wide variety of eukaryotic cells has been grown on LbL films demonstrating their use in cell culture [90, 91, 161, 162]. The use of LbL films has been found to help in the acquisition of a more natural morphology in the case of smooth muscle cells [73, 74]. Other cellular characteristics like adhesion [161], proliferation [163] have been found to be substantially influenced by LbL proving the utility of these films.

LbL-assembled films though similar to SAMs in that the features have additional advantages like the diversity in the composition of the films, amorphous structure with interpenetrating layers. At the same time, some of the difficulties of LbL films are the difficulties in controlling the molecular arrangements and gradients [15]. But these difficulties are offset by the diverse number of other features controlling the nanoscale architecture like the molecules assembled, the number of layers which can be very high, concentration, charge density [164] and ionic strength [165].

LbL films help in the realization of complex structures with biomimetic properties [117, 166, 167]. Cells cultured on LbL films have responded to the multilayers of the LbL films. Retinal neural cells grown on micropatterned polyelectrolyte multilayer lines had a more elongated morphology compared to cells cultured on polystyrene [168]. Cells were found to interact with proteins embedded in LbL films through a combination of cellular extension up to the proteins and the local degradation of the films [169].

The limited examples above, along with various others, are testimony to the ability of the LbL films to influence the cellular behavior and their utility as cell culture substrates. Most of the materials used in the LbL films are biocompatible, adding value to their utility. But details regarding specific interactions between cells and LbL-assembled



materials are still missing, particularly, the influence of the composition at the nanolevel and physical arrangement of the surfaces. [15]

## **2.2 Micropatterned Substrates**

From the discussion in the previous sections it becomes obvious that cells can interact with a wide variety of natural, artificial or hybrid environmental factors through physicochemical cues, and respond by changes in cell morphology, adhesion, orientation and several other processes. Micro-nanoscale patterning offers superior control over many important features, especially spatiotemporal control [15]. Patterning helps in the control and manipulation of cell-cell, cell-medium and cell-substrate interactions helping in a better understanding of the intricate cellular processes and creation of better biomaterial scaffolds [66, 91, 169-176].

Cellular functions, such as adhesion, differentiation, orientation and migration have been found to be affected by microgrooves and ridges produced using micropatterning technology [177]. While the above mentioned is true, not much progress has been made in micropatterning methods for controlling cell adhesion [61]. Further, though many studies have aimed at the retention of the phenotype of chondrocytes, there is still much to be understood and achieved in this regard, especially due to the labile nature of the chondrocyte phenotype. Also, a better understanding of stem cells and progenitor cells like chondrocytes and osteoblasts is possible only by a superior control over spatial architecture and delivery of the required factors like growth factors and peptides. Random co-cultures fail to achieve the control required for the homotypic and heterotypic cell-cell interactions and a better understanding of the differentiation of the stem cells into different lineages. Micropatterned co-cultures of hepatocytes and

fibroblasts and hepatocytes and parenchymal cells have helped in a superior preservation and modulation of the hepatocyte phenotype [178] and improvement in hepatocyte functions like increased albumin secretion as a direct consequence of the distance between the cell patterns [66, 179]. While there have been demonstrations of stem-cell differentiation into multiple lineages [180], many questions still remain. The need for a fundamental understanding of the response of stem cells to various controlled spatiotemporal signals is all the more due to the increasing implication of stem cells in a wide variety of diseases, notably cancer [52]. The resulting biomimetic co-culture systems would be ideal platforms for studying stem cell differentiation and interactions between stem cells and various progenitor cells.

### **2.3 Two-Dimensional (2-D) vs. Three-Dimensional (3-D) Substrates**

Most of the earliest cell cultures studies were done on flat and two-dimensional surfaces. These 2-D surfaces cannot replicate the 3-D *in vivo* settings. Thus 3-D substrates are more relevant for the study of the biological activities of the cells. Hydrogel-based substrates like agarose and alginate are well-exemplified 3-D matrices [181]. Substrates studying 3-D matrix interactions between fibroblasts and ECM exhibited increased cell functions and narrowed integrin usage when compared with 2-D substrates. Also the 3-D matrix cell adhesions showed differences in structure and localization in relation to traditional *in vitro* adhesions [182]. Cells grown in 3-D matrices show faster morphological changes, migration and proliferation than most 2-D matrices or collagen gels demonstrating the importance of dimensions and dynamicity of matrix substrates in the responses of cells to ECM [183]. The phenotype and function of

vascular SMCs were modulated using *in vitro* biochemical stimulation but these effects were dependent on the nature of the ECM of the 3-D matrices used for the growth of the cells [184]. These limited results exemplify the importance of the substrates used for cell culture and growth.

Nanotechnology offers the ability to build superior biomaterial scaffolds with enhanced mechanical, physical, optical and other properties [177]. Different materials like 3-D nanofibrous scaffolds, electrospun fibers [185, 186] are some of the examples resulting from nanotechnology.

## **2.4 Cell Adhesion**

### **2.4.1 Cell Adhesion and Cell Culture**

One of the most important components in the above discussion of microsubstrates is the requirements for an adhesive surface for cells to attach, grow and maintain different functions. Thus cell adhesion plays an important role in cell and tissue culture. Cell adhesion proteins and their receptors play a key role in different cellular processes like anchorage, migration and provide signals for polarity, position and differentiation [187]. Different kinds of cell adhesion mechanisms dictate the organization of cells into tissues. Regulation of tissue morphogenesis is a complex interplay of adhesion receptors, cytoskeleton, and the diverse network signaling pathways. There is a very strong relationship between the physical aspects of tissue generation with cell growth and differentiation required for the patterning of cells into tissues [188].

With regard to cell culture, cell adhesion is important for the maintenance of cell morphology and functionality. Chondrocytes rapidly lose their rounded configuration in monolayer culture and get dedifferentiated. The rounded phenotype is regained when the

cells are grown on agarose gels [136]. But efforts are still underway to obtain chondrocytes of the optimum configuration, especially in the tissue engineering of artificial cartilage. A variety of hormones [189, 190], growth factors [191, 192], and cytokines [193-196], influence the chondrocyte phenotype. All these essential items mentioned above are required for the growth and maintenance of the differentiated state of the chondrocytes especially in *in vitro* and *ex vivo* settings.

#### **2.4.2 Cell Adhesion and 2D, 3D, and Coated Culture Substrates**

Different factors necessary for the adhesion and growth of cells have been engineered onto substrates using different technologies. Besides being necessary to better understand the different events of cellular biology, these are also useful in tissue engineering, creation of biosensors, drug testing, and implant coatings. Different materials are being continually evaluated for testing cell adhesion. Polymers have been excellent candidates for tissue engineering applications because of their biocompatibility [197, 198]. A wide variety of polyelectrolytes and polypeptides are being used in the various surface modification techniques utilized by nanotechnology [118, 199-203]. These studies have demonstrated the utility and advantages offered by the above-mentioned materials for cell culture. For example, smooth muscle cells showed increasing adhesion with increasing stiffness on LbL films [204]. In another study, SaOS-2 osteoblast-like cells and human periodontal ligament (PDL) cells were grown on polyelectrolyte multilayers. With the exception of PEI, all the other materials were found to be biocompatible for the cells [118]. Chondrosarcoma cells (HCS-2/8) grown on different polyelectrolyte films showed increased cell adhesion in the early stages on all with one exception being PSS where the cell adhesion was slightly lower [124].

Micropatterned polystyrene substrates coated with laminin improved the cell adhesion and spreading of cytoskeletal filaments significantly in rat type-1 astrocytes [205]. Thus it can be seen that a variety of polyelectrolytes and proteins have been used to enhance the adhesion of cells on substrates.

The characteristic markers of differentiated chondrocytes include collagens II and IX and aggrecans. The differentiated phenotype of chondrocytes from different animal species is generally associated with a round or a polygonal morphology and can be maintained in high-density cultures. But the round or polygonal morphology is lost and a spread or flattened morphology arises when chondrocytes are maintained in low-density cultures. The differentiated phenotype of chondrocytes is subject to extensive modulation in cell culture, and the mechanisms regulating differential gene expression are just beginning to be known. Thus maintenance of the rounded phenotype of chondrocytes is a major factor in the retention of the normal physiology of the chondrocyte cell type and this issue still needs addressing.

## **2.5 Cartilage and Chondrocytes**

The composition of various connective tissues is a reflection of the functional requirements. Cartilage is an example of tissues subjected to compressional loads which have irregularly arranged collagen fibers and an abundant ECM composed of proteoglycans, ions and water. The predominant proteoglycan is a large chondroitin sulfate-rich molecule which forms aggregates with hyaluronic acid [56]. Cartilage is aneural, alymphatic and avascular. The major cell type in cartilage is a chondrocyte. Chondrocytes are mature cartilage cells and are specialized cells of mesenchymal origin. These are metabolically active, do not normally divide after adolescence and are ascribed

to live in a hypoxic environment due to the limited blood supply. However, Shapiro et al. concluded that chick growth plate chondrocytes are not oxygen deficient *in vivo* [206]. Chondrocytes have a highly labile phenotype and show two distinct phenotypes. They exhibit a flattened morphology during anchorage-dependent culture and spherical or rounded morphology during anchorage-independent culture. The differentiated phenotype of chondrocyte is rapidly lost during *in vitro* culture by a process termed 'dedifferentiation'.

## **2.6 Chondrocyte Cytoskeleton, Morphology, and Phenotype**

### **2.6.1 Chondrocyte Cytoskeleton**

The cytoskeleton is that part of the cytoplasm that remains when organelles and internal membrane systems are removed. It is unique to eukaryotic cells. It is a dynamic three-dimensional structure that fills up the cytoplasm. The cytoskeleton is responsible for providing cell shape, mechanical strength, and motility, chromosome separation in mitosis and meiosis and intracellular transport of organelles. The cytoskeleton consists of three kinds of protein filaments: microtubules, intermediate filaments and actin filaments (also called microfilaments). The actin cytoskeleton provides a structural framework helping in the cell shape and polarity in all eukaryotic cells [207].

Articular cartilage is a load-bearing component of the body, and this loading is essential for the normal physiology of the chondrocytes. The cytoskeleton has been pointed as the main load-bearing organelle in the chondrocyte by various studies. Investigations of the 3-D structure of the chondrocyte cytoskeleton in response to mechanical loads have demonstrated that actin distribution is unaffected while the

vimentin cytoskeleton is disassembled. The probable reason is the counteraction of loading to the swelling pressure of tissue [208].

Earlier studies have pointed out that the mechanical environment of the chondrocytes may be altered in osteoarthritis [209]. A very recent study proposes that microfilaments and possibly intermediate filaments are the key elements in the rendering of viscoelastic properties of the chondrocytes, and the changes in the structure and properties of these elements may be reflective of the changes of chondrocytes with osteoarthritis [210]. Thus, a better understanding of different types of chondrocytes (both normal and diseased) would lead to therapeutic advances of especially debilitating diseases like osteoarthritis.

### **2.6.2 Focal Adhesion Plaques**

Cell ligation to ECM results in integrin aggregation triggering increased tyrosine phosphorylation of various intracellular proteins [211-213]. Focal adhesions are specialized organelles consisting of concentrated integrin clusters which also have bundles of actin and associated cytoskeletal proteins like vinculin, talin, paxillin, etc. [214, 215]. Focal adhesions are the sites of cell adhesion to a substrate. These are complex multimolecular assemblies which link the ECM and the cell cytoskeleton through membrane-bound receptors [216, 217]. These sites act as the transmitters of forces to the substrate [218]. A study by Balaban et al. using elastic micropatterned substrates revealed that the direction of force applied at each mature focal adhesion correlated with the main axis of the elongation. The disruption of focal adhesions was dependent on the relaxation of the force and the force exerted by the cell through

actomyosin contraction at its focal adhesion site determined the assembly of the cells [218].

### **2.6.3 Integrins**

Integrins, a family of cell surface receptors attach cells to the ECM and transmit the mechanical and chemical signals from it. These signals help in the regulation of the activities of cytoplasmic kinases, growth factor receptors, and various ion channels and help control the organization of the intracellular actin cytoskeleton [219]. Integrins play crucial roles in cell adhesion, migration, and signaling by providing transmembrane links between the extracellular matrix and the cytoskeleton [187]. Several studies have been conducted on the relevance of integrins to chondrocytes [220-229]. These studies emphasize the importance of Integrin-mediated cell adhesion to extracellular matrices in providing signals essential for chondrocyte cell cycle progression and differentiation.

## **2.7 Patterned Self-Assembled Films**

Two of the most commonly used techniques to produce patterned self-assembled films have been soft lithography and photolithography. Dip-pen nanolithography (DPN) is used for the deposition of nanoscale features onto self-assembled nanofilms. But there are numerous other patterning techniques mostly used for specialized applications [15].

### **2.7.1 Soft Lithography**

A wide variety of soft lithographic techniques have been used along with SAMs and LbL self-assembly [230-232]. Soft lithography utilizes an elastomeric poly(dimethylsiloxane) (PDMS) stamp or mold to transfer an organic/inorganic monolayer or cells onto the surface of a substrate. A wide variety of techniques have been developed from this such as microcontact printing ( $\mu$ CP) [71, 233, 234], replica molding



(REM), microtransfer molding ( $\mu$ TM), micromolding in capillaries (MIMIC), solvent-assisted micromolding (SAMIM), 3D micromolding in capillaries (3D MIMIC) [147], patterning using microfluidic networks ( $\mu$ FN), elastomeric membranes [235, 236], chemically templated surfaces [32, 231], multilayer transfer printing (MTP) [237, 238].

Though the different soft lithographic techniques mentioned above have several advantages like rapid prototyping, lower costs, good biocompatibility, and the ability to pattern non-planar substrates [147], there is a limit on the repeatability of pattern transfer as it depends on myriad factors like quality of the patterns on the mold/stamp, hydrophobicity of the mold/stamp and the material itself used for molding/stamping, and several other factors that are not repeatable. There are various other drawbacks like the complexity associated with 3D microfluidic systems, the constraints on the choice of materials and the stringent deposition conditions of chemically patterned templates, etc. [15]. Some other drawbacks of the structures associated with soft lithography are their non-rigid nature with a risk of collapse [239].

### **2.7.2 Photolithography**

Photolithographic techniques have been constantly and extensively refined and adjusted for advanced applications in integrated circuit (IC) technology and microelectromechanical systems (MEMS). Also, the mold/stamp used in all of the soft lithographic applications is created using the conventional lithography processes [15]. Now, photolithography is being applied for patterning of self-assembled nanofilms [240-242]. Issues of biocompatibility have been addressed by the studies on biocompatible photolithographic processes [243] that utilize chemically amplified photoresists and dilute aqueous base developers [244-246]. Photolithography in conjunction with LbL

self-assembly is a powerful methodology for the fabrication of well-defined structures of differing functionality in close proximity [247]. “LbL-LO”, a recently developed technique combining photolithography and LbL processes with a single lift-off (LO) step has been successfully utilized to create patterned multilayer nanofilms of biomolecules [74], and extended to the production of multiprotein patterns [91] for the successful culture and growth of SMCs and neuronal cells. The use of acetone in the LbL-LO methodology was not a deterrent for the adhesion and growth of the different types of mammalian eukaryotic cells.

Thus, the most important advantages of using conventional photolithography over soft lithography are the ease in fabrication processes, precise alignment and undistorted features of the patterns generated, and the unrestrained choice of materials.

## CHAPTER 3

### EXPERIMENTAL DESIGN

#### 3.1 Layer-by-Layer Assembly

The diagram in Figure 3.1 depicts the LbL technique. This technique has been described in sufficient detail in section 2.1.2 of Chapter Two. In the present study, LbL was used to build multilayer architectures of varying configurations and chondrocytes from different species were tested on these multilayer beds consisting of different biomaterials.

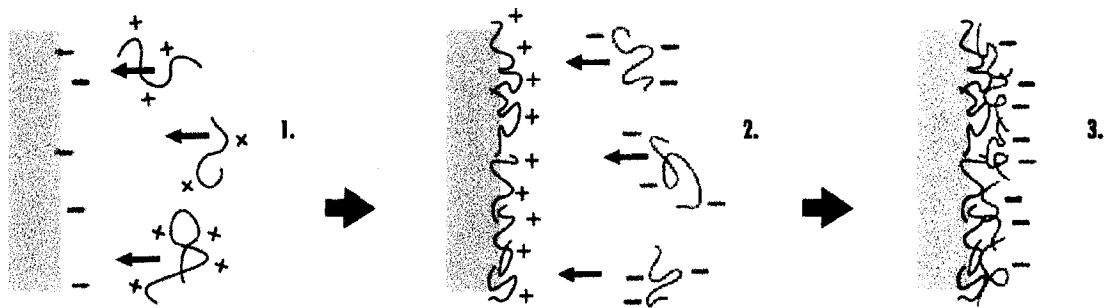


Figure 3.1 LbL assembly.

#### 3.1.1 Multilayer Architectures

Different multilayer configurations made up of eleven different biomaterials were constructed using the LbL technique for use in this study. These biomaterials consisted of polyelectrolytes and polypeptides. The various biomaterials used were poly(ethyleneimine)(PEI), poly(dimethyldiallyl-ammoniumchloride) (PDDA), poly(styrene-sulfonate) (PSS), polyethylene glycol amine (PEG-NH<sub>2</sub>), collagen,

fibronectin, poly-L-lysine (PLL), poly-D-lysine (PDL), laminin, bovine serum albumin (BSA), and chondroitin sulfate (CS). Unmodified tissue-culture polystyrene (TCPS) was used as the standard control. Mono-, bi-, and tri-layers of these biomaterials were prepared and PBAC were grown on these layers. Table 3.1 depicts the different biomaterials, their molecular weights, charges, the different LbL layer configurations and the concentrations of the materials used.

Table 3.1 Molecular weights, pH, charges, LbL architectures and concentrations of the different biomaterials used in this study.

Material	Molecular weight	pH	Charge	Monolayer	Bilayer	Trilayer	Concentration
Polystyrenesulfonate (PSS)	1000000	7	-	PSS	(PSS/PEI)/PSS	(PSS/PEI) <sub>2</sub> /PSS	2 mg/ml
Polydimethylallylammoniumchloride (PDAA)	150000	7	+	PSS/PDAA	(PSS/PDAA) <sub>2</sub>	(PSS/PDAA) <sub>3</sub>	2 mg/ml
Polyethylenimine (PEI)	750000	7	+	PSS/PEI	(PSS/PEI) <sub>2</sub>	(PSS/PEI) <sub>3</sub>	2 mg/ml
Fibronectin	450000	7.4	-	Fibronectin	(PSS/PEI)/Fibronectin	(PSS/PEI) <sub>2</sub> /Fibronectin	100 µg/ml
Poly-L-lysine (PLL)	84000	7.4	+	PSS/PLL	(PSS/PLL) <sub>2</sub>	(PSS/PLL) <sub>3</sub>	125 µg/ml
Poly-D-lysine (PDL)	125100	7.4	+	PSS/PDL	(PSS/PDL) <sub>2</sub>	(PSS/PDL) <sub>3</sub>	125 µg/ml
Bovine serum albumin (BSA)	66430	7.4	-	BSA	(BSA/PEI)/BSA	(BSA/PEI) <sub>2</sub> /BSA	125 µg/ml
Laminin	900000	7.4	-	Laminin	(PSS/PEI)/Laminin	(PSS/PEI) <sub>2</sub> /Laminin	86 µg/ml
Chondroitin Sulfate (CS)	502.5	7.4	-	CS	(CS/PEI)/CS	(CS/PEI) <sub>2</sub> /CS	125 µg/ml
Polyethylene glycol amine (PEG-NH <sub>2</sub> )	10000	5.1	+	PSS/PEG-NH <sub>2</sub>	(PSS/PEI)/PSS/PEG-NH <sub>2</sub>	(PSS/PEI) <sub>2</sub> /PSS/PEG-NH <sub>2</sub>	125 µg/ml
Collagen	100000	4	+	PSS/Collagen	(PSS/Collagen) <sub>2</sub>	(PSS/Collagen) <sub>3</sub>	1 mg/ml

As a step towards further evaluation of the effects of varying multilayer architectures on different species of chondrocytes, human chondrosarcoma cells were grown on 5- and 10-bilayers and canine chondrocytes were grown on monolayers, 5-, 10, and 20-bilayers. These multilayer beds consisted of the same eleven different biomaterials which were used earlier for testing PBAC. Table 3.2 depicts the different

biomaterials and the different LbL architectures – monolayer, 5-, 10- and 20-bilayer multilayer configurations.

Table 3.2 LbL architectures of the different biomaterials used in this study.

Material	Monolayer	5-Bilayers	10-Bilayers	20-Bilayers
Polystyrenesulfonate (PSS)	PSS	(PSS/PEI) <sub>4</sub> /PSS	(PSS/PEI) <sub>9</sub> /PSS	(PSS/PEI) <sub>19</sub> /PSS
Polydimethyldiallyl-ammoniumchloride (PDDA)	PSS/PDDA	(PSS/PDDA) <sub>5</sub>	(PSS/PDDA) <sub>10</sub>	(PSS/PDDA) <sub>20</sub>
Polyethylenimine (PEI)	PSS/PEI	(PSS/PEI) <sub>5</sub>	(PSS/PEI) <sub>10</sub>	(PSS/PEI) <sub>20</sub>
Fibronectin (FN)	Fibronectin	(PSS/PEI) <sub>4</sub> /Fibronectin	(PSS/PEI) <sub>9</sub> /Fibronectin	(PSS/PEI) <sub>19</sub> /Fibronectin
Poly-L-lysine (PLL)	PSS/PLL	(PSS/PLL) <sub>5</sub>	(PSS/PLL) <sub>10</sub>	(PSS/PLL) <sub>20</sub>
Poly-D-lysine (PDL)	PSS/PDL	(PSS/PDL) <sub>5</sub>	(PSS/PDL) <sub>10</sub>	(PSS/PDL) <sub>20</sub>
Bovine serum albumin (BSA)	BSA	(BSA/PEI) <sub>4</sub> /BSA	(BSA/PEI) <sub>9</sub> /BSA	(BSA/PEI) <sub>19</sub> /BSA
Laminin	Laminin	(PSS/PEI) <sub>4</sub> /Laminin	(PSS/PEI) <sub>9</sub> /Laminin	(PSS/PEI) <sub>19</sub> /Laminin
Chondroitin Sulfate (CS)	CS	(CS/PEI) <sub>4</sub> /CS	(CS/PEI) <sub>9</sub> /CS	(CS/PEI) <sub>19</sub> /CS
PEG Amine (PEG-NH <sub>2</sub> )	PSS/PEG-NH <sub>2</sub>	(PSS/PEI) <sub>4</sub> /PSS/PEG-NH <sub>2</sub>	(PSS/PEI) <sub>9</sub> /PSS/PEG-NH <sub>2</sub>	(PSS/PEI) <sub>19</sub> /PSS/PEG-NH <sub>2</sub>
Collagen	PSS/Collagen	(PSS/Collagen) <sub>5</sub>	(PSS/Collagen) <sub>10</sub>	(PSS/Collagen) <sub>20</sub>

## **CHAPTER 4**

### **MATERIALS AND METHODS**

#### **4.1 Chondrocytes**

##### **4.1.1 Cell Culture**

Three chondrocyte lines were used in this study – a primary cell line, bovine articular chondrocytes and two secondary lines, human chondrosarcoma cells and canine chondrocytes. The secondary cell lines were obtained from commercial sources.

##### **4.1.1.1 PBAC**

Ham's F-12 medium (GibcoBRL, Life technologies) containing 10% Fetal Bovine Serum (FBS) (Biosource, Camarillo, CA) supplemented with 1% Penicillin-Streptomycin (Pen-Strep) (Biosource, Camarillo, CA) was used to culture the cells. Cell counting was done using a hemocytometer. Trypsin (Atlanta Biologicals, Lawrenceville, GA) and mechanical agitation with sterile transfer pipettes were used for the dissociation of cells from their attachment areas.

##### **4.1.1.2 Human Chondrosarcoma Cells**

Human chondrosarcoma cells, a chondrocyte-like cell line [SW 1353, Humerus (HTB-94)] were obtained from ATCC (Manassas, VA). Leibovitz's L-15 medium containing 10% Fetal Bovine Serum (FBS) supplemented with 1% Penicillin-

Streptomycin (Pen-Strep) (all from Biosource, Camarillo, CA) was used to culture the cells. Cell counting was done using a hemocytometer.

#### **4.1.1.3 Canine Chondrocytes**

Canine chondrocytes were obtained from Cell Applications (San Diego, CA). The medium supplied by the company was used for culturing the cells.

#### **4.1.2 Substrates**

LbL nanofilms were deposited on 24-well plates and 96-well black well plates (BD Falcon, BD Biosciences, San Jose, CA). Black well plates were used in the absorbance and the fluorescence plate readers. Before the LbL film assembly, these plates were cleaned with a cleaning solution [60% de-ionized (D.I.) water, 39% ethyl alcohol (70%) and 1% KOH] to eliminate the cell-attachment layer on the black-well plates. The typical cell-attachment layer is either poly-D-lysine or type I collagen.

#### **4.1.3 Biomaterials (Polyelectrolyte and Polypeptide) Preparation**

All chemicals were purchased from Sigma-Aldrich unless otherwise specified. PDDA (Mw ~ 100k-200k), PSS (Mw ~ 1M) solutions were prepared at concentrations of 2 mg/ml with 0.5 M KCl and a PEI (Mw ~ 750k) solution of 2 mg/ml were prepared in deionized (DI) H<sub>2</sub>O for use in LbL self-assembly. PLL (Mw ~ 84,000), PDL were prepared with a concentration of 125 µg/ml while BSA (Mw ~ 66,430), PEG-NH<sub>2</sub>, chondroitin sulfate and collagen (Cohesion, Palo Alto, CA) were prepared at a concentration of 120 µg/ml while laminin was prepared at a concentration of 86 µg/ml and Fibronectin at a concentration of 100 µg/ml. All solutions were prepared using deionized water with a resistivity of 18.2 MΩ.cm (Millipore systems). Proteins were vortexed before their use in the LbL process.

Different parameters like Cell morphology and attachment, viability, cell metabolic activity, and functionality were determined using bright field microscopy, Live/Dead viability assay, MTT assay, and anti-type II collagen and aggrecan immunocytochemistry, respectively. PEI served as the precursor layer in all the cases.

#### **4.1.4 Fabrication Techniques**

The fabrication technique was very simple and performed using pipettes. To prevent infection of cells due to contamination, the entire nanofilm deposition procedure was performed under a laminar flow-hood adopting strict sterile techniques. For every layer, about 100  $\mu$ l or 200  $\mu$ l was used for 96- and 24-well plates respectively. PEI was the precursor layer in all the cases. Successive layers of positive and negative polyelectrolytes/polypeptides were built upon one another to achieve the desired LbL configurations. The intermediate drying step with nitrogen was eliminated. After the completion of fabrication the multilayer plates were kept under UV light in a laminar flow-hood overnight. Later these plates were transferred to 4°C until further use. Before cell-seeding, these plates were filled with 70% ethanol for 30 minutes followed by a five minutes wash with HBSS (without calcium and magnesium) (Biosource).

#### **4.1.5 Characterization Techniques**

##### **4.1.5.1 AFM**

AFM has emerged as the method of choice for the evaluation of different nanoengineered surfaces because of the inherent advantages this method offers. One of the most important advantages of this method is the generation of 3-D images of surfaces with resolution at nearly the atomic level [248]. In the present study, an Atomic force microscope (Quesant, Model 250) was used in tapping mode with silicon cantilevers to



measure the roughness of the different nanofilms. Silicon substrates were used for the film deposition.

#### **4.1.5.2 Ellipsometry**

A spectroscopic ellipsometer (SENTECH, Model-SE 850) measured the thickness of 5-, 10-, and 20-nanometer nanofilms on silicon wafers.

#### **4.1.6 MTT Assay**

A MTT assay kit (Sigma, St. Louis, MO) was used in the assay to determine chondrocyte cell metabolic activity [249]. An absorbance/cell number curve (calibration) was obtained with known cell numbers after cell-attachment. The MTT assay was performed on the fourth day *in vitro* after seeding chondrocytes. Three different densities were used: 500, 1000 and 1500 cells/ml. The absorbance was measured using an absorbance plate reader at a wavelength of 570 nm. All the results were corrected for background (MTT solvent at a wavelength of 690 nm) and normalized to TCPS control (relative activity).

#### **4.1.7 Live-Dead Assay**

Live-Dead viability assay (Molecular Probes, Eugene, OR) was performed on the sixth day after seeding chondrocytes. The assay utilizes the hydrolysis of membrane permeant calcein-AM fluorescence dye by esterases in live cells which leads to cytoplasmic green fluorescence and membrane-impermeant ethidium homodimer-1 dye which labels the nucleic acids of membrane-compromised cells with red fluorescence [250]. The fluorescence intensity was measured at 485 nm of excitation and 530 nm of emission by a Tecan fluorescence plate reader and all results were normalized to TCPS control (% Live). Live-Dead assay was performed on the sixth day *in vitro*.

#### **4.1.8 Statistical Analyses**

ANOVA and Tukey analyses were used for analyzing the interactions between density, layers and the different biomaterials for the different assays used. SAS statistical software was used for the analysis. The tests were performed with a significance level  $p$  equal to 0.05.

### **4.2 Micropatterned Surfaces**

#### **4.2.1 Substrates**

Number #2 microscope cover slips (18 x 18 mm<sup>2</sup>, Electron Microscopy Sciences) were used as the substrates for micropatterns. These substrates were chosen to ease the LbL assembly and patterning process. To help withstand the centrifugal force during spin coating, the glass coverslips were attached onto silicon wafers using a PR 1813 photoresist.

#### **4.2.2 Chemicals**

Nano-strip<sup>TM</sup> from CYANTEK corporation; positive photoresist, PR 1813, and positive resist developer, MF-319 from Shipley were used. All the chemicals were purchased from Sigma-Aldrich unless otherwise specified. All commercial chemicals were used in the condition they were received.

#### **4.2.3 Preparation of Polyelectrolyte and Polypeptide Solutions**

PDDA, PSS, PEI, collagen and CS solutions were prepared and used for the LbL assembly as described previously in section 3.1.3.

#### **4.2.4 Mask Design**

The mask used for pattern transfer contained 80  $\mu\text{m}$  wide stripe patterns separated by 100  $\mu\text{m}$ .

#### **4.2.5 Fabrication**

Based upon the results obtained with canine chondrocytes in chapter four, five different materials which showed the highest cell metabolic activity were selected. The five materials were PDDA, PEI, PSS, collagen and CS. The substrates were patterned with these five different materials as five and ten bilayers each.

#### **4.2.6 Substrate Pretreatment**

The substrates were first incubated in Nano-strip™ at 70°C for one hour followed by DI water rinsing and drying using N<sub>2</sub>. This procedure removed any sort of organic material and created a uniform negative charge on the substrates. Based on previous results with smooth muscle cells [74] and neuronal cells [91], a precursor layer of PDDA was deposited onto the substrates to render a cytophobic background on the substrates. One point to be mentioned here is that any cytophobic material other than PDDA can also be used.

#### **4.2.7 Photolithography**

The glass substrates were attached onto silicon wafer pieces using photoresist and heated at 165°C for 5 minutes (min) to hard bake the photoresist. After this, positive photoresist was spun on the PDDA-coated substrates (1000 rpm-100 r s<sup>-1</sup>-10 sec, 3000 rpm-500 r s<sup>-1</sup>-50 sec), soft baked at 115°C for one minute, and photo-patterned using UV radiation (400 nm, 7 Mw cm<sup>-2</sup>) for 18 sec. At the end, the patterns were developed for 15 sec using MF-134, and the substrates were quickly rinsed in DI water and dried using N<sub>2</sub>.

#### **4.2.8 LbL Self-Assembly**

The micropatterned substrates were then modified using LbL self-assembly. The substrates were dipped in the polyelectrolyte and protein solutions for 10 minutes and 30

minutes respectively. Either PSS or PEI was the polyanions used in the multilayer configurations. After every layering step, the substrates were rinsed in DI water and then dried using N<sub>2</sub>. Thus the following configurations were built – (PSS/PDDA)<sub>5</sub>, (PSS/PDDA)<sub>10</sub>; (CS/PEI)<sub>4</sub>/CS, (CS/PEI)<sub>9</sub>/CS; (PSS/PEI)<sub>5</sub>, (PSS/PEI)<sub>10</sub>; (PSS/Collagen)<sub>5</sub>, (PSS/Collagen)<sub>10</sub>; and (PSS/PEI)<sub>4</sub>/PSS, (PSS/PEI)<sub>9</sub>/PSS.

#### **4.2.9 Lift-Off**

Lift-off was performed by sonicating the substrates in acetone for about 5-10 min. The photoresist and the nanofilms were removed during the lift-off process and the cover-slip glasses removed from the silicon wafers. The main parameters in this step were the sonication strength and sonication time. Surprisingly, the use of acetone has been shown not to affect the biological functions of the molecules used in the lithographic process [15].

#### **4.2.10 Characterization**

Phase-contrast microscopy was used to demonstrate the successful creation of the micropatterns.

### **4.3 Micropatterned Co-Culture Platforms**

#### **4.3.1 Substrates**

43 x 70 mm microscope glass cover-slips (Thomas Scientific, USA) – No. 2 thickness were cut into two halves and used as the substrates for film patterning.

#### **4.3.2 Chemicals**

Nano-Strip from Cyantek, poly(diallyldiethylammonium chloride) (PDDA) (M<sub>w</sub> ~ 100 k-200k), poly(sodium 4-styrenesulfonate) (PSS) (M<sub>w</sub> ~ 1M), poly(ethyleneimine) (PEI) (M<sub>w</sub> ~ 750 k) and vitronectin (M<sub>w</sub> ~ 70 k) from Innovative Research were used in

the assembly of the patterns. Positive photoresist, PR1813, and positive resist developer, MF-319 from Shipley were used. The anti-CD 44 rat monoclonal (Calbiochem) and the mouse monoclonal anti-rat osteopontin (MPIIB10<sub>1</sub>) antibodies obtained from the Developmental Studies Hybridoma Bank were used. Solutions with concentrations of 2 mg/ml PDDA and PSS in 0.5 M KCl and a solution of 2 mg/ml PEI were prepared for use in LbL assembly. FITC and TRITC obtained from Sigma-Aldrich were used for fluorescent tagging of proteins. Protein solutions were separated from unreacted dyes using disposable PD-10 desalting columns obtained from Amersham Pharmacia Biotech.

#### **4.3.3 Mask Design**

The mask used for pattern transfer contained 80 μm squares separated by a distance of 80 μm.

#### **4.3.4 Instrumentation**

A Nikon (Model-Eclipse TS100) microscope was used to image and characterize the substrates. A lightlever (LL-AFM) with Nano-R™ SPM from Pacific Nanotechnology Inc. was used for fine-feature analysis and a surface profiler (KLA-Tencor Alpha Step IQ) was used for the surface topography analysis of the patterns on the substrates.

#### **4.3.5 Fabrication**

Substrates were patterned with (vitronectin/PEI)<sub>4</sub>/vitronectin with anti-CD 44 rat monoclonal antibody atop and (fibronectin/PEI)<sub>4</sub>/fibronectin with mouse monoclonal anti-rat osteopontin (MPIIB10<sub>1</sub>) atop in a checkerboard (chessboard) pattern.

#### **4.3.6 Substrate Pretreatment, Photolithography, LbL Assembly, and Lift-Off**

These steps were performed as described earlier [91]. The charge on the substrates was eliminated by using Nano-Strip. Next, a monolayer of PDDA was built on the substrates. The PDDA-coated substrates were attached onto Silicon wafer pieces (<100>) using photoresist and photoresist was spun on the PDDA-coated substrates. Subsequently, LbL was performed twice with the following configurations -- (PSS/PDDA)<sub>3</sub>/(vitronectin-FITC/PEI)<sub>4</sub>/vitronectin-FITC/anti-CD44 rat monoclonal antibody and (PSS/PDDA)<sub>3</sub>/(fibronectin-TRITC/PEI)<sub>4</sub>/fibronectin-TRITC/anti-rat osteopontin (MPIIB10<sub>1</sub>). The immersion times were 10 minutes each for all the polyelectrolytes – PSS, PDDA and PEI. For the fluorescently labeled proteins, immersion times of one hour each for the first four layers were adopted while the final layer was developed after over-night incubation. The adsorption times for the antibodies were one hour each at room temperature and the concentration of the antibodies was 50 µmg/ml each (dissolved in sterile PBS, pH 7.4).

#### **4.3.7 Characterization**

AFM was used to characterize the checker board co-culture patterns. Nano-R™ AFM was used in tapping mode (close contact mode – 2B) with silicon nitride (Si<sub>3</sub>N<sub>4</sub>) cantilevers. The NanoRule software accompanying the AFM was used for the analysis of the acquired AFM images.

## CHAPTER 5

### RESULTS AND DISCUSSION

#### **5.1 *In Vitro* Evaluation of Chondrocytes on Layer-by-Layer Assembled Nanofilms**

##### **5.1.1 PBAC on TCPS**

PBAC were obtained from cows' knee joints by routine pronase/collagenase enzymatic dissociation techniques. The joints were obtained from the abattoir at Louisiana Tech University. All necessary aseptic precautions were taken for the isolation of cells. Cells from passages three and four were used in all experiments. Figure 5.1 depicts passage three PBAC grown on TCPS tissue culture dishes.



Figure 5.1 (a), (b) Passage Three PBAC grown on TCPS.

##### **5.1.2 Functionality – PBAC**

Anti-type II collagen & aggrecan immunocytochemistry was performed using a Vectastain Avidin Biotin-conjugate kit to demonstrate the functionality of PBAC. Immunocytochemical analysis was performed on these cells after fixation with 95% ethyl alcohol. The immunocytochemical procedure followed was as follows: The fixed cells were washed quickly in phosphate buffered saline-tween 20 (PBS-T)

thrice followed by 3 five minutes washes each. Then, blocking treatment provided in the ABC kit was applied and incubated for 30 minutes at room temperature. Next, primary antibodies (undiluted) were applied onto the cells and incubated for one hour at 37°C followed by the PBS-T washings as described earlier. Following this, biotinylated secondary antibodies were added and incubated for one hour at room temperature followed by the washing steps with PBS-T. Excess buffer around the cells was wiped off, and Avidin Biotin-conjugate reagent complex was applied and incubated for 30 minutes at room temperature. At the end, 3,3-diaminobenzidine substrate was applied and the cells were incubated in dark. The reaction was terminated after five minutes by gently washing in running water. Figure 5.2 depicts the immunocytochemical results.

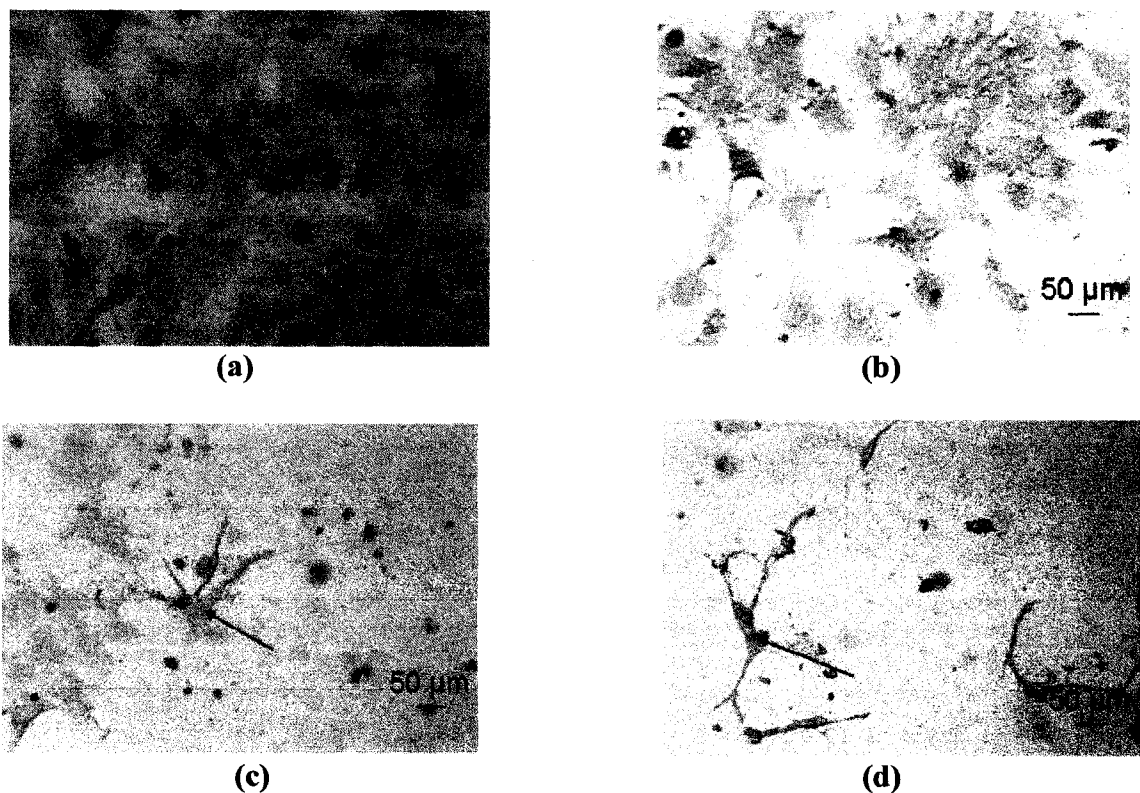


Figure 5.2 (a) Anti-type II collagen, (b) Anti-aggrecan immunocytochemistry of PBAC; controls for (c) Anti-type II collagen and (d) Anti-aggrecan immunocytochemistry of PBAC [arrows indicate chondrocytes].



### 5.1.3 AFM-Monolayer, Bilayers, and Trilayers

Different surface characterization methods including fluorescence and confocal microscopy, surface profilometry and AFM have been used for the characterization of multilayer nanofilms [90, 91, 98, 106, 125, 162, 251-256]. In the present study, AFM was employed for surface-characterization of the different multilayer films. The AFM data depicted in Table 5.1 indicate that roughness increased with increasing number of layers for most of the biomaterials except for fibronectin which displayed a decreasing trend in the roughness with increase in the number of layers while laminin showed a sharp decrease for the bilayers and increased again for the trilayers.

Table 5.1 Average roughnesses of the monolayer, bilayer, and trilayer nanofilms of the different biomaterials [Mean  $\pm$  Standard Deviation) ( $n=3$ )].

Material	Roughness (nm)		
	Monolayer	Bilayer	Trilayer
PEG-NH <sub>2</sub>	2.28 $\pm$ 0.8	5.04 $\pm$ 0.79	5.51 $\pm$ 1.09
PDDA	1.64 $\pm$ 0.42	3.94 $\pm$ 0.88	7.35 $\pm$ 1.15
BSA	1.37 $\pm$ 0.27	6.42 $\pm$ 0.86	17.11 $\pm$ 3.54
PDL	1.76 $\pm$ 0.32	5.34 $\pm$ 0.61	9.19 $\pm$ 0.19
Chondroitin Sulfate	1.18 $\pm$ 0.16	2.72 $\pm$ 1.04	9.11 $\pm$ 1.90
PEI	1.80 $\pm$ 0.26	2.49 $\pm$ 0.28	8.51 $\pm$ 2.92
Collagen	2.75 $\pm$ 0.20	6.43 $\pm$ 0.66	9.75 $\pm$ 1.08
PLL	2.37 $\pm$ 0.54	5.02 $\pm$ 0.69	8.46 $\pm$ 1.84
Fibronectin	7.08 $\pm$ 2.91	4.04 $\pm$ 0.70	6.0 $\pm$ 1.41
PSS	1.42 $\pm$ 0.15	3.38 $\pm$ 0.46	4.13 $\pm$ 0.49
Laminin	10.16 $\pm$ 1.89	3.38 $\pm$ 0.71	9.82 $\pm$ 3.78

Representative AFM images (Figures 5.3 and 5.4) of monolayer, bilayer and trilayer nanofilms with PDL and CS as the terminating layers are displayed below.

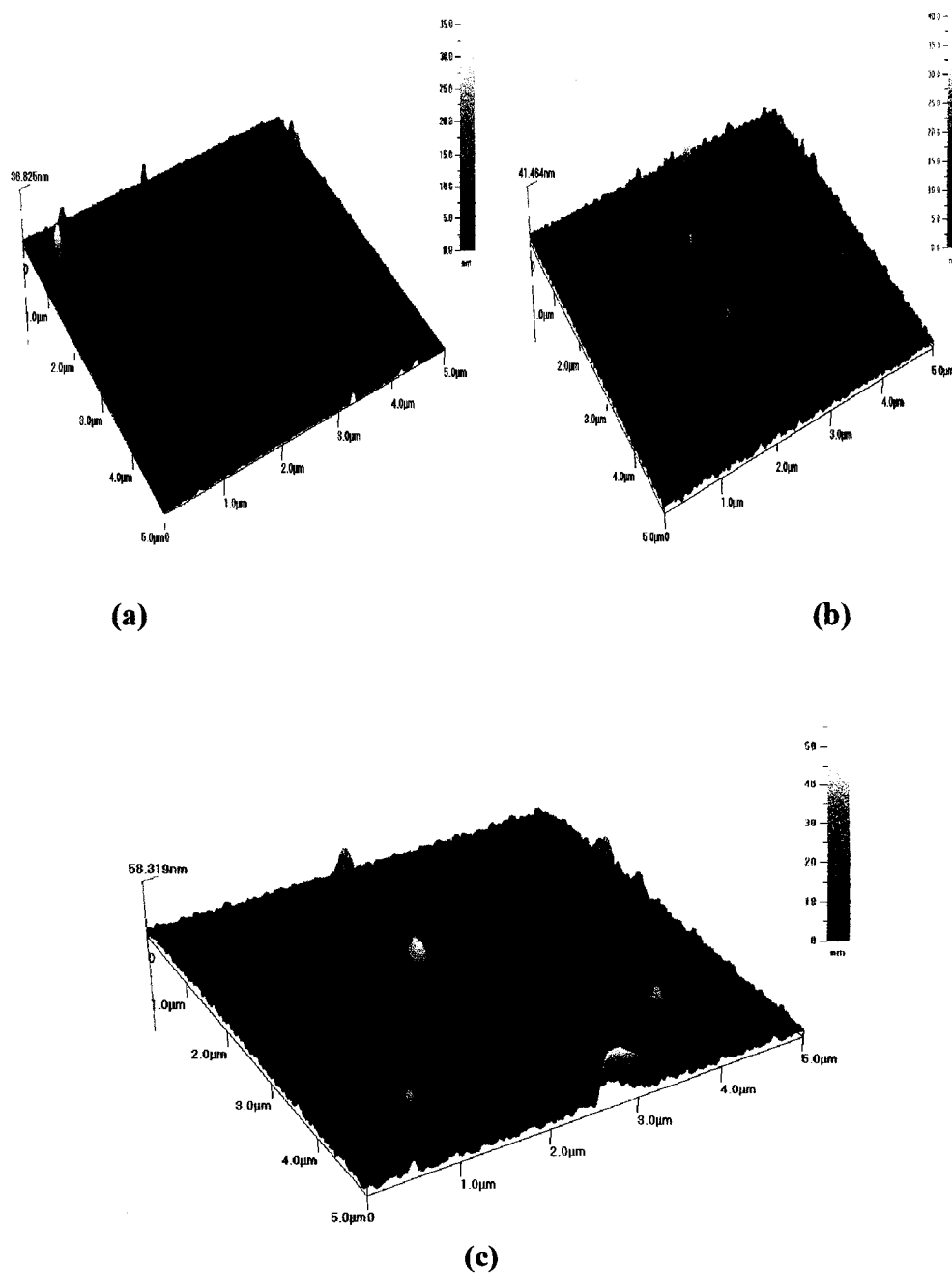


Figure 5.3 AFM images of (a) PSS/PDL, (b) (PSS/PDL)<sub>2</sub>, (c) (PSS/PDL)<sub>3</sub>.

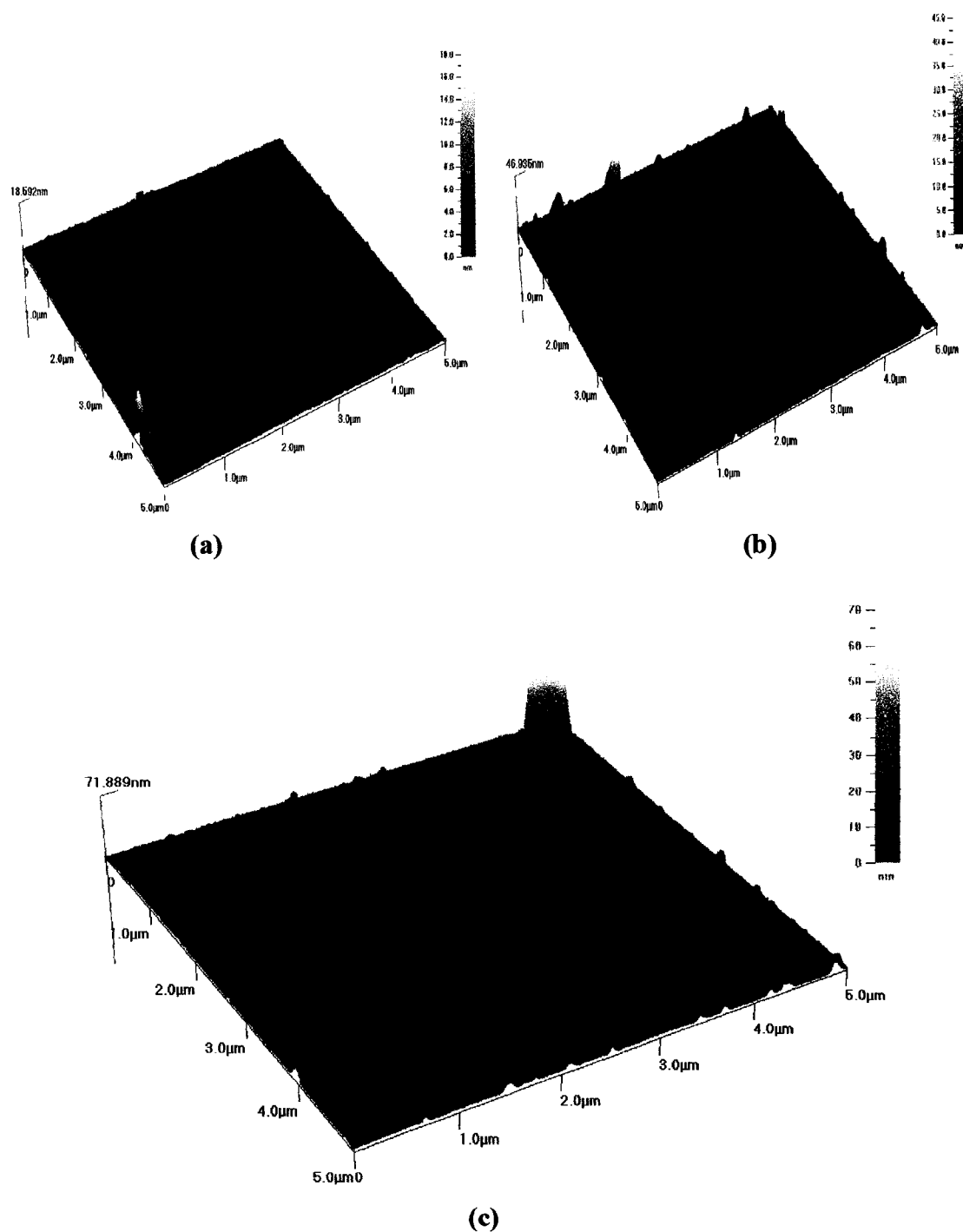


Figure 5.4 AFM images of (a) (CS/PEI)/CS, (b) (CS/PEI)<sub>2</sub>/CS, and (c) (CS/PEI)<sub>3</sub>/CS.

It can be observed from the images above that as the number of layers increases, the surfaces display increasing roughness. These results corroborate the results of other research findings [102, 141-143].

#### **5.1.4 Morphological Observations – PBAC on Different Biomaterials**

Morphological observations demonstrate that chondrocytes can be successfully grown on the nanofilms. Chondrocytes tolerated nearly all the materials favorably. A representative sample of cells on the different biomaterials is provided in Figures 5.5–5.16. All the images displayed below unless otherwise specified are of chondrocytes seeded at density one (5000 cells/ml).

##### **5.1.4.1 PBAC on TCPS**

The cells on TCPS (Figure 5.5) have a typical fibroblast phenotype.

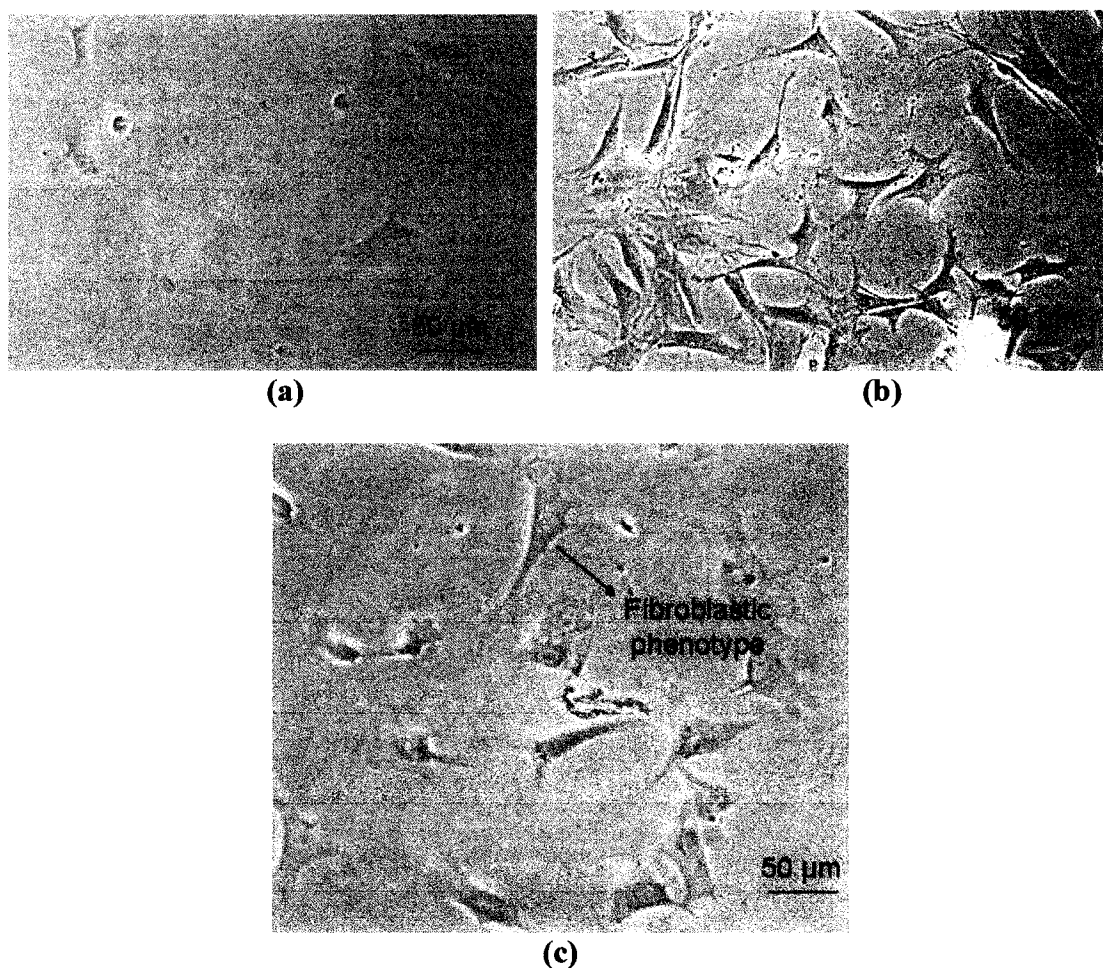


Figure 5.5 PBAC on TCPS: (a) After 34 hours; (b), (c) After 72 hours.

#### 5.1.4.2 PBAC on PEG-NH<sub>2</sub>

On PEG-NH<sub>2</sub> (Figure 5.6), it can be observed that the cells tend to acquire a far less fibroblast phenotype and tend towards a slightly rounded to orthogonal phenotype (SROP).

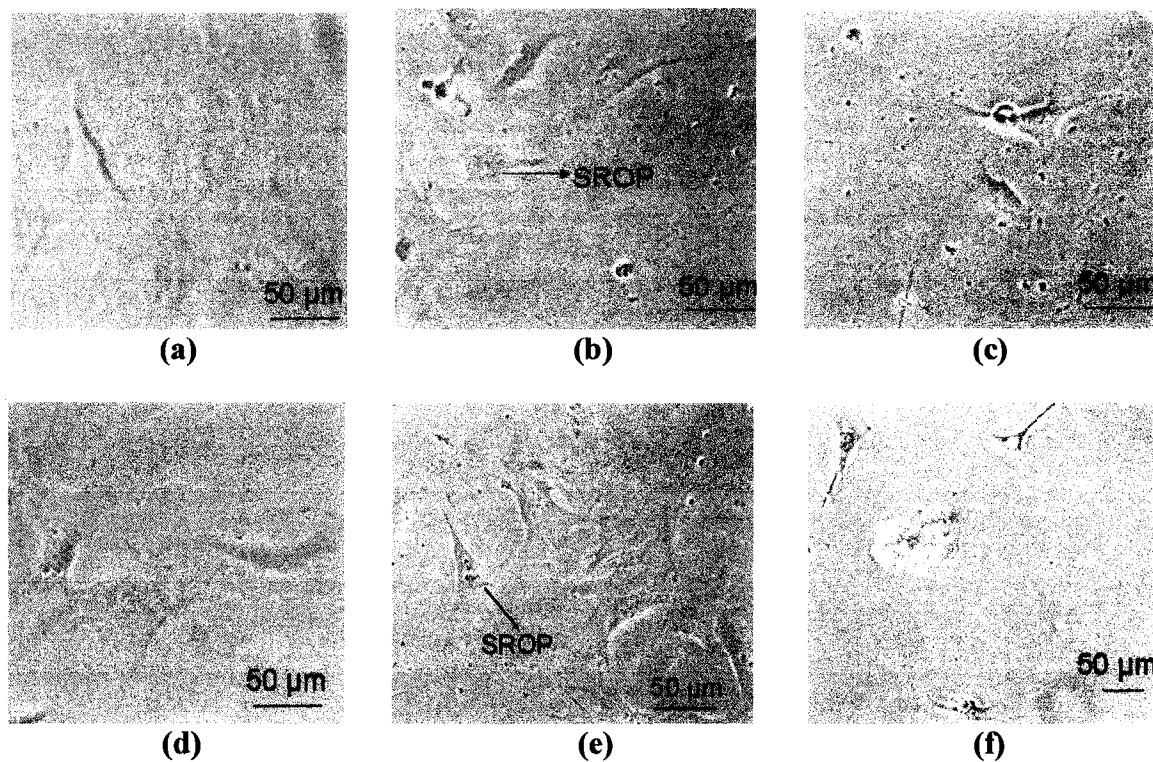


Figure 5.6 PBAC on PEG- NH<sub>2</sub>: After 34 hours – (a) On monolayer, (b) On bilayers, (c) On trilayers; after 72 hours –(d) On monolayer, (e) On bilayers, (f) On trilayers.

### 5.1.4.3 PBAC on PDDA

PDDA (Figure 5.7), a polyelectrolyte, tends to stabilize the phenotype of the chondrocytes to a SROP. Unlike PEG-NH<sub>2</sub>, the SROP is more pronounced on both bilayers and trilayers after 72 hours.

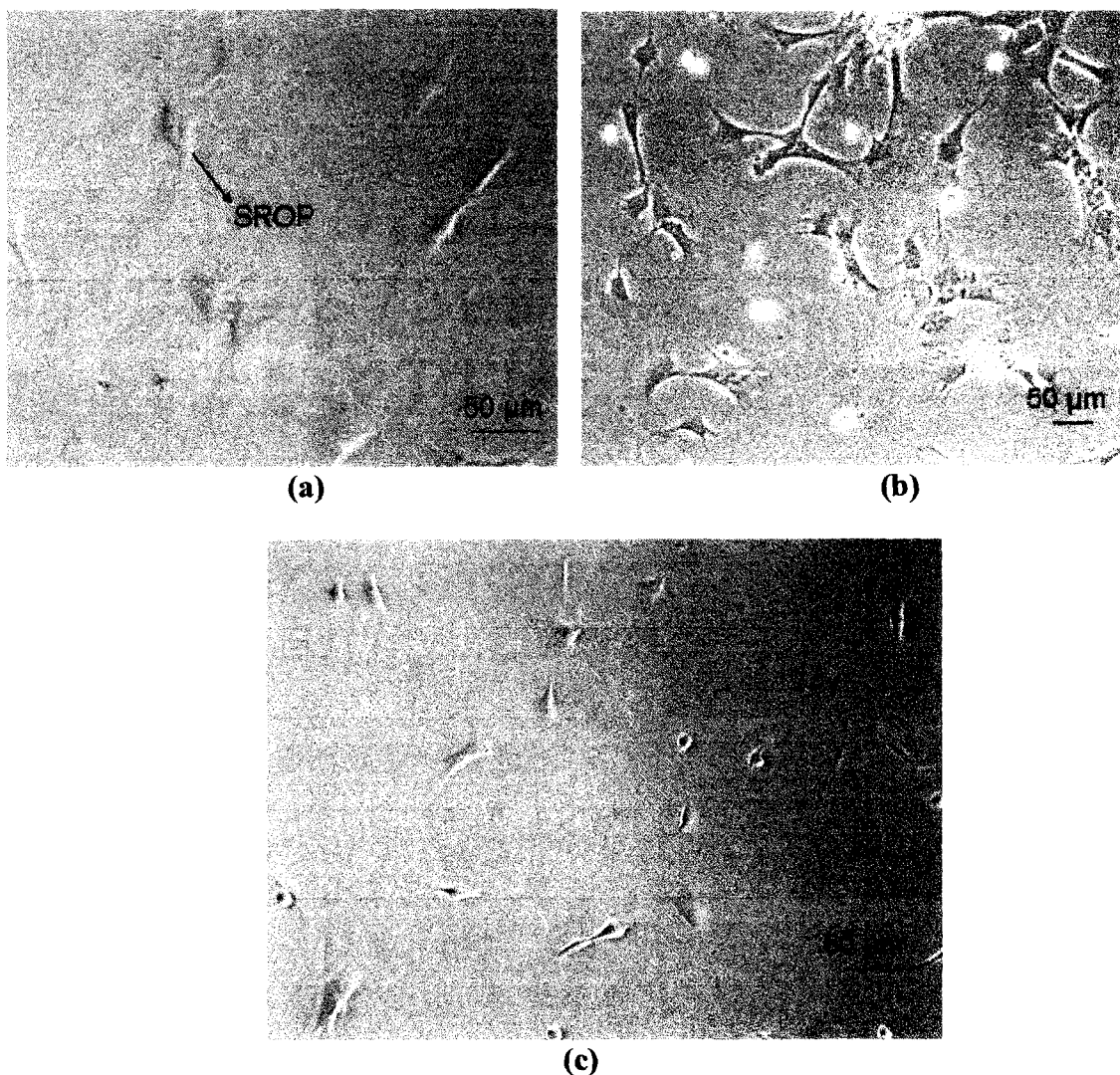


Figure 5.7 PBAC on PDDA: After 34 hours – (a) On bilayers; after 72 hours – (b) On bilayers, (c) On trilayers.

#### 5.1.4.4 PBAC on BSA

BSA (Figure 5.8) appears to stabilize the phenotype of the chondrocytes towards a more rounded phenotype. The roundedness is more pronounced on monolayer and bilayers after 72 hours whereas one can observe SROP on trilayers.

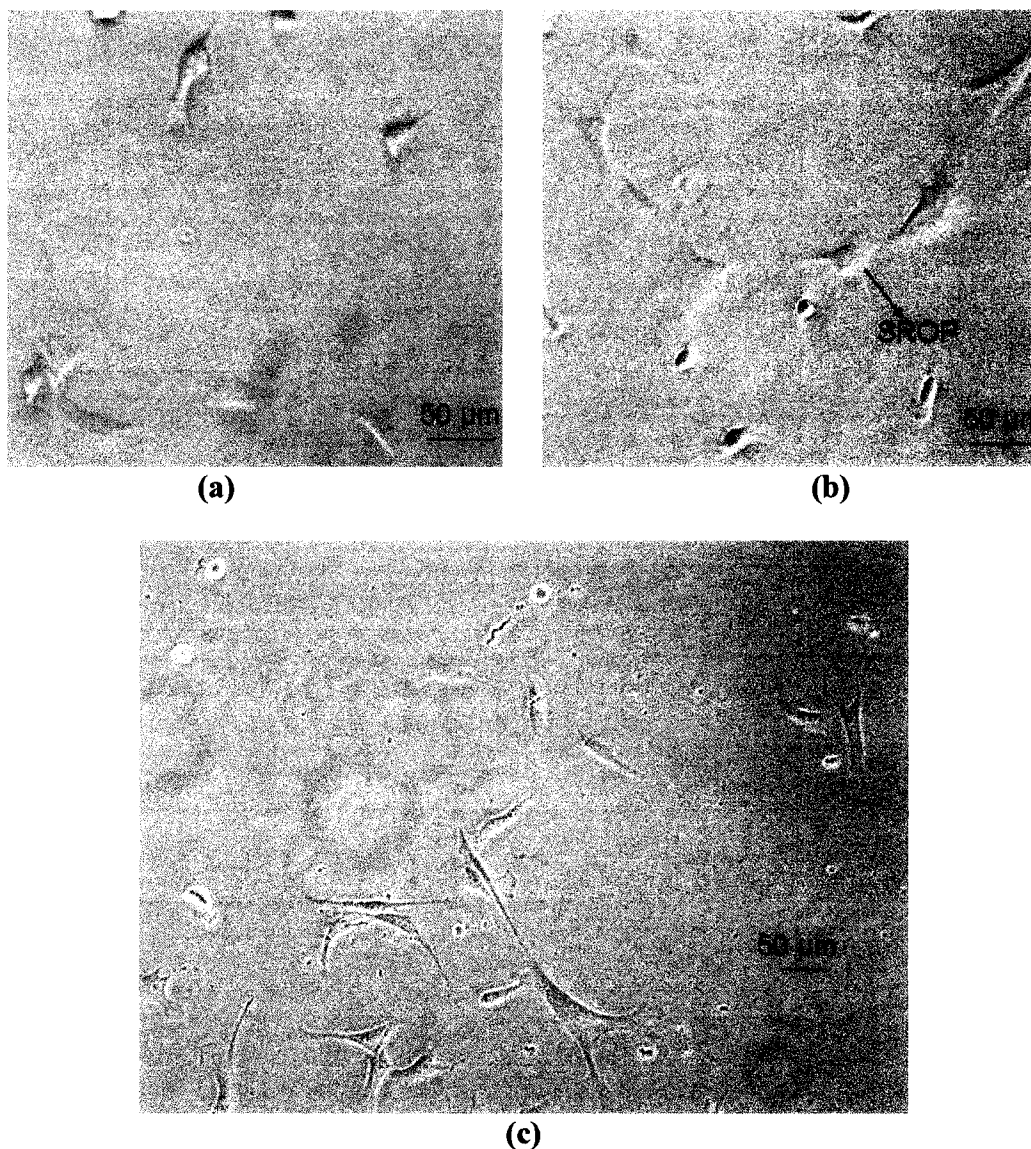


Figure 5.8 PBAC on BSA: After 72 hours – (a) On monolayer, (b) On bilayers, (c) On trilayers.

#### 5.1.4.5 PBAC on PDL

The chondrocytes on PDL (Figure 4.9) exhibit SROP on bilayers while it is slightly less pronounced on the trilayers.

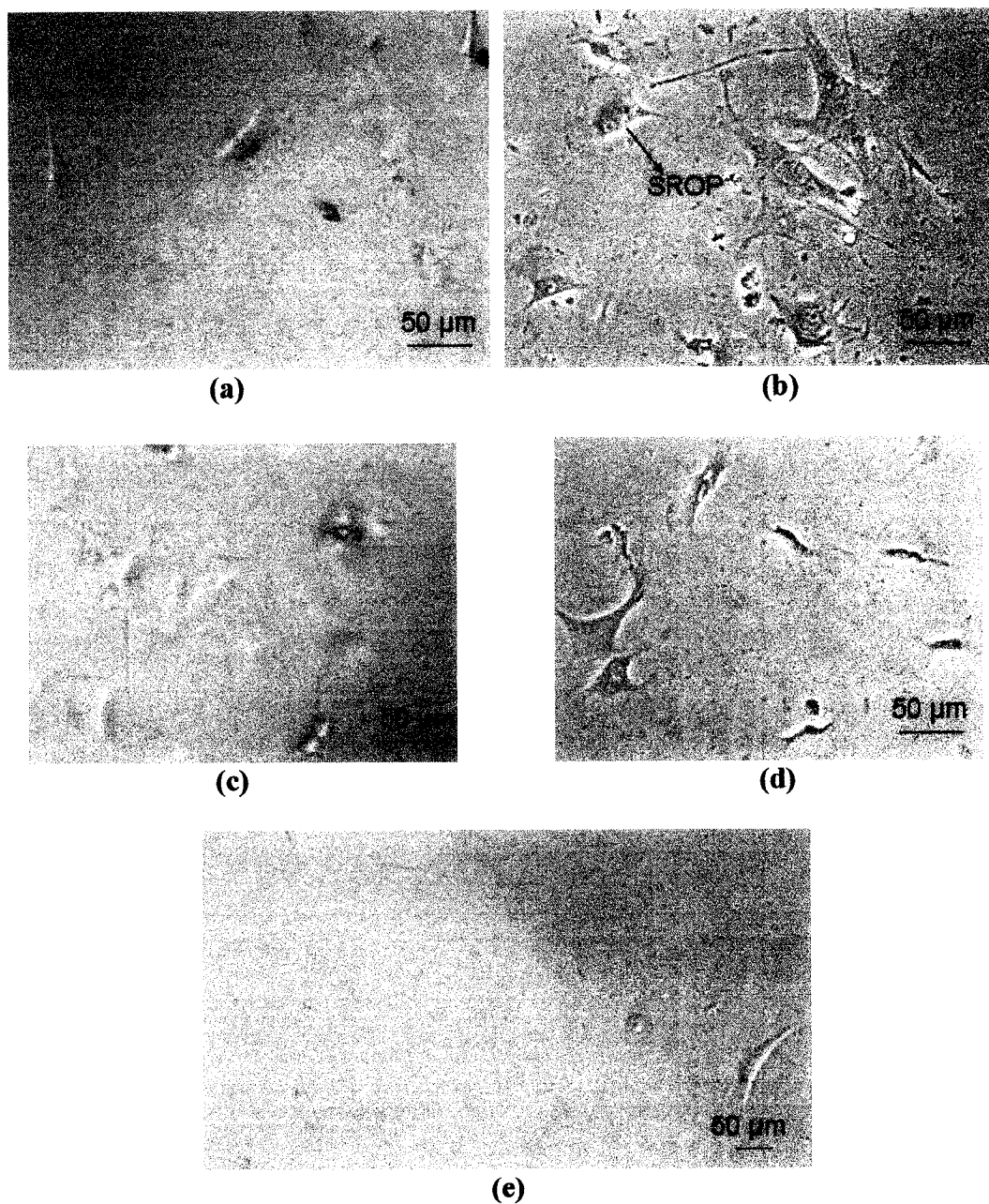


Figure 5.9 PBAC on PDL: After 34 hours – (a) On bilayers, (b) On trilayers; after 72 hours – (c) On monolayer, (d) On bilayers, (e) On trilayers.



#### 5.1.4.6 PBAC on CS

CS (Figure 5.10), like the other proteins above, shows the similar trend of chondrocytes having a more SROP and less of a fibroblast phenotype compared with the other materials.

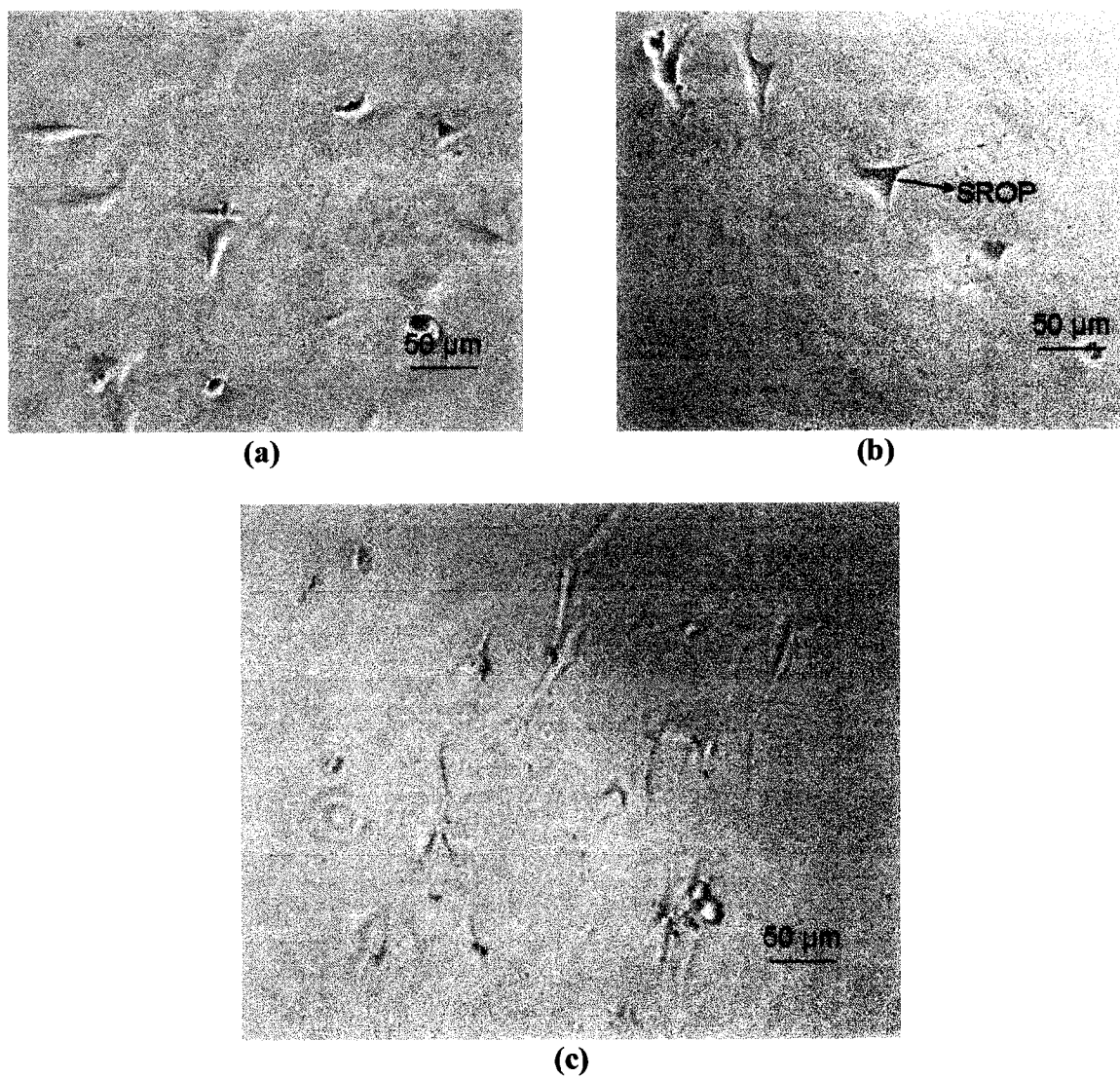


Figure 5.10 PBAC on CS: After 34 hours – (a) On bilayers, (b) On trilayers; after 72 hours – (c) On trilayers.

#### 5.1.4.7 PBAC on PEI

Figure 5.11 displays the SROP of chondrocytes on PEI.

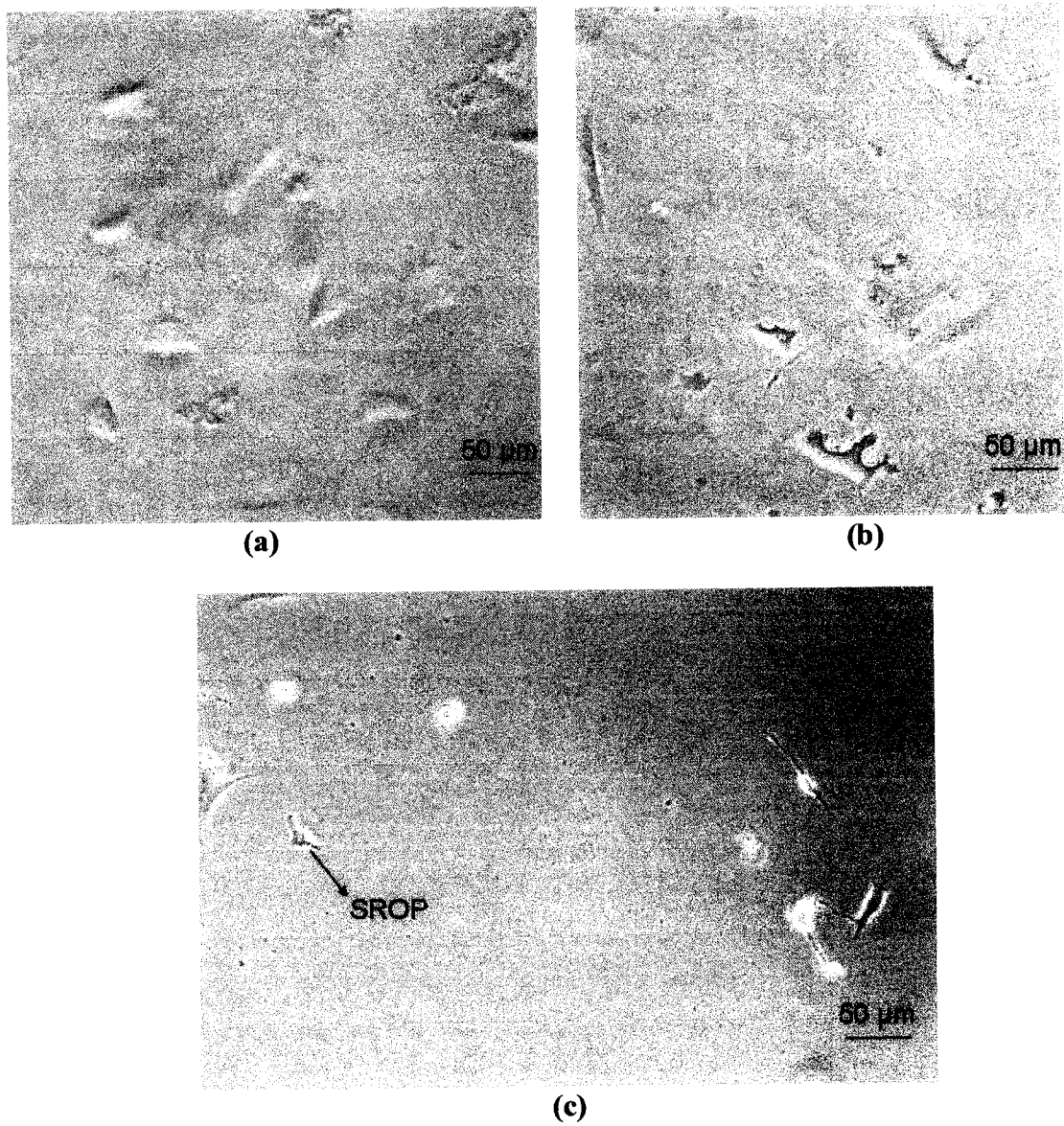


Figure 5.11 PBAC on PEI: After 34 hours – (a) On monolayer, (b) On bilayers; after 72 hours – (c) On trilayers.

#### 5.1.4.8 PBAC on Collagen

Figure 5.12 exhibits the SROP of chondrocytes on the different layers.

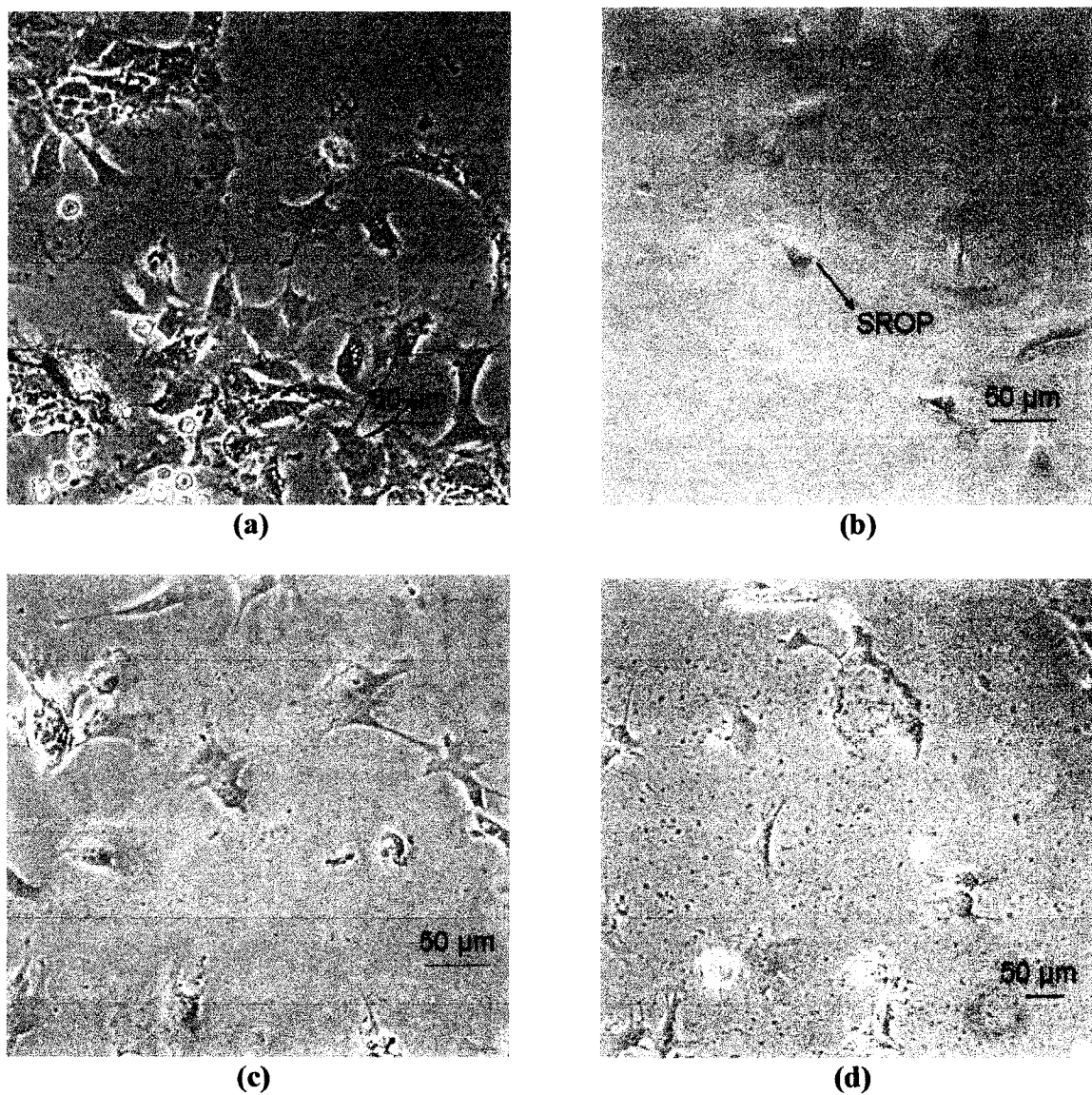


Figure 5.12 PBAC on collagen: After 34 hours – (a) On trilayers; after 72 hours – (b) On monolayer, (c) On bilayers, (d) On trilayers.

#### 5.1.4.9 PBAC on PLL

Figure 5.13 displays the SROP of chondrocytes on PLL. Very few cells are present on trilayers with marked cell death.

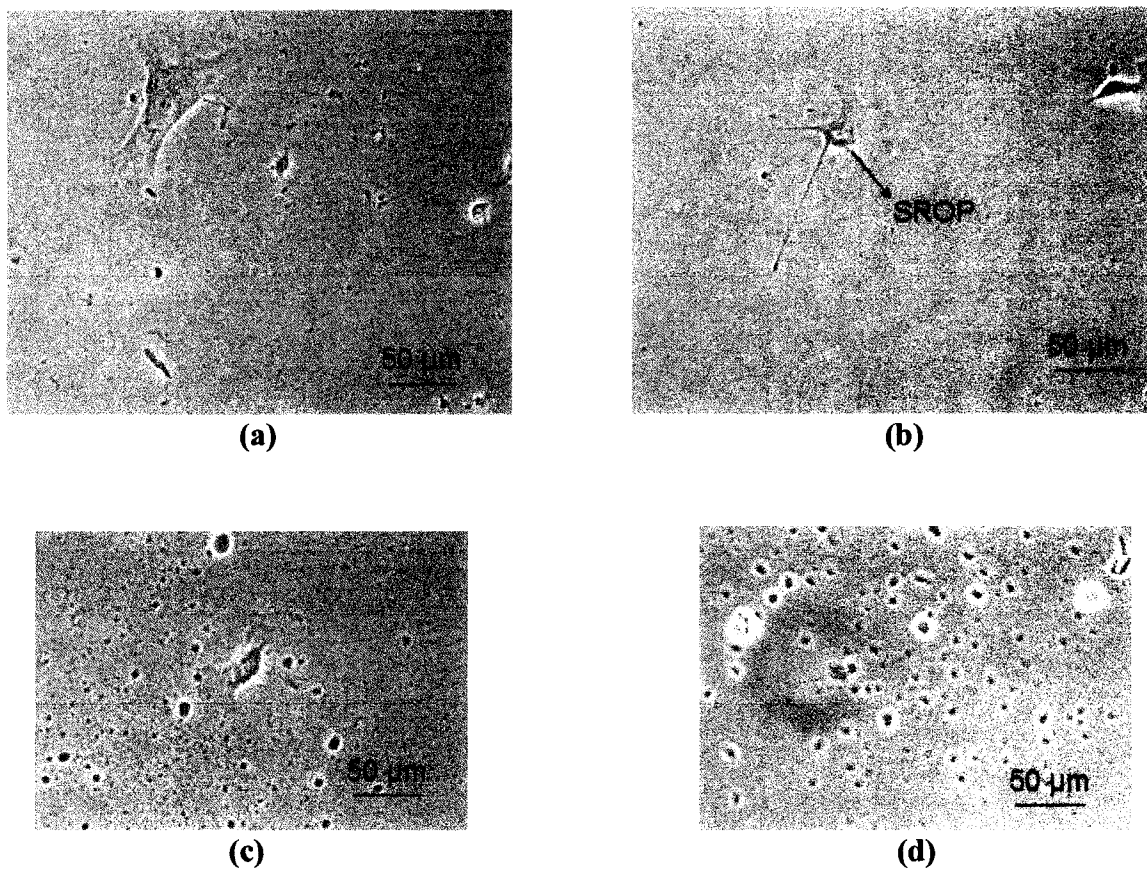


Figure 5.13 PBAC on PLL: After 34 hours – (a) On monolayer, (b) On bilayers, (c) On trilayers; after 72 hours – (d) On trilayers

#### 5.1.4.10 PBAC on Fibronectin

The chondrocytes on fibronectin (Figure 5.14) exhibit SROP.

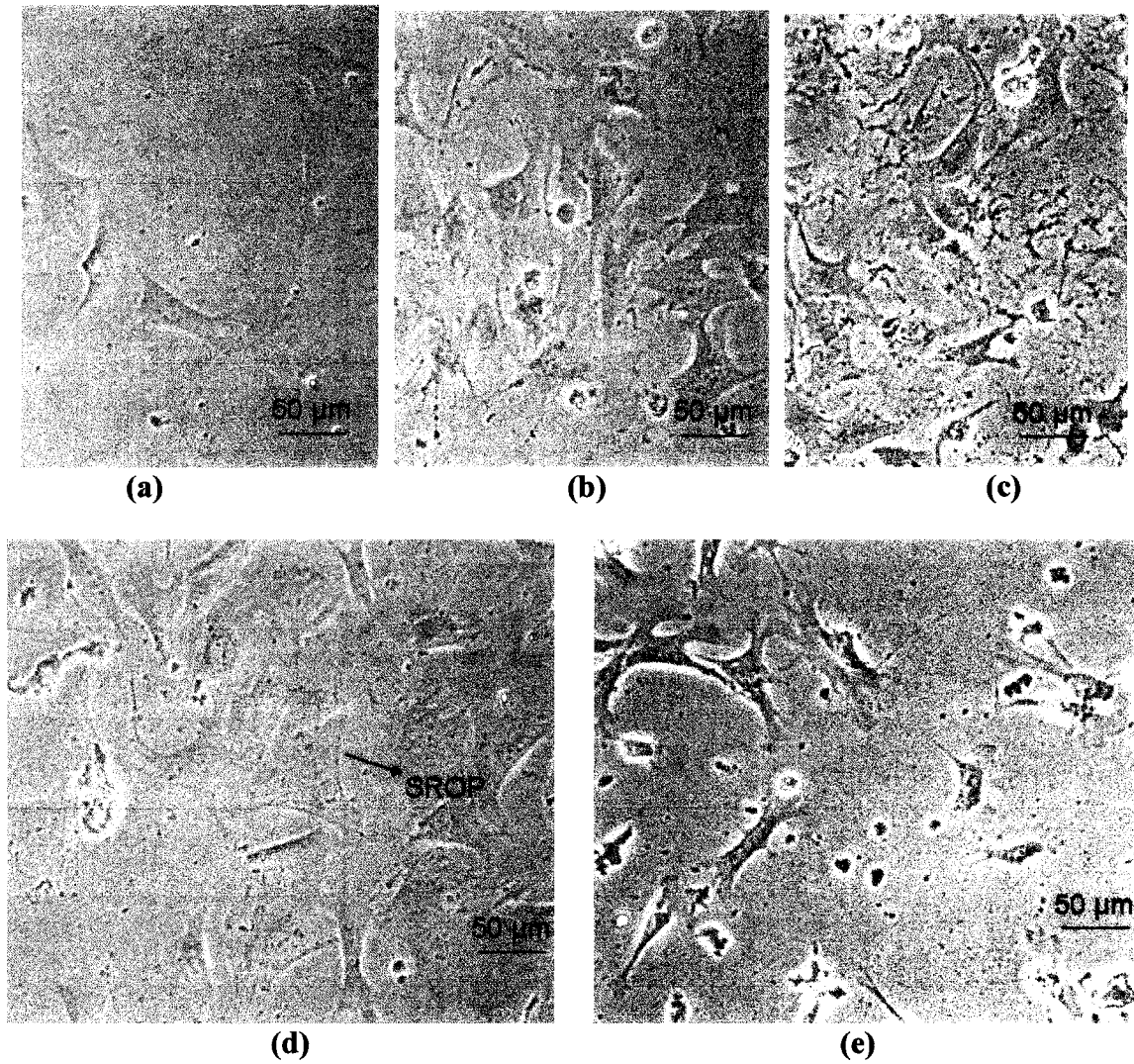


Figure 5.14 PBAC on fibronectin: After 34 hours – (a) On monolayer, (b) On bilayers, (c) On trilayers; after 72 hours – (d) On monolayer, (e) On bilayers.

#### 5.1.4.11 PBAC on PSS

The chondrocytes on PSS (Figure 5.15) show a SROP on all the layers.

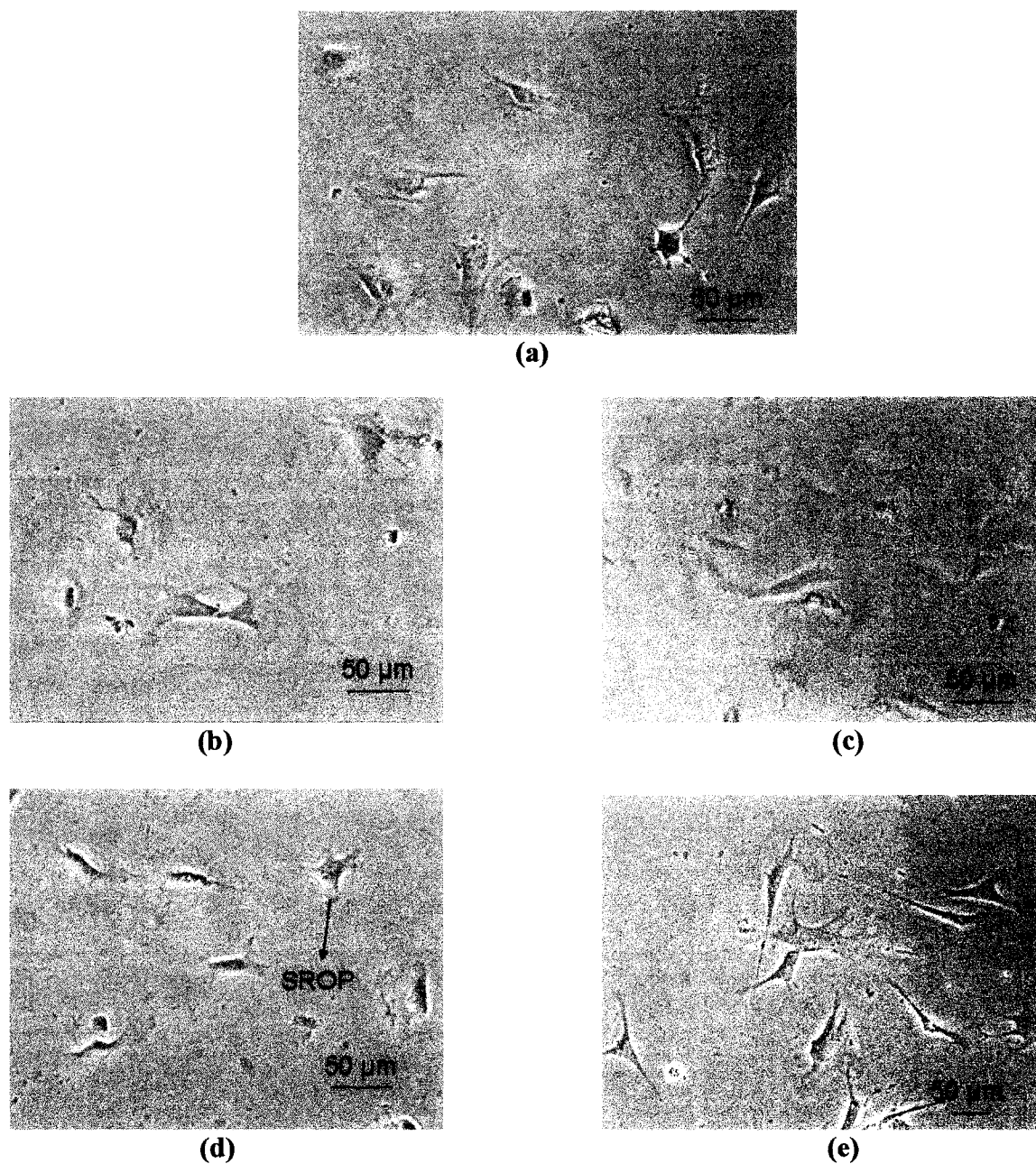


Figure 5.15 PBAC on PSS: After 34 hours – (a) On monolayers (b) On bilayers, (c) On trilayers; after 72 hours – (d) On bilayers, (e) On trilayers.

#### 5.1.4.12 PBAC on Laminin

Cells on laminin (Figure 5.16) exhibit SROP along with their typical characteristics. Lamellopodia and filopodia of the chondrocytes are more pronounced on this material than any other. But these are more pronounced on the bi- and trilayers as compared to monolayers.

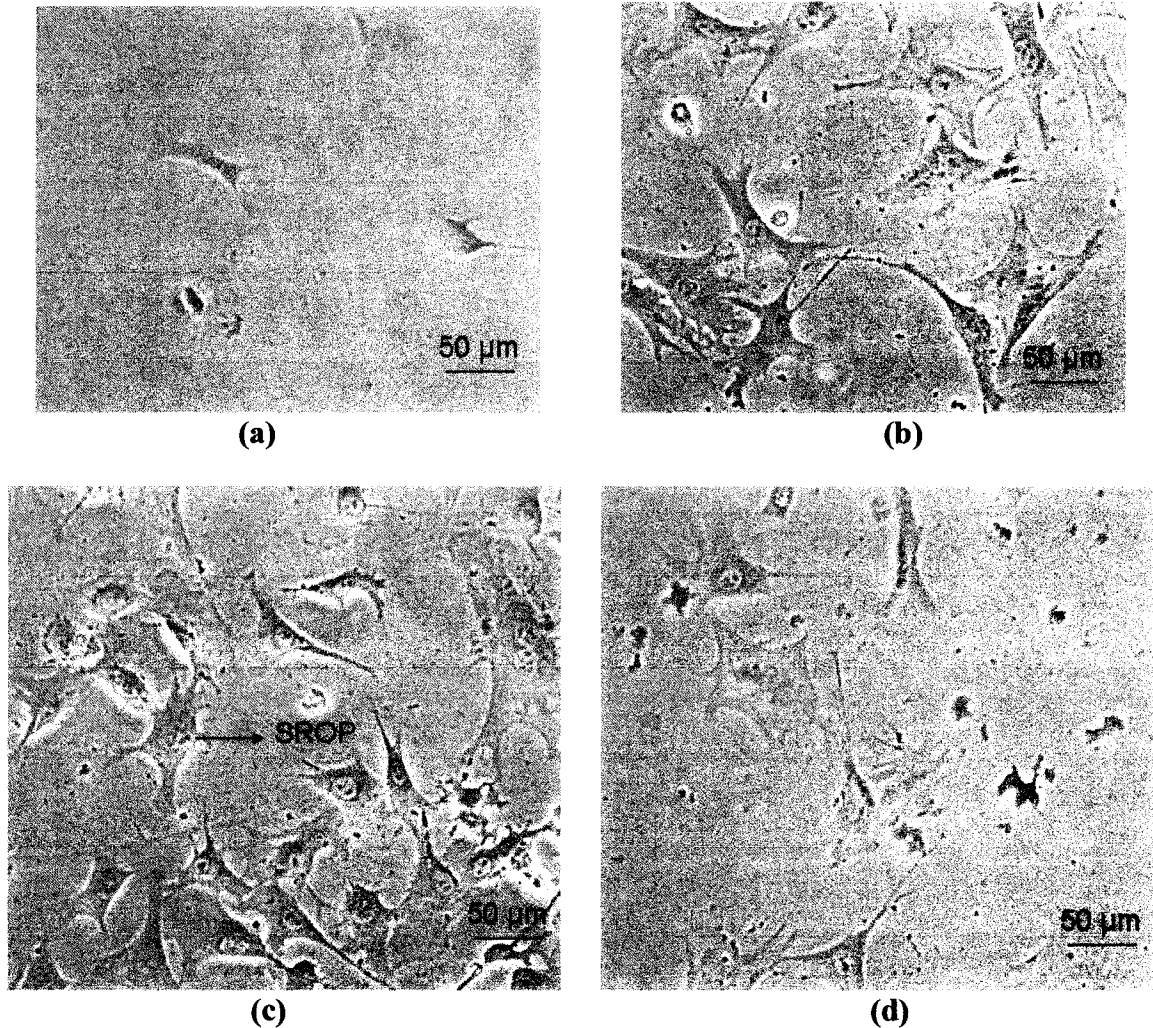


Figure 5.16 PBAC on laminin: After 34 hours – (a) On monolayer, (b) On bilayers, (c) On trilayers; after 72 hours – (d) On bilayers.

Table 5.2 displays the phenotypes observed on monolayer, bilayers, and trilayers of the different biomaterials used in this study. These observations are from a mixture of the images acquired after 34 and 72 hours. It can be observed from the above table that PBAC exhibit slightly rounded to orthogonal phenotype (SROP) on most of the biomaterials. This raises the exciting possibility of the utilization of LbL-assembled multilayer nanofilms for the stabilization of the phenotype of chondrocytes. But there is a necessity of testing the growth of chondrocytes on multilayer nanofilms having more number of bilayers than the ones used in this study. Table 5.2 displays the summary of the morphological observations.

Table 5.2 Summary of morphological observations of phenotypes exhibited by PBAC on monolayer, bilayers, and trilayers (Cell density 1 – 5000 cells/ml).

<b>Biomaterial</b>	<b>Monolayer</b>	<b>Bilayers</b>	<b>Trilayers</b>
PEG-NH <sub>2</sub>	SROP	SROP	SROP
PDDA	SROP	SROP	SROP
BSA	Rounded	Rounded	SROP
PDL	SROP	SROP	Fibroblast
CS	SROP	SROP	SROP
PEI	SROP	SROP	SROP
Collagen	SROP	SROP	SROP
PLL	SROP	SROP	Cell death
Fibronectin	SROP	SROP	SROP
PSS	SROP	SROP	SROP
Laminin	SROP	SROP	SROP

### **5.1.5 Results from Viability Studies on PBAC**

Representative samples of the growth of bovine articular chondrocytes on different materials assessed using Live-dead assay are displayed in Figures 5.17–5.28. Only images of live cells are shown below to highlight the differences in morphology of the cells on different layered nanofilms. All the images displayed below are from the cells seeded at cell density one (5000 cell/ml).



### 5.1.5.1 PBAC on TCPS

Figure 5.17 depicts the PBAC on TCPS. The cells have a fibroblast phenotype.

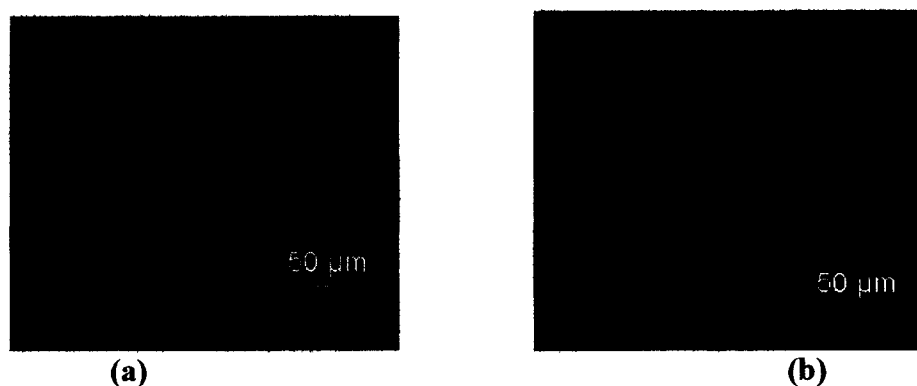


Figure 5.17 (a), (b) Live PBAC on TCPS.

### 5.1.5.2 PBAC on PEG-NH<sub>2</sub>

Cells on PEG-amine (Figure 5.18) have SROP and are well spread. Thus PEG-amine is favorable for the growth and viability of chondrocytes.

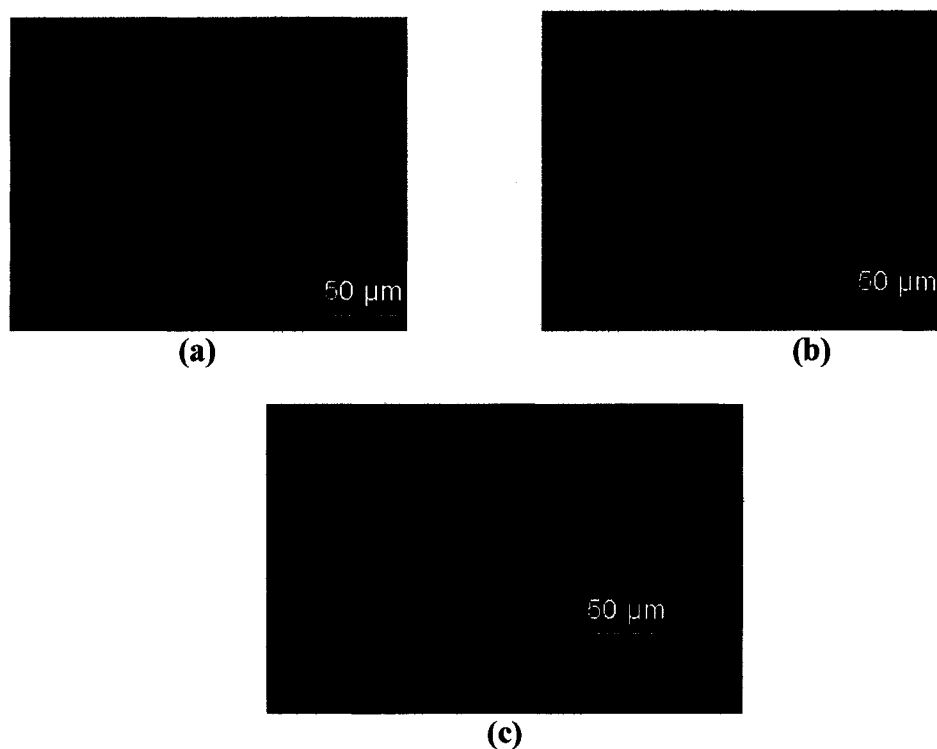


Figure 5.18 Live PBAC on PEG-amine: (a) monolayer, (b) bilayers, (c) trilayers.

### 5.1.5.3 PBAC on PDDA

Figure 5.19 displays the cells on monolayer, bilayers and trilayers of PDDA. Cells on monolayer and trilayers are round and floating, but there are many live cells displaying SROP on bilayers. It can be observed that there is a difference in the size of the chondrocytes in between the different layers. For example, cells on bilayers are bigger in size compared to the cells on monolayer and trilayers.

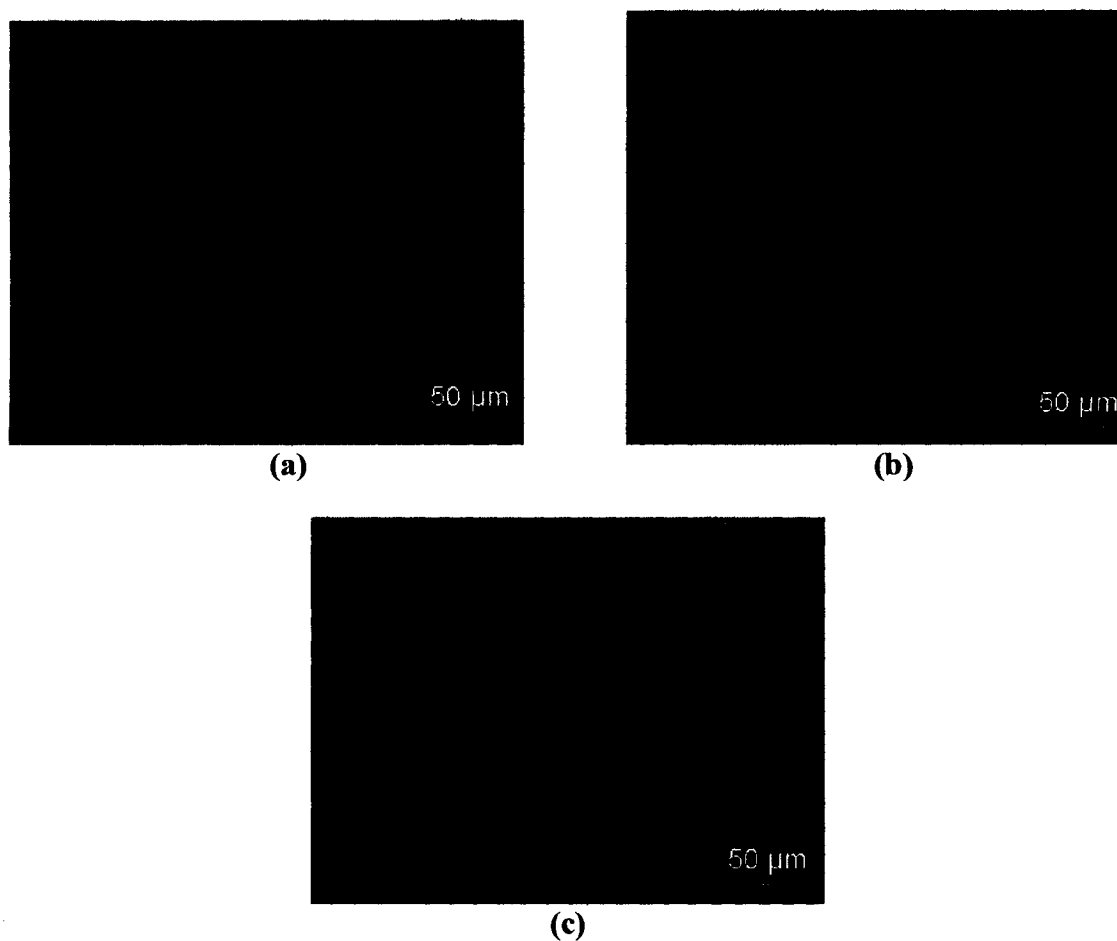


Figure 5.19 Live PBAC on PDDA: (a) monolayer), (b) bilayers, (c) trilayers.

#### 5.1.5.4 PBAC on BSA

Cells on BSA (Figure 5.20) are round and floating in a few wells. Cells on bilayers are better-attached than cells on other layers.

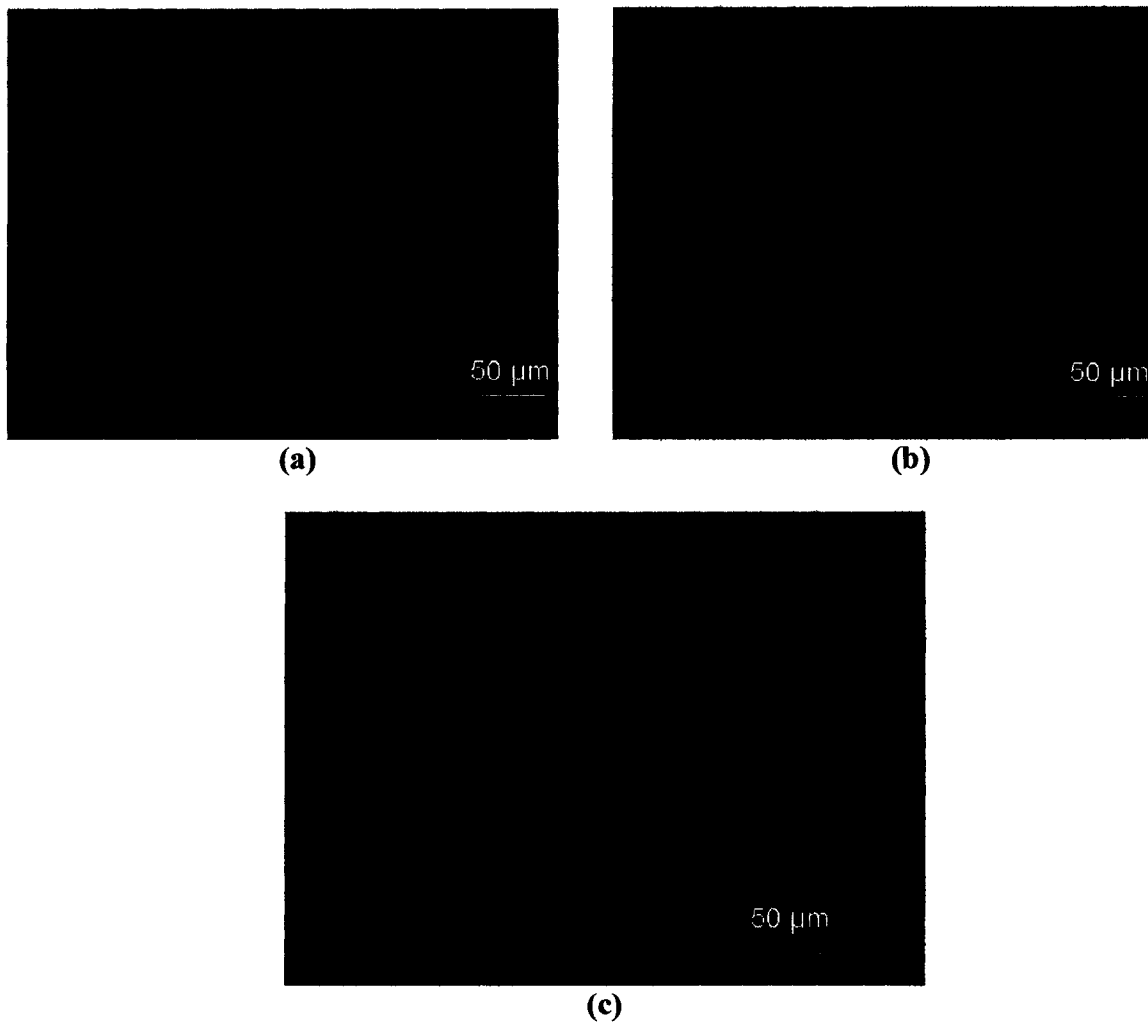


Figure 5.20 Live PBAC on BSA: (a) monolayer, (b) bilayers, (c) trilayers

### 5.1.5.5 PBAC on PDL

Cells on PDL (Figure 5.21) have more SROP than PEG-amine, are well attached and wide spread. It can be observed that the highest number of cells is on trilayers which display fibroblast phenotype while there are very few cells on bilayers.

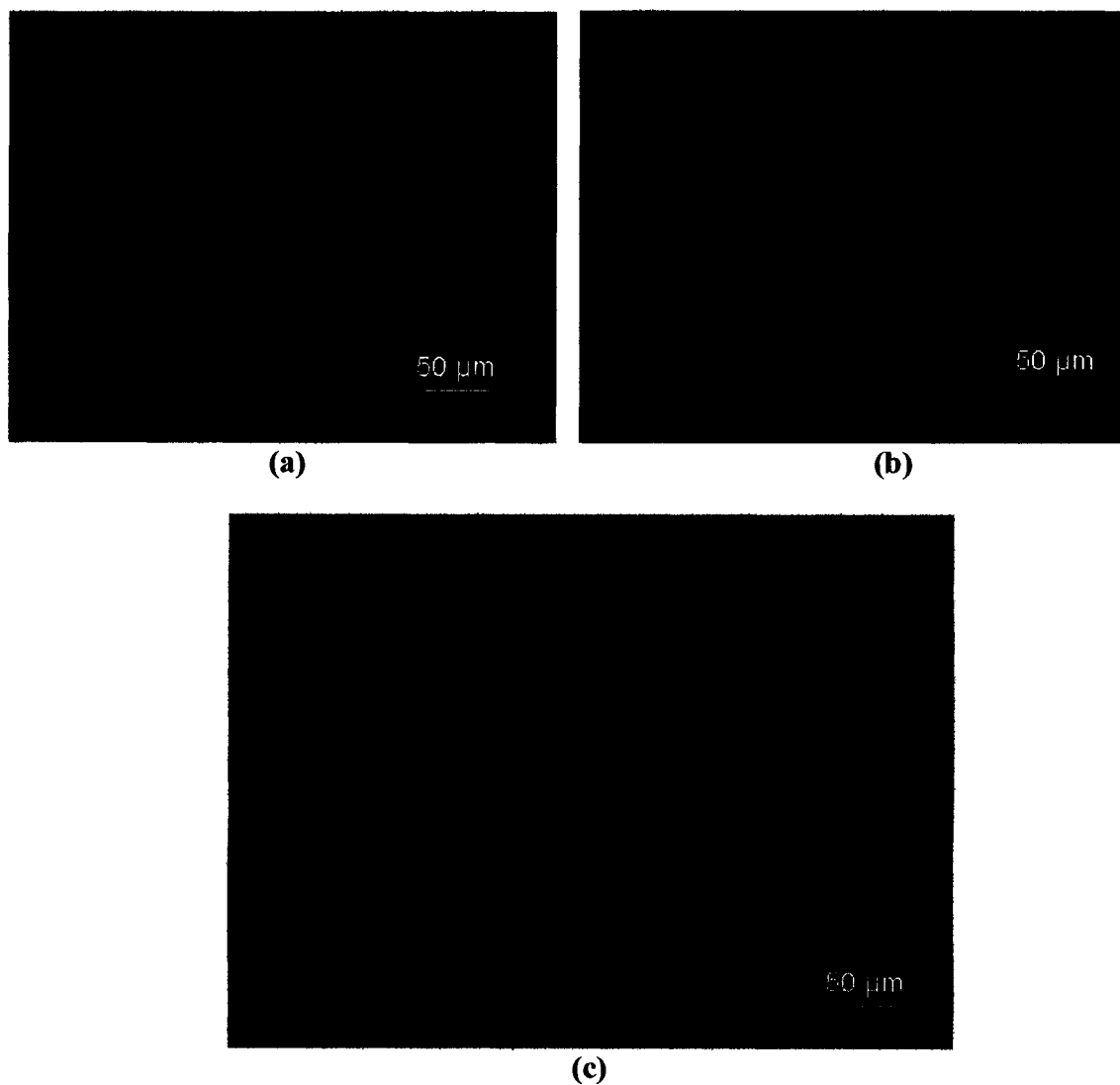


Figure 5.21 Live PBAC on PDL: (a) monolayer, (b) bilayers, (c) trilayers.

### 5.1.5.6 PBAC on CS

Cells on CS (Figure 5.22) are well attached and widespread. There are a few rounded cells, and some of the cells display SROP. The cellular extensions are longer and in some ways resemble cells on laminin. Cell viability is greater indicating that chondroitin sulfate is more favorable for chondrocyte growth and viability.

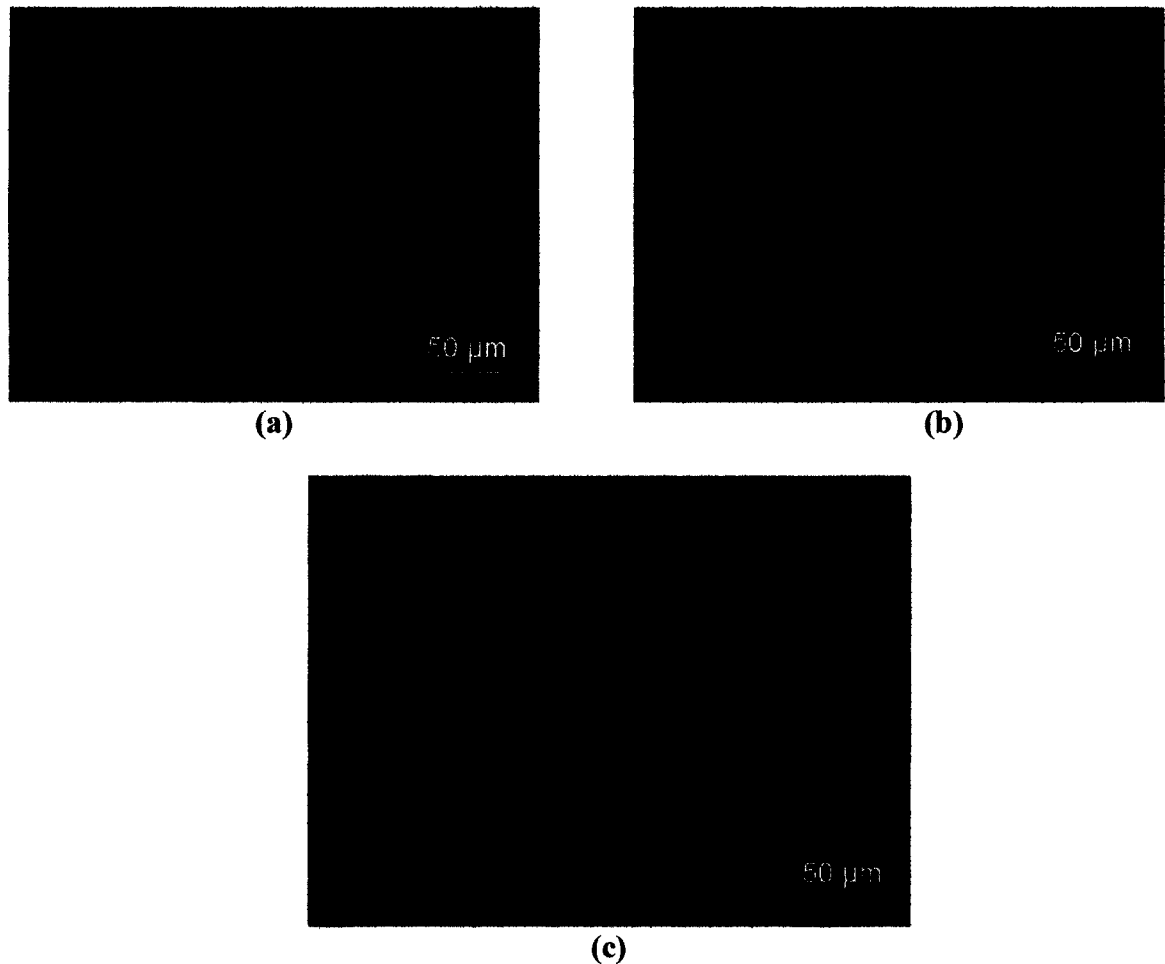


Figure 5.22 Live PBAC on CS: (a) monolayer, (b) bilayers, (c) trilayers.

### 5.1.5.7 PBAC on PEI

Cells on PEI (Figure 5.23) are well attached; display SROP and well spread in most cases indicating that PEI is favorable for chondrocyte growth and viability.

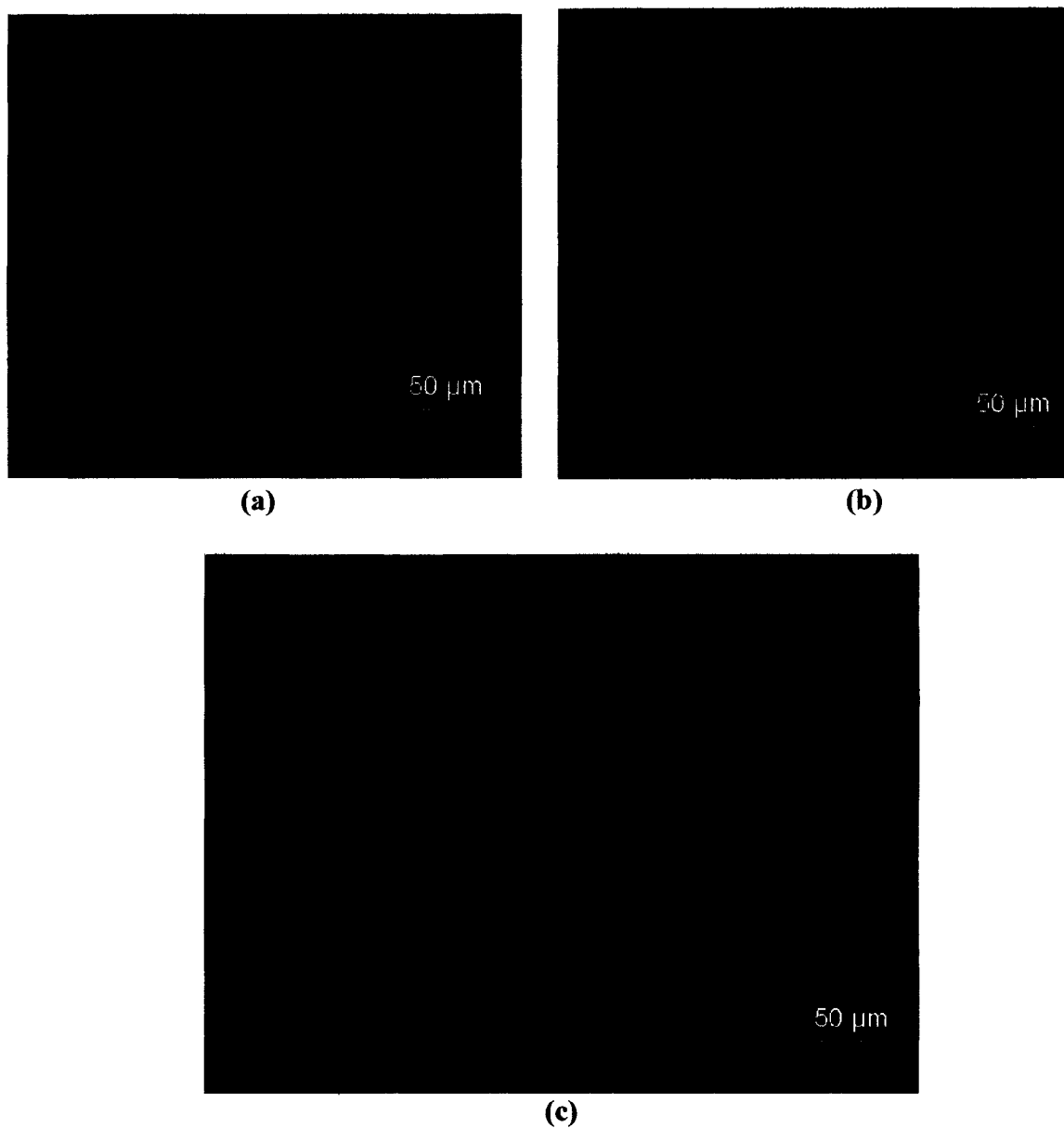


Figure 5.23 Live PBAC on PEI: (a) monolayer, (b) bilayers, (c) trilayers.

### 5.1.5.8 PBAC on Collagen

Cells on monolayer and bilayers of collagen (Figure 5.24) are few in number while there is a large number of cells present on the trilayers. It can be observed that cells on the trilayers are well-attached and show SROP.

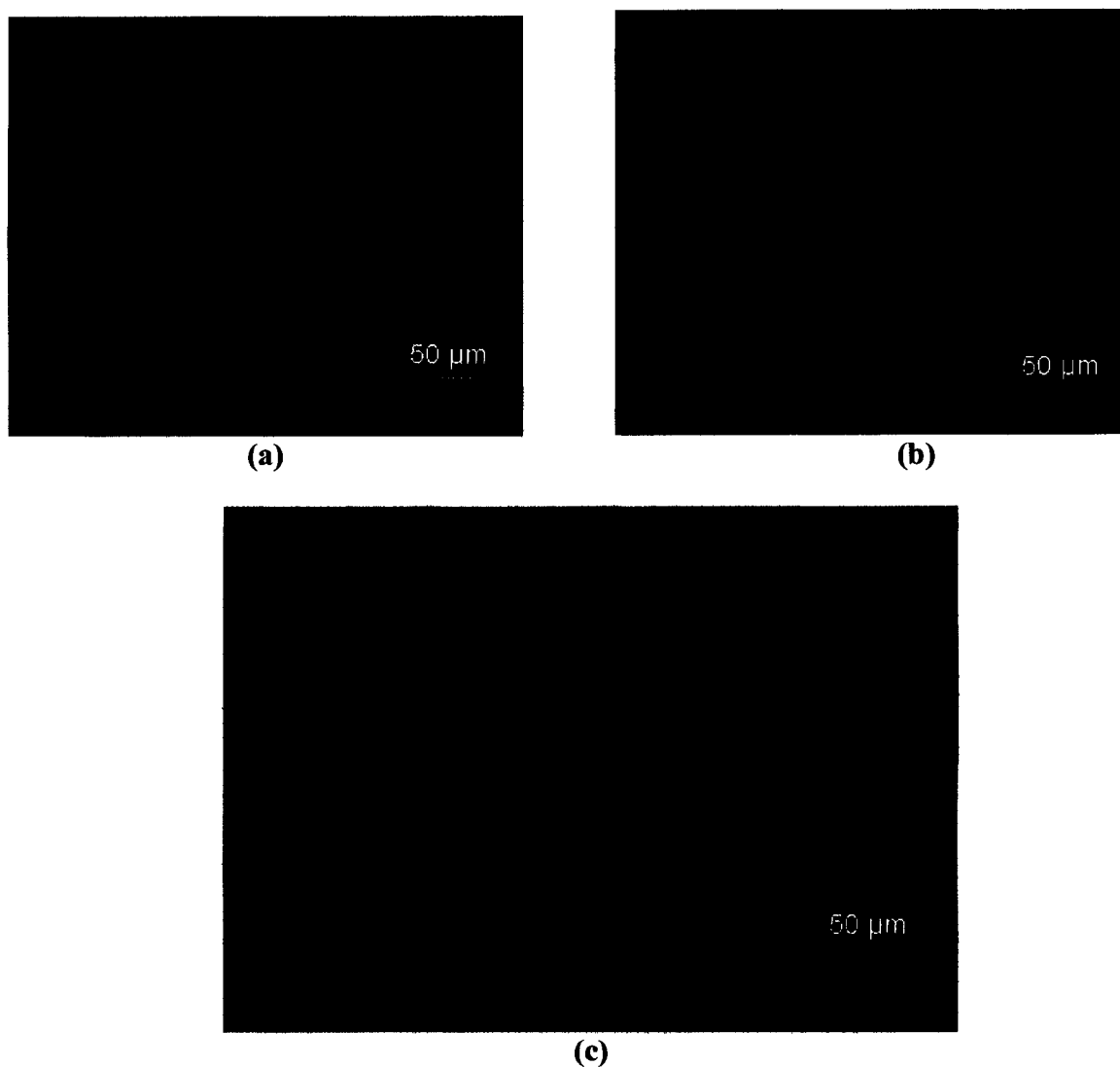


Figure 5.24 Live PBAC on Collagen: (a) monolayer, (b) bilayers, (c) trilayers.

### 5.1.5.9 PBAC on PLL

Cells on PLL (Figure 5.25) display SROP, are well attached and wide spread. Cells display slightly longer extensions on this material as well. Cell viability is more indicating that PLL is favorable for chondrocyte growth and viability. Cells on bilayers appear to be bigger in size compared to the cells on other layers.

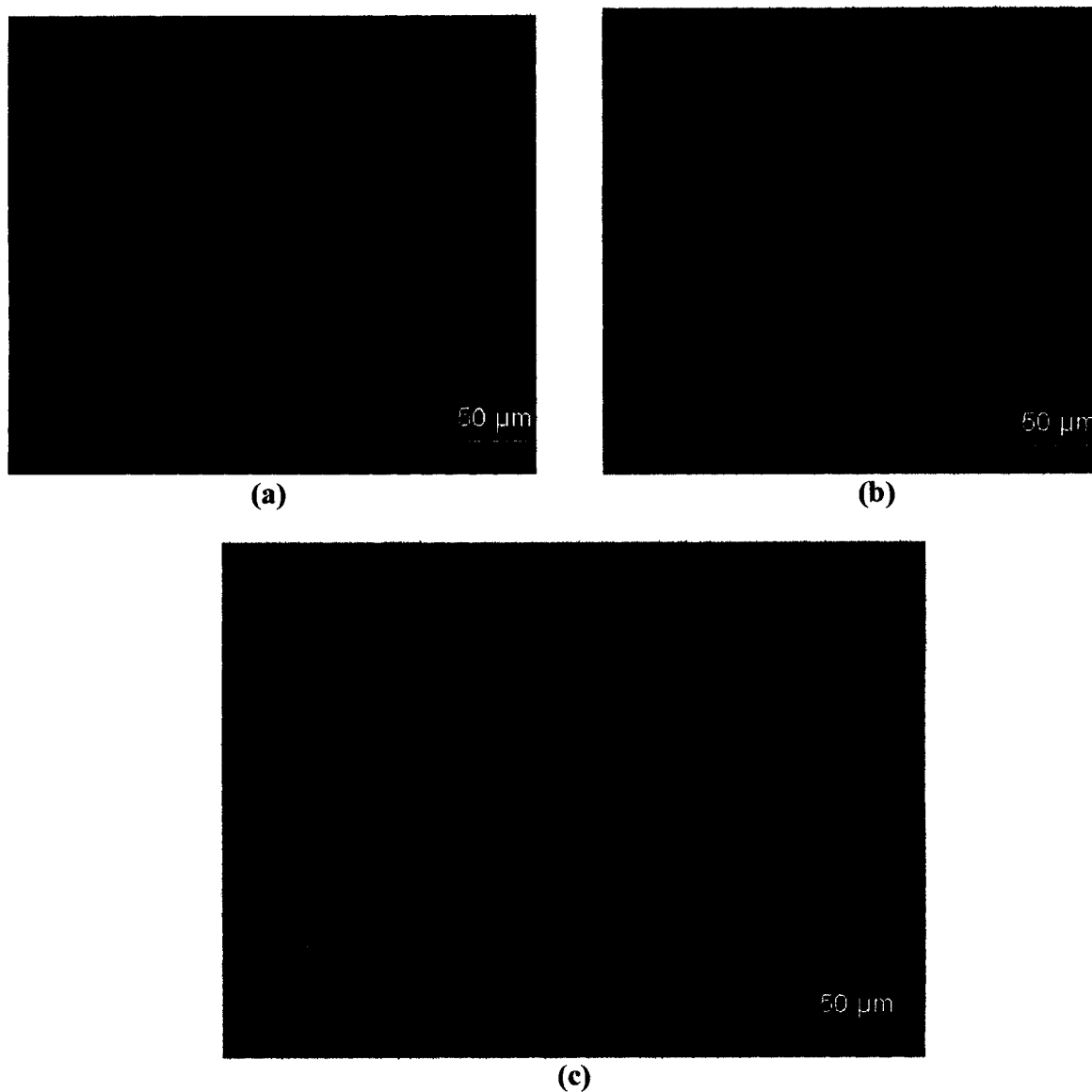


Figure 5.25 Live PBAC on PLL: (a) monolayer, (b) bilayers, (c) trilayers



### 5.1.5.10 PBAC on Fibronectin

Cells on fibronectin (Figure 5.26) display SROP, are well attached and widespread. Cell viability is the best among all the materials indicating that fibronectin is the most favorable for chondrocyte growth and viability.

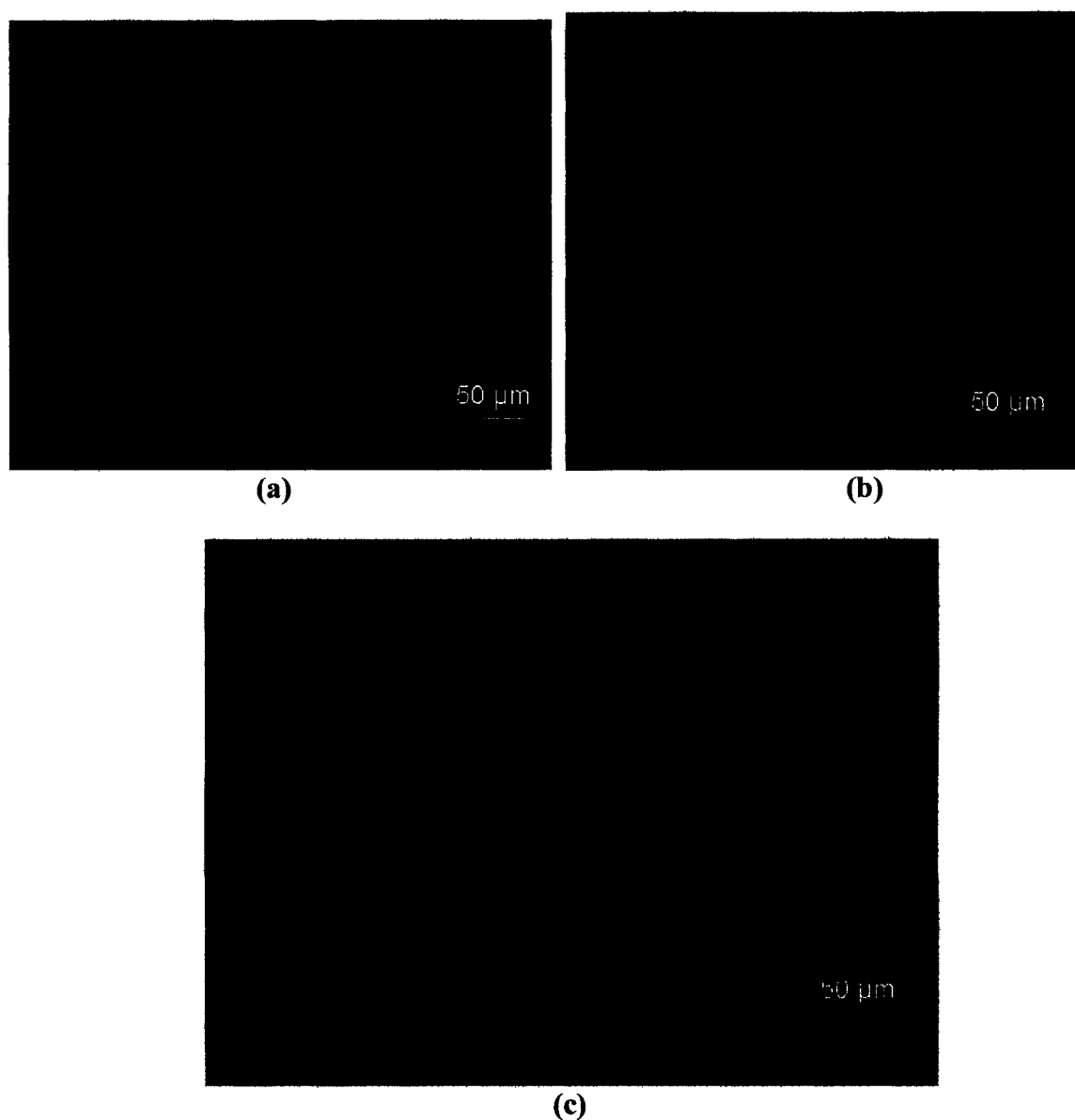


Figure 5.26 Live PBAC on Fibronectin: (a) monolayer, (b) bilayers, (c) trilayers.

### 5.1.5.11 PBAC on PSS

Cells on PSS (Figure 5.27) display SROP, are attached and well spread in most cases indicating that PSS is favorable for chondrocyte growth and viability. The cells on the bilayers are bigger in size compared to the cells on monolayer and trilayers.

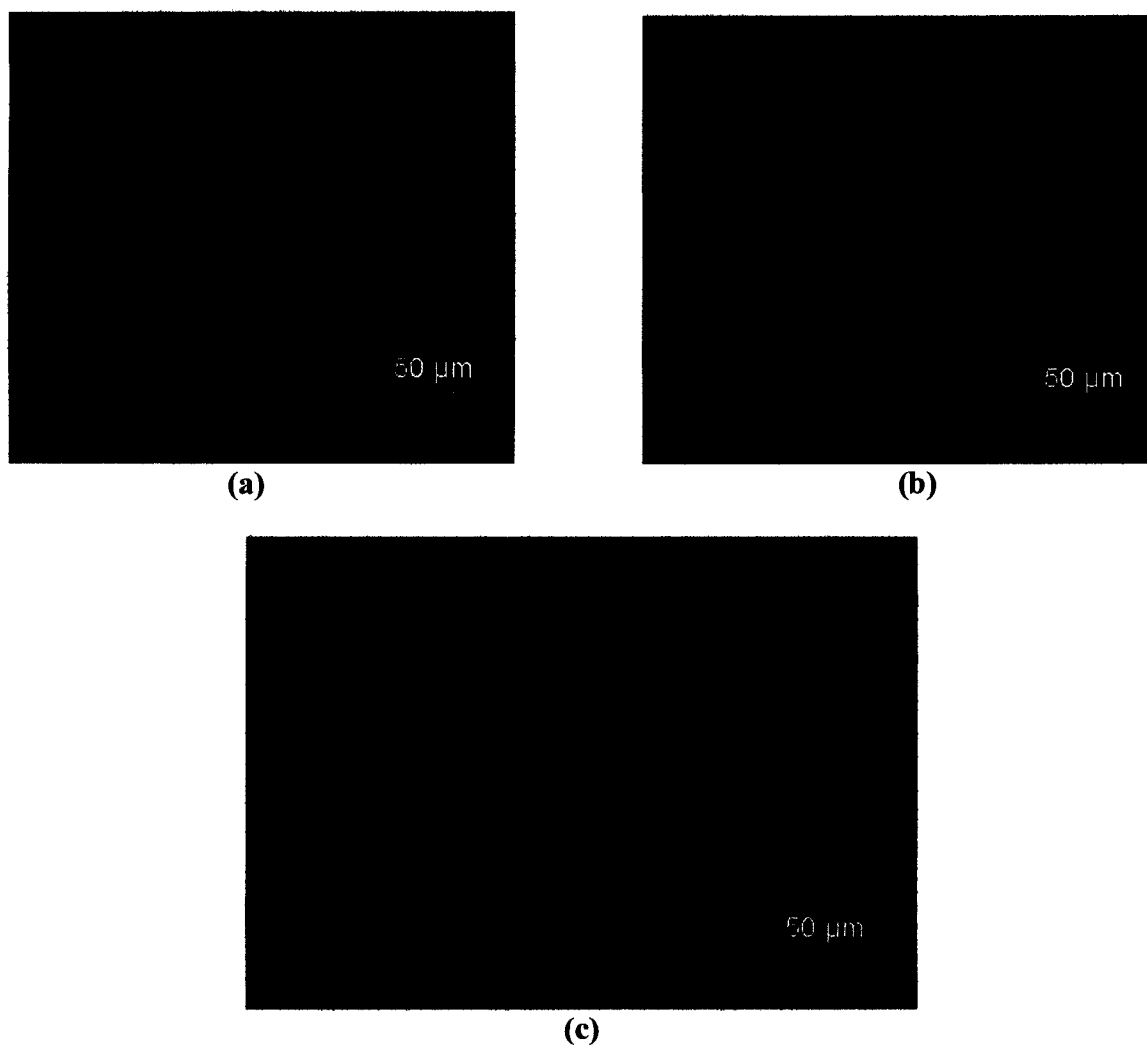


Figure 5.27 Live PBAC on PSS: (a) monolayer, (b) bilayers, (c) trilayers.

### 5.1.5.12 PBAC on Laminin

Cells on laminin (Figure 5.28) are attached in some cases and display SROP on monolayer and bilayers. There were a large number of dead cells on trilayers hence they have been displayed here.

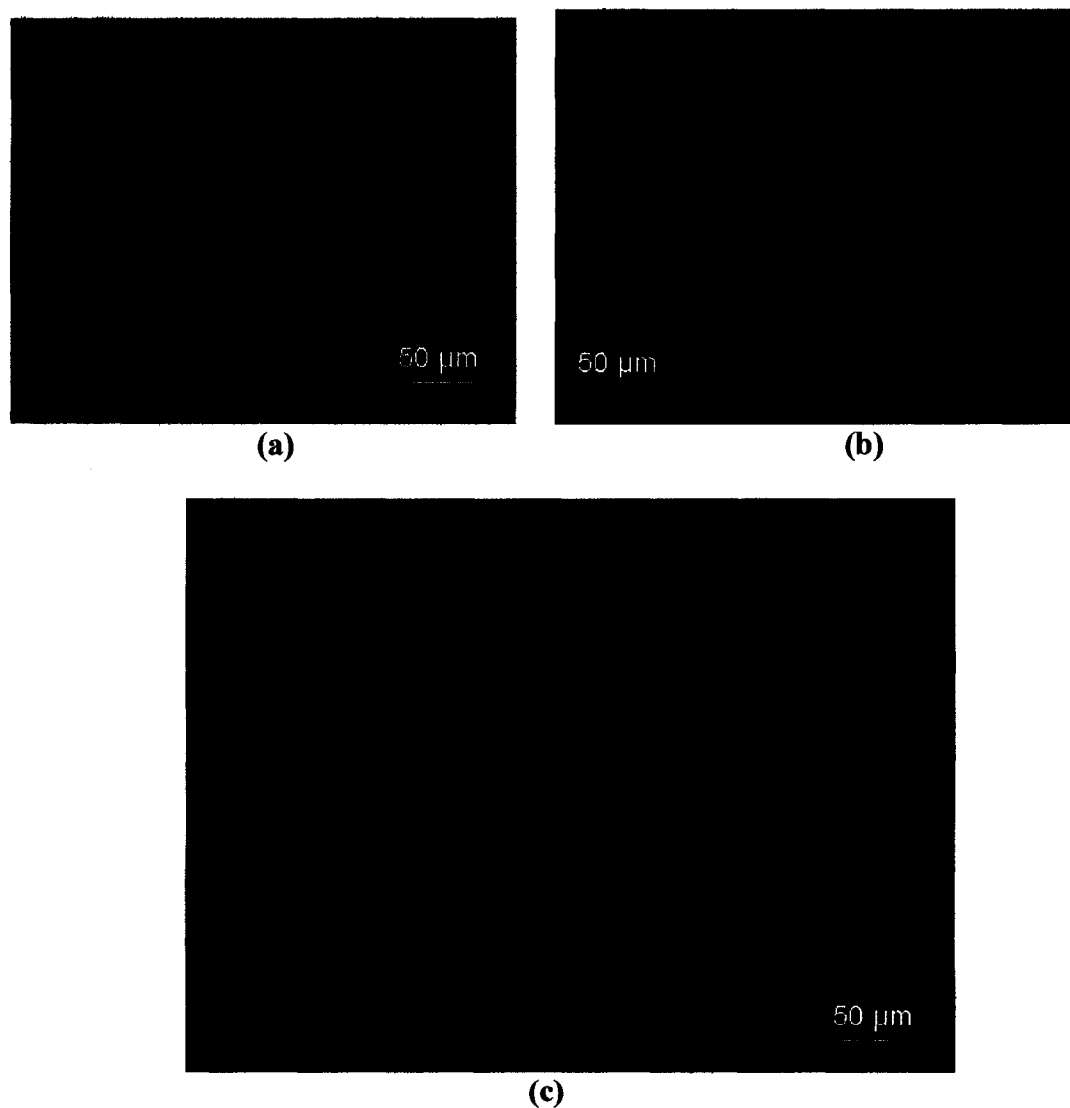


Figure 5.28 Live PBAC on laminin: (a) monolayer, (b) bilayers; dead PBAC on laminin: (c) trilayers.

PBAC grew on all the LbL-modified biomaterials favorably. Morphological observations indicated that all the biomaterials tolerated the chondrocytes fairly well. On most of the biomaterials tested, chondrocytes exhibited slightly rounded to orthogonal

phenotype (SROP). On some of the materials, the chondrocytes showed a rounded morphology for a few days after seeding.

The most important observations were that cells on bilayers of PDDA, PLL and PSS were bigger in size as compared to cells on layers of PDDA, PLLA and PSS. Also cells on bilayers of BSA showed better cell attachment when compared to cells on other layers of BSA. From the live/dead morphological observations, it is suggested that PEG-amine, PDL, chondroitin sulfate, PEI, PLL, fibronectin and PSS were more favorable for the growth and viability of chondrocytes than other materials used and were even an improvement over the control (TCPS). Table 5.3 summarizes the morphological observations of Live-Dead Images.

Table 5.3 Summary of morphological observations of phenotypes exhibited by PBAC after Live-Dead Analysis on monolayer, bilayers, and trilayers (Cell density 1 – 5000 cells/ml).

<b>Biomaterial</b>	<b>Monolayer</b>	<b>Bilayers</b>	<b>Trilayers</b>
PEG-NH <sub>2</sub>	SROP	SROP	SROP
PDDA	Rounded	SROP	Rounded
BSA	Rounded	SROP	Rounded
PDL	SROP	SROP	Fibroblast
CS	SROP	SROP	SROP
PEI	SROP	SROP	SROP
Collagen	Rounded	Rounded	SROP
PLL	SROP	SROP	SROP
Fibronectin	SROP	SROP	SROP
PSS	SROP	SROP	SROP
Laminin	SROP	SROP	Cell death

### 5.1.6 Live/Dead Data

Figures 5.29 – 5.31 depict the viability of the PBAC seeded at the densities of 5000, 15000, and 25000 cells/ml respectively.

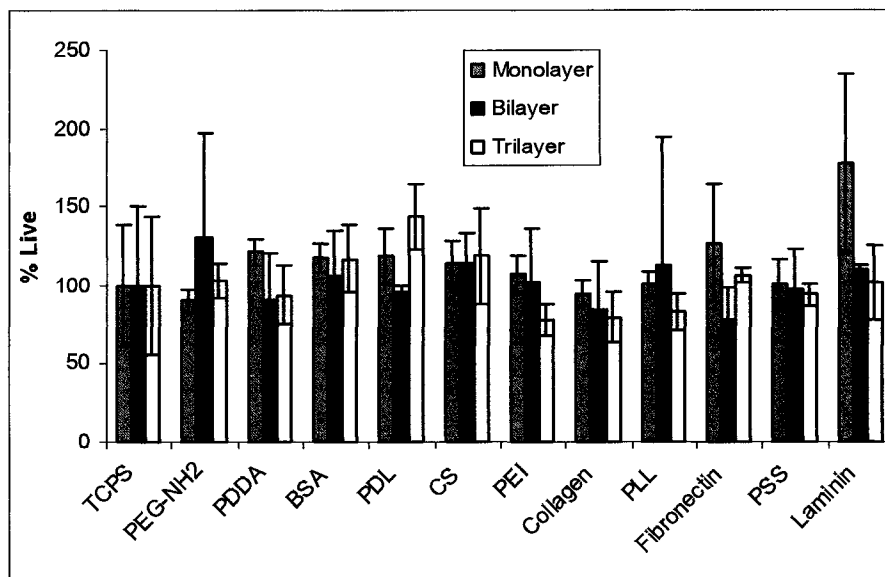


Figure 5.29 Viability exhibited by PBAC on different biomaterials at Cell Density 1 (5000 cells/ml).

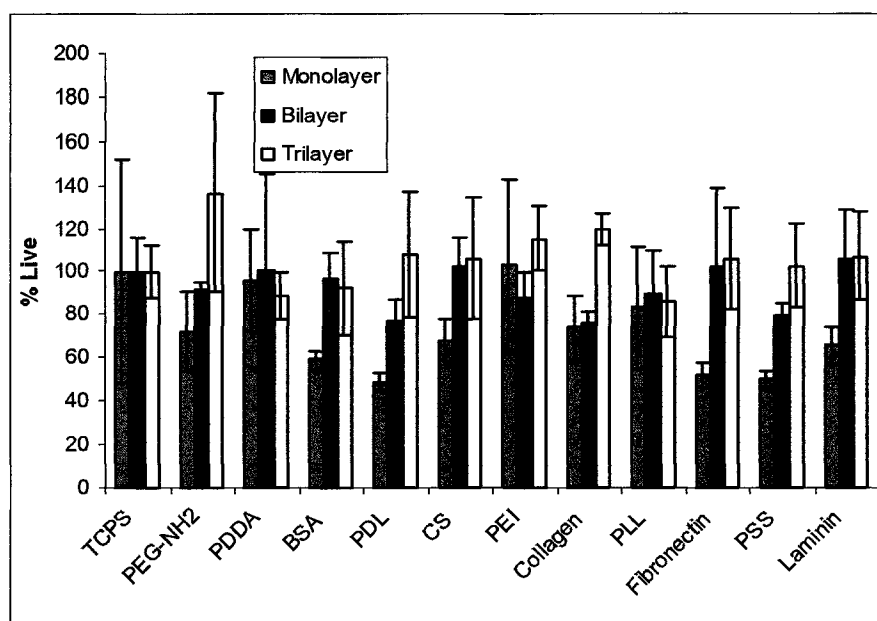


Figure 5.30 Viability exhibited by PBAC on different Biomaterials at Cell Density 2 (15000 cells/ml).

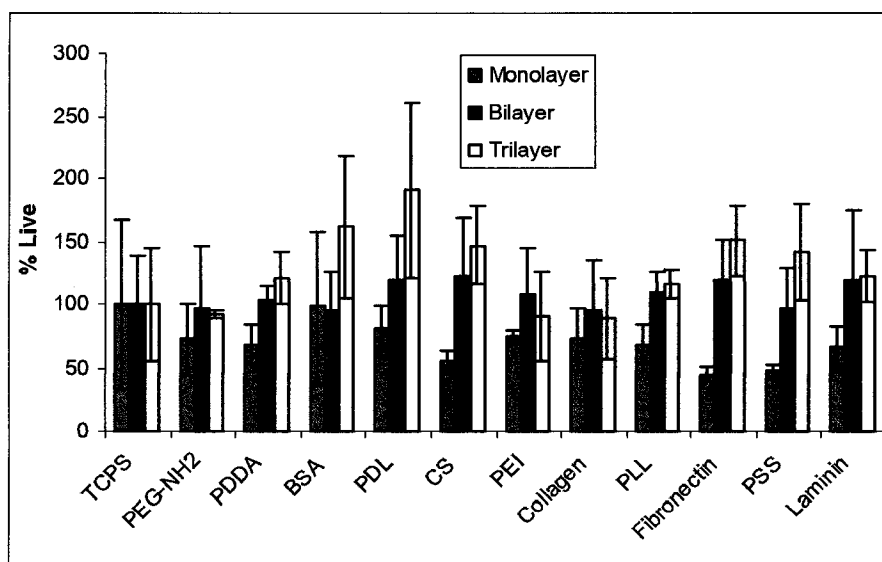


Figure 5.31 Viability exhibited by PBAC on different biomaterials at Cell Density 3 (25000 cells/ml).

#### 5.1.6.1 Cell Density One (5000 cells/ml)

CS exhibits increasing viability of the cells with increasing number of layers at cell density one. Many materials like PEI, PSS, collagen and laminin actually exhibit a decrease in viability with increase in the number of layers. The standard deviations were high for some of the materials for specific types of layers. For example, PEG-NH<sub>2</sub> and PLL exhibited high standard deviation while laminin exhibits the same for monolayers. It has to be noted that all of the materials which exhibit high standard deviations are proteins and polypeptides. At the same time, laminin shows the least standard deviation for bilayers. PEG-NH<sub>2</sub> and PLL show an increase in viability only for bilayers while PDDA, BSA, PDL and fibronectin show a decrease in viability for bilayers compared to other layers.

#### 5.1.6.2 Cell Density Two (15000 cells/ml)

Many biomaterials like PEG-NH<sub>2</sub>, PDL, CS, collagen, fibronectin, PSS and laminin show increasing viability of the cells with increasing number of layers. No

material exhibits decreasing viability with increasing number of layers. PDDA, BSA, PLL – these materials exhibit increased viability for bilayers while PEI shows decreased viability for bilayers. The monolayer for TCPS and trilayers for PEG-NH<sub>2</sub> show high standard deviations.

### **5.1.6.3 Cell Density Three (25000 cells/ml)**

The consistent trend of viability of the cells with increasing number of layers continues here, i.e., cell density three. PDDA, PDL, CS, PLL, fibronectin and PSS show increasing viability with increasing number of layers. Once again as with cell density two, no material is showing decreasing viability with increasing number of layers. The trilayers for BSA and PDL show high standard deviations. PEG-NH<sub>2</sub>, PEI and collagen show an increased viability for bilayers while for BSA, there is a slight decrease in viability for bilayers whereas there is a pronounced increase in the viability for trilayers.

Thus the following biomaterials showed the highest viabilities: Laminin, PEG-NH<sub>2</sub>, PDL, PEI, TCPS, BSA, CS and Fibronectin. Table 5.4 displays the highest viabilities exhibited by PBAC on the different biomaterials.

Table 5.4 Highest viabilities exhibited by PBAC on the different biomaterials.

Density (cells/ml)	Monolayer	Bilayer	Trilayer
5000	Laminin	PEG-NH <sub>2</sub>	PDL
15000	PEI, TCPS	Laminin	PEG-amine
25000	BSA, TCPS	PDL, CS, Fibronectin, Laminin	PDL

Studies with several eukaryotic cells have revealed the benefits of increasing number of layers through LbL on different cellular functions. For example, human

umbilical vein endothelial cells displayed improved activity and cell proliferation on LbL-modified 1-, 3-, and 5- bilayers of aminolyzed poly(L-lactic acid) (PLLA) with chitosan as the outermost layer compared with the control – unmodified, virgin PLLA as well as TCPS. The endothelial cells also displayed good spreading and improved morphology. It was also found that PSS was not as effective as chitosan in promoting cytocompatibility due to either the former's charge repulsion or unfavorable surface chemistry. But in the present study, bovine articular chondrocytes grew reasonably well on PSS and displayed increasing number of live cells for cell densities two and three (15000 and 25000 cells/ml respectively). Previous studies with rabbit ear chondrocytes grown on ECM-like LbL modified PDL have revealed the benefits of LbL assembly. Cell viability, total intracellular protein content, and cell morphology showed improved levels on PEI/gelatin multilayers modified PDL [133, 134].

Apart from agarose gels [136], collagen and alginate gels [257, 258] too have been used to culture chondrocytes. Collagen gels have helped in the achievement of the chondrocyte phenotype though only for short time periods [258]. Specifically, bovine articular chondrocytes which are the topic of the present study maintained their phenotype and proliferated on collagen gels [259]. Also it was proved that bovine articular chondrocytes maintained a better phenotype on floating type I collagen compared with attached or monolayer collagen gels [260]. The Live-Dead viability results in the current study reveal the presence of rounded chondrocytes on a few materials like PDDA, BSA, CS, and collagen. These results suggest that LbL films could be further modified to achieve the rounded phenotype of chondrocytes. To maintain the rounded phenotype, the cells can be removed as soon as they achieve the rounded



phenotype and then transferred onto tissue engineering substrates. This transfer could be done at sub-confluence levels. Also, nanofilms could be incorporated with enzymes and other necessary growth factors to stabilize the rounded phenotype further. The enzymes and other factors could be released in a sequential manner [108-110, 261, 262].

### 5.1.7 Live/Dead Image Analysis

Image J software was used as an adjunct to the Live-Dead viability analysis for counting cells from the Live-Dead Images. Each image was divided into three randomly selected regions, analyzed and the mean of the resultant cell counts obtained. The results (Figures 5.32 – 5.34) for live cells for the different densities and layers are displayed below.

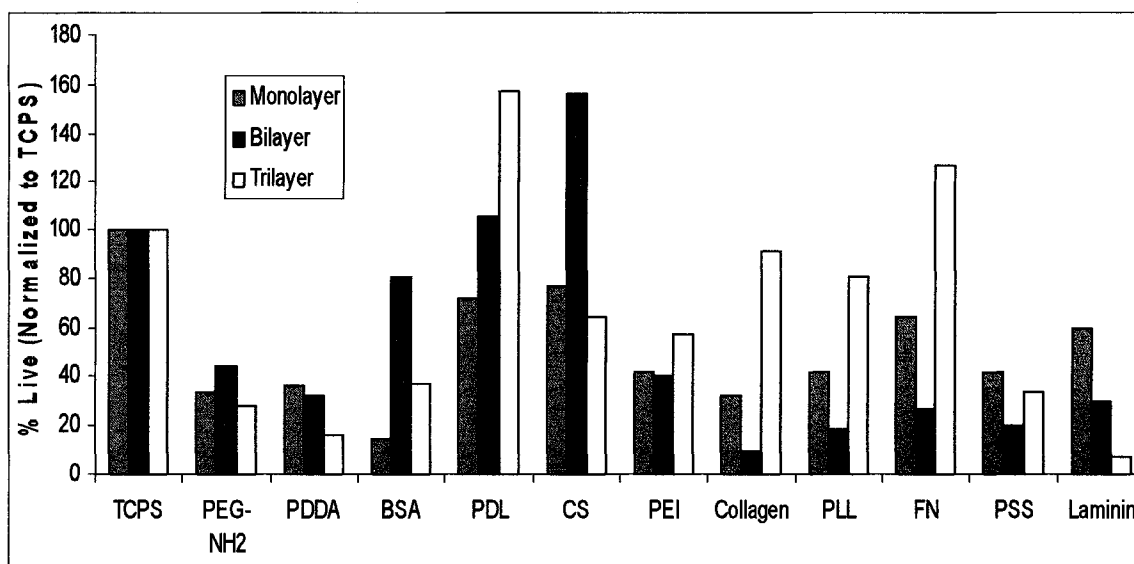


Figure 5.32 Live-Dead Image Analysis results of PBAC on different biomaterials: Cell Density 1 (5000 cells/ml).

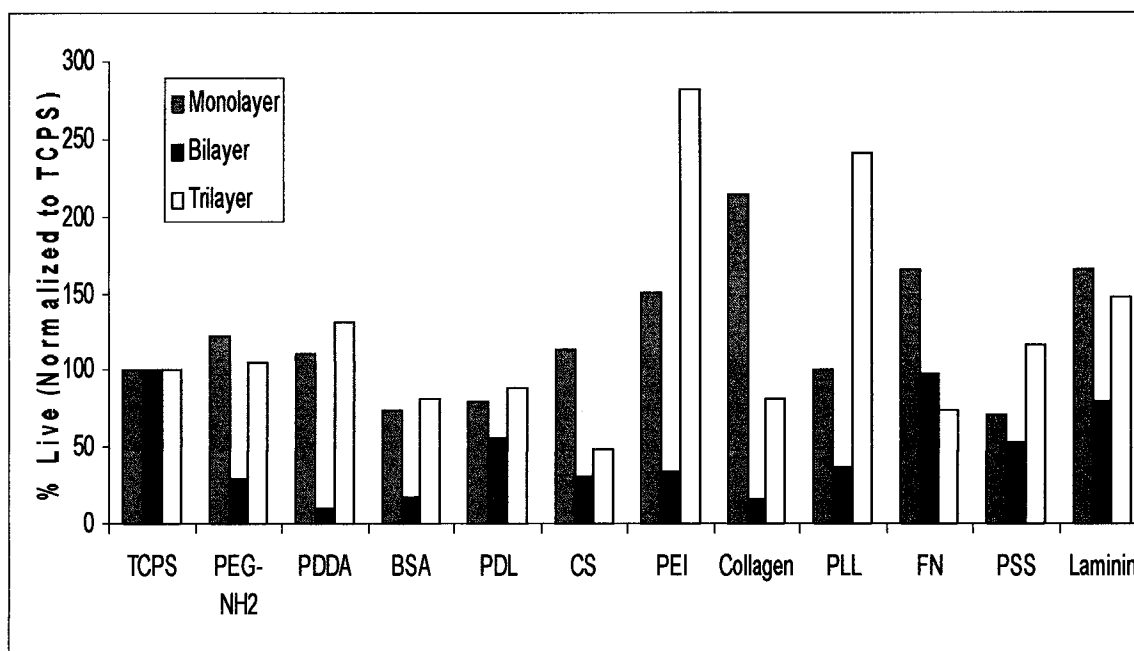


Figure 5.33 Live-Dead Image Analysis results of PBAC on different biomaterials: Cell Density 2 (15000 cells/ml).

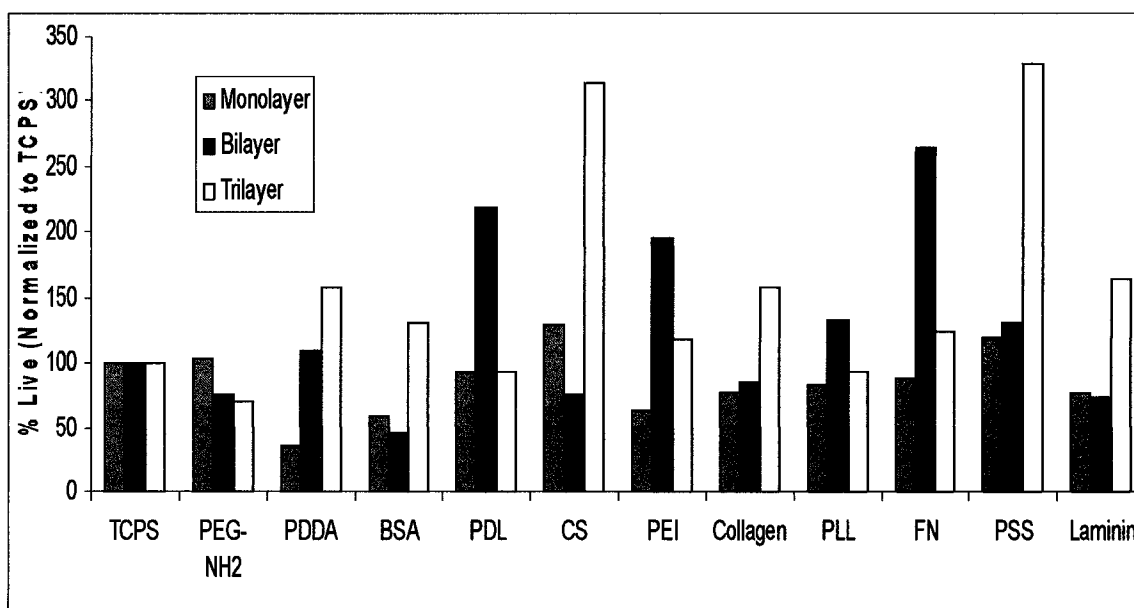


Figure 5.34 Live-Dead Image Analysis results of PBAC on different biomaterials: Cell Density 3 (25000 cells/ml).

#### **5.1.7.1 Cell Density One (5000 cells/ml)**

PDL exhibits increasing number of live cells with increasing layers. PEI, collagen, fibronectin and PSS too exhibit the same behavior: increasing number of live cells with increasing layers except for a slight drop in case of bilayers. Laminin and PDDA exhibit the opposite behavior, decreasing number of cells with increasing layers. In case of PEG-NH<sub>2</sub>, BSA and CS; bilayers exhibit the largest number of live cells. These results are comparable to those obtained from Live-Dead spectrofluorometric analysis.

#### **5.1.7.2 Cell Density Two (15000 cells/ml)**

PDDA, BSA, PDL, PEI, PLL and PSS exhibit an increase in the number of live cells with density but exhibit large drop in numbers for the bilayers, especially PDDA, BSA and PEI. Fibronectin exhibits a steady decline in the number of cells with increasing layers while PEG-NH<sub>2</sub>, CS, collagen and laminin exhibit the same behavior except for a drop in the number of cells for bilayers.

#### **5.1.7.3 Cell Density Three (25000 cells/ml)**

PDDA, collagen and PSS exhibit increasing number of live cells with increasing layers while BSA, CS and laminin exhibit the same behavior except for a drop in the number of live cells for bilayers. In the case of PDL, PEI, PLL and fibronectin, bilayers show the largest number of live cells.

### 5.1.8 MTT Data

Figures 5.35 – 5.37 depict the viability of the PBAC seeded at the densities of 5000, 15000, and 25000 cells/ml respectively.

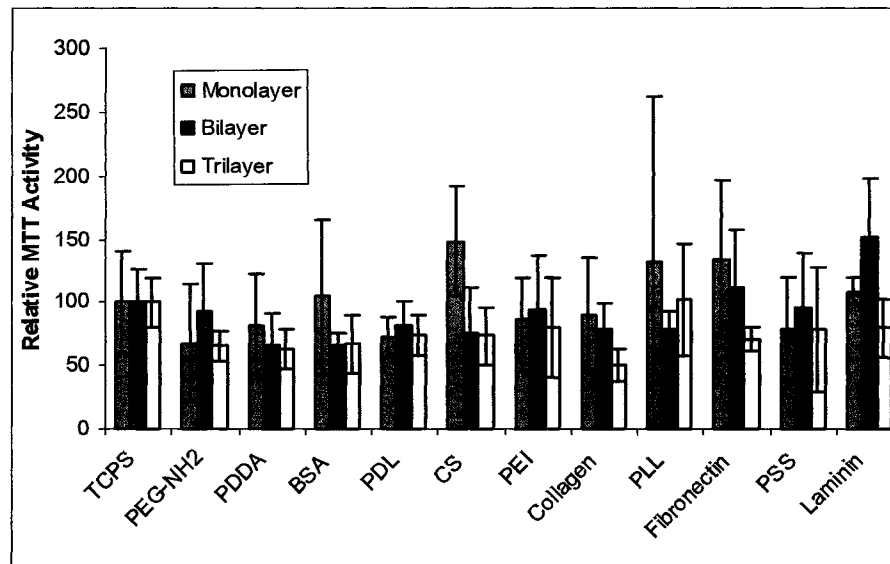


Figure 5.35 Cell metabolic activity exhibited by PBAC on different biomaterials at Cell Density A (500 cells/ml).

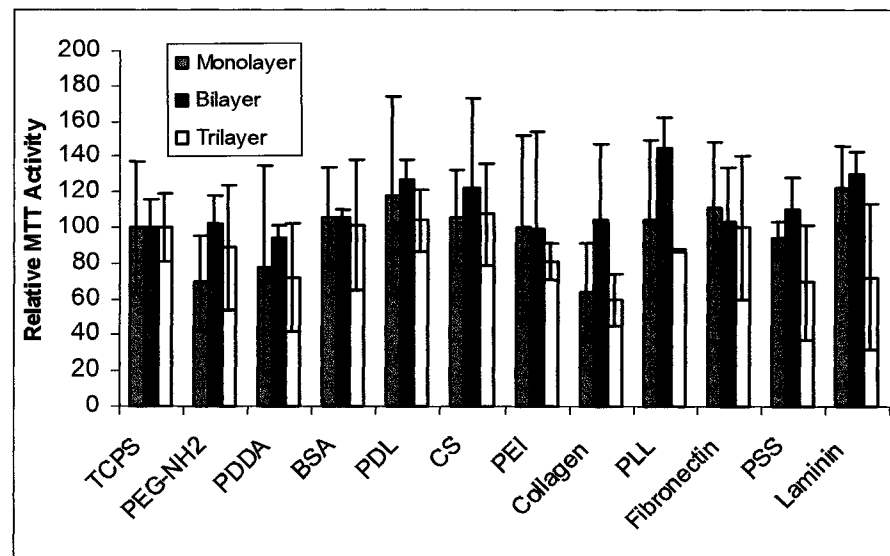


Figure 5.36 Cell metabolic activity exhibited by PBAC on different biomaterials at Cell Density B (1000 cells/ml).

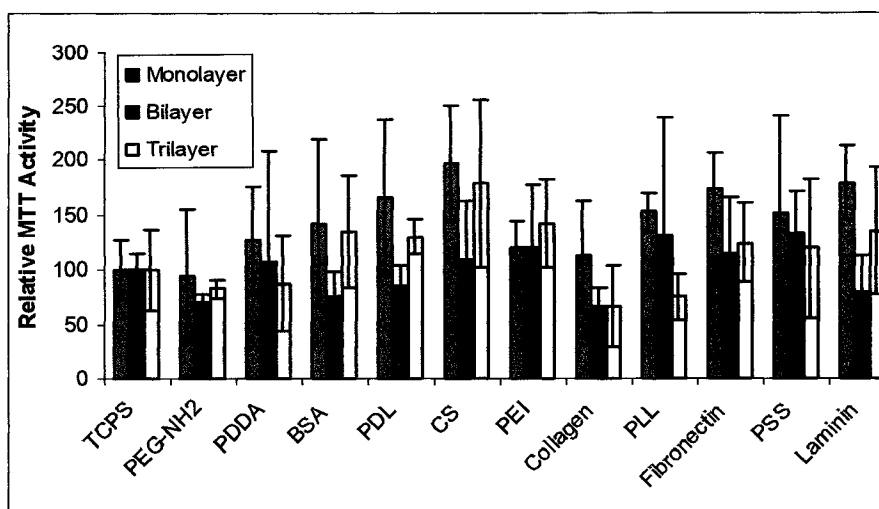


Figure 5.37 Cell metabolic activity exhibited by PBAC on different biomaterials at Cell density C (1500 cells/ml).

#### 5.1.8.1 Cell Density A (500 cells/ml)

PDDA, CS, collagen and fibronectin show decreasing cell metabolic activity with increasing number of layers while BSA shows increased cell metabolic activity for monolayers and nearly equal cell metabolic activity for both bilayers and trilayers. PLL, fibronectin and BSA show high standard deviations for monolayers. Once again it has to be noted that all of the materials which show high standard deviations are proteins and polypeptides. PEG-NH<sub>2</sub>, PDL, PEI, PSS and laminin – all these materials show increased cell metabolic activity for bilayers while PLL shows decreased cell metabolic activity for bilayers.

#### 5.1.8.2 Cell Density B (1000 cells/ml)

PEI and fibronectin showed decreasing cell metabolic activity with increasing number of layers while PEG-NH<sub>2</sub>, PDDA, PDL, CS, collagen, PLL, PSS and laminin showed increased cell metabolic activity for bilayers.

### 5.1.8.3 Cell Density C (1500 cells/ml)

PEI showed increasing cell metabolic activity with increasing number of layers. Decreasing cell metabolic activity with increasing number of layers was observed for PDDA, PLL and PSS. PEG-NH<sub>2</sub>, BSA, PDL, fibronectin and laminin too showed decreasing cell metabolic activity with increasing number of layers, but in all of these materials, monolayers showed the highest cell metabolic activity with the trilayers following and the bilayers showing the least cell metabolic activity. Collagen showed the highest cell metabolic activity for monolayers followed by bilayers and trilayers which showed almost equal cell metabolic activity. Figure 5.37 displays the cell metabolic activity results for cell density C. Thus, the cell metabolic activities varied with both density as well as the number of layers underscoring the importance of both. Only for density C, one can observe a consistent result for all the three layers. Thus the following materials exhibited the highest cell metabolic activities-CS, laminin, PLL, TCPS, fibronectin, PDL and BSA. Table 5.5 displays the highest cell metabolic activities of PBAC on the different biomaterials.

Table 5.5 Highest cell metabolic activities exhibited by PBAC on the different biomaterials.

Density (cells/ml)	Monolayer	Bilayer	Trilayer
500	CS	Laminin	PLL, TCPS
1000	Laminin	Fibronectin	PDL, BSA, CS and TCPS
1500	CS	CS	CS

### 5.1.9 Statistical Analyses

#### 5.1.9.1 Live-Dead Assay

Table 5.6 displays the various statistics obtained by performing three-way ANOVA and Tukey analyses using SAS.

Table 5.6 Statistical analysis results of Live-Dead Assay on PBAC.

<b>3-Way ANOVA Statistic</b>	<b>Density</b>	<b>Material</b>	<b>Layer</b>
2.53 (<.0001)	43.98 (<.0001)	1.17 (0.3064)	6.34 (0.0021)
<b>DensityxMaterial</b>	<b>DensityxLayer</b>	<b>MaterialxLayer</b>	<b>DensityxMaterialxLayer</b>
1.25 (0.2077)	13.14 (<.0001)	1.69 (0.0315)	0.90 (0.6491)

**Note:** Each value represents the F-Statistic with the P-Value in brackets.

The above results of the statistical analyses reveal no significant three-way interactions among density, biomaterial and layers for the Live-Dead Assay Data. But the interactions between density and layer, material and layer are significant.

#### 5.1.9.2 MTT Assay

Table 5.7 displays the various statistics obtained by performing three-way ANOVA and Tukey analyses using SAS.

Table 5.7 Statistical analysis results of MTT Assay on PBAC.

<b>3-Way ANOVA Statistic</b>	<b>Density</b>	<b>Material</b>	<b>Layer</b>
1.11 (0.2553)	2.38 (0.0949)	3.00 (0.001)	3.08 (0.0479)
<b>DensityxMaterial</b>	<b>DensityxLayer</b>	<b>MaterialxLayer</b>	<b>DensityxMaterialxLayer</b>
0.61 (0.9171)	5.73 (0.0002)	0.67 (0.8691)	0.55 (0.9902)

**Note:** Each value represents the F-Statistic with the P-Value in brackets.

There are no three way-interactions between density, material and layer for the MTT assay. The interactions between density and layer are significant for this assay.

The above results indicate the importance of multilayers on cell behavior, more so in the case of viability in this study and the probable requirement of a multilayer configuration with more number of layers like 5-, 10-, and 20-bilayers which may lead to the achievement of the elusive rounded phenotype of the chondrocytes. With this aim in mind, multilayer architectures consisting of 5-, 10-, and 20-bilayers were constructed using LbL. Besides AFM which was used to measure the roughness of the nanofilms, ellipsometry was used to measure the thickness of the various multilayer nanofilms. For the ellipsometric measurements, the films were assembled on silicon wafers.

#### 5.1.10 Biomaterial Thickness Profiles

PEG-NH<sub>2</sub>, PDDA, PEI, fibronectin, PLL, PSS showed a substantial increase in the thickness of the nanofilms as the number of bilayers progressed from five to twenty. Among all of these materials, PDDA had the most thickness for all the bilayers. With regard to laminin, PDL, PSS, the increase was considerable. Collagen showed a slight increase. BSA showed a reverse trend – there was a decrease in the thickness of the layers as the number of bilayers increased. Table 5.8 depicts the thicknesses of 5-,10-, and 20-bilayers of the various biomaterials used in this study.

Table 5.8 Thickness profiles of 5-, 10-, and 20-bilayers of the biomaterials [(Mean ± Standard Deviation) (*n*=3)].

Material	Thickness (nm)		
	5 Bilayers	10 Bilayers	20 Bilayers
PEG-NH <sub>2</sub>	36.99 ± 1.23	123.09 ± 4.18	369.23 ± 5.13
Chondroitin Sulfate	11.01 ± 1.75	34.58 ± 2.20	46.27 ± 1.15
PDDA	59.61 ± 4.07	251.58 ± 6.28	425.91 ± 8.02
PEI	40.18 ± 1.63	101.39 ± 5.31	259.62 ± 5.01
Fibronectin	51.12 ± 1.22	102.51 ± 5.85	262.93 ± 4.93
Laminin	47.10 ± 1.12	87.52 ± 5.60	261.70 ± 5.08
Collagen	54.39 ± 4.29	55.72 ± 4.41	62.06 ± 5.78
PDL	38.73 ± 1.14	58.63 ± 4.23	95.75 ± 5.79
PLL	37.31 ± 1.15	111.95 ± 4.96	216.02 ± 6.60
BSA	9.32 ± 0.65	7.15 ± 0.49	6.17 ± 0.48
PSS	30.69 ± 1.58	115.98 ± 4.7	232.88 ± 4.90



### 5.1.11 Roughness Profiles of the Biomaterials

PDDA and fibronectin showed a substantial increase in the roughness with the increase in the number of bilayers while PEI, laminin, PLL and PSS showed considerable increase. CS showed an increase in roughness up to ten bilayers but showed a decrease for the 20-bilayer configuration. PEG-NH<sub>2</sub> showed a slight decrease from the five to ten bilayers configuration but showed a substantial jump for the 20 bilayers configuration. PDL and collagen showed a slight decrease in the roughness from five- to ten-bilayers and then showed a slight increase for the 20-bilayers configuration. BSA showed the same trend as displayed in the thickness profile- there was a slight decrease in the roughness as the number of bilayers increased. Table 5.9 depicts the various roughnesses of 5-, 10-, and 20-bilayers of the different biomaterials used in this study.

Table 5.9 Roughness profiles of 5-, 10-, and 20-bilayers of the biomaterials [(Mean  $\pm$  Standard Deviation) ( $n=3$ )].

Material	Roughness (nm)		
	5 Bilayers	10 Bilayers	20 Bilayers
PEG-NH <sub>2</sub>	59.70 $\pm$ 5.82	58.32 $\pm$ 6.86	119.66 $\pm$ 6.53
Chondroitin Sulfate	21.86 $\pm$ 2.22	36.76 $\pm$ 7.03	18.15 $\pm$ 6.43
PDDA	29.13 $\pm$ 6.00	110.93 $\pm$ 19.23	294.21 $\pm$ 66.00
PEI	63.30 $\pm$ 12.76	74.61 $\pm$ 7.56	124.22 $\pm$ 10.57
Fibronectin	62.31 $\pm$ 25.08	132.88 $\pm$ 32.20	141.82 $\pm$ 38.17
Laminin	45.62 $\pm$ 10.51	52.89 $\pm$ 10.41	180.43 $\pm$ 94.57
Collagen	58.60 $\pm$ 8.98	53.60 $\pm$ 9.48	56.26 $\pm$ 8.40
PDL	54.47 $\pm$ 14.93	51.24 $\pm$ 9.89	61.41 $\pm$ 2.68
PLL	52.19 $\pm$ 15.67	60.46 $\pm$ 10.60	181.30 $\pm$ 68.72
BSA	3.77 $\pm$ 0.24	2.57 $\pm$ 0.24	2.55 $\pm$ 0.18
PSS	50.83 $\pm$ 17.31	129.20 $\pm$ 18.93	146.94 $\pm$ 53.85

The AFM results correspond with the results obtained by other researchers- some proteins and polypeptides showed no appreciable differences in surface roughness while polyelectrolytes showed increasing roughness with increasing number of bilayers [102, 141-143]. Representative AFM images of two biomaterials are depicted below. Figures

(5.38 and 5.39) depict AFM images of monolayer, 5-, 10-, and 20-bilayer nanofilms with collagen and PDL as the terminating layers.

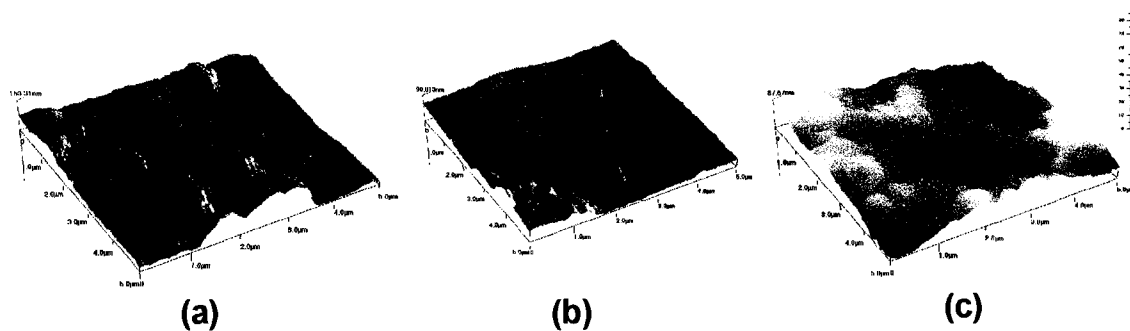


Figure 5.38 AFM images of (a)  $(\text{PSS/Collagen})_5$ , (b)  $(\text{PSS/Collagen})_{10}$ , and (c)  $(\text{PSS/Collagen})_{20}$ .

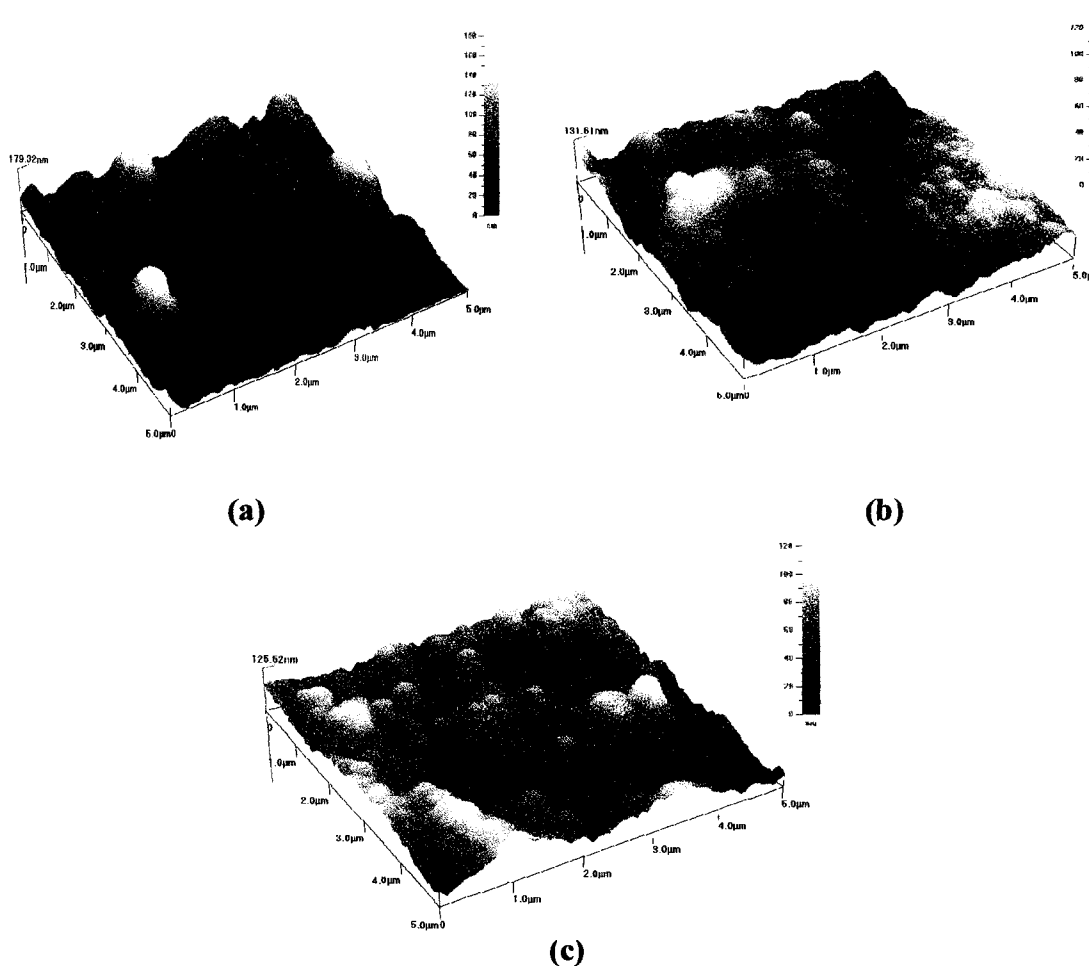
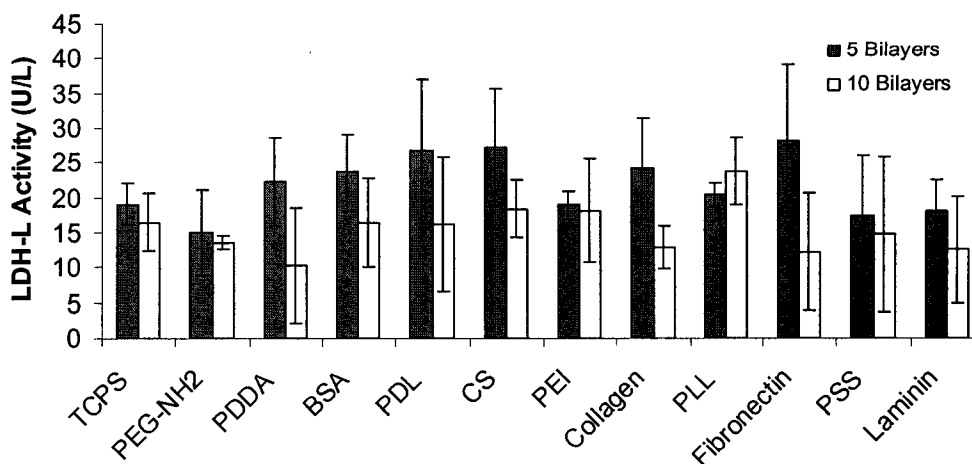


Figure 5.39 AFM images of (a)  $(\text{PSS/PDL})_5$ , (b)  $(\text{PSS/PDL})_{10}$ , and (c)  $(\text{PSS/PDL})_{20}$ .

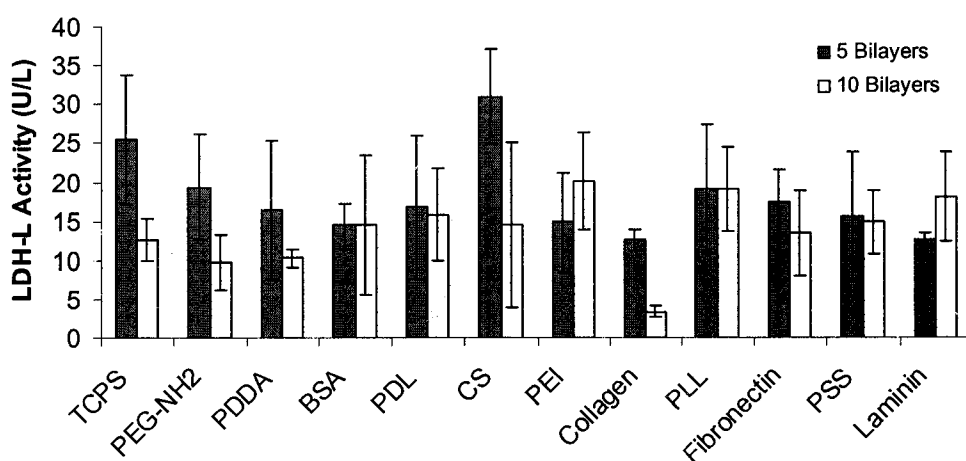
### **5.1.12 LDH-L Assay–Chondrosarcoma Cells**

A few studies have been undertaken on chondrosarcoma cells on LbL assembled films [116, 119, 124, 263, 264]. Divergent opinions exist as to the influence of the LbL films on these cells too. Some researchers have hypothesized that the underlying layers have no influence on the cells at all with only the outermost layer having any effect at all on the cells grown; others have stated that the underlying layers too have an influence on the cells grown on top of these films. Vautier et al. stated that chondrosarcoma cells failed to detect the underlying layers of LbL films and detected the presence of only the uppermost layer. But the horseradish peroxidase assay performed by Vautier et al. suggested dependence on both the underlying layers as well as the upper layer. Also stronger adhesion was observed on positively charged layers than on the negatively charged layers. The results of Vautier et al. corresponded with those of Tryoen-Toth et al. in that early adhesion is promoted on positively charged surfaces [118, 124]. In another study, adhesion of chondrosarcoma cells was higher on PLL films compared with poly(L-glutamic acid) acid (PGA) films [264].

In the present study, chondrosarcoma cells were grown on 5-, and 10-bilayers and evaluated using the LDH-L cytotoxicity assay (Thermo Electron, Louisville, CO). The cells were grown until the required confluence was achieved for performing LDH-L assay [265, 266]. The medium was collected on the fifth day and stored in black-colored vials at 4°C until the assay was performed. The biomaterial which exhibited the least cytotoxicity was collagen. Based upon visual inspection of the results of this assay (Figure 5.40), one can observe that the 10-bilayer nanofilms exhibited lesser cytotoxicity compared with their five-bilayer counterparts. 10-bilayers collagen (density – 25000 cells/ml) showed the least cytotoxicity among all the materials.



(a)



(b)

Figure 5.40 LDH-L assay profile of chondrosarcoma cells (a) Cell Density 1 – 5000 cells/ml, (b) Cell Density 2 – 25000 cells/ml.

### 5.1.13 Canine Chondrocytes–MTT Assay

Passage two canine chondrocytes were cultured in 96-well plates containing mono-, 5-, 10-, and 20-bilayer nanofilms of the same biomaterials as used earlier. An MTT assay was performed as described earlier. An optimal density of 2000 cells/ml was used for the MTT assay. Figure 5.41 exhibits the cell metabolic activity data of the different biomaterials for the four types of layers – monolayers, 5-, 10-, and 20-bilayers.

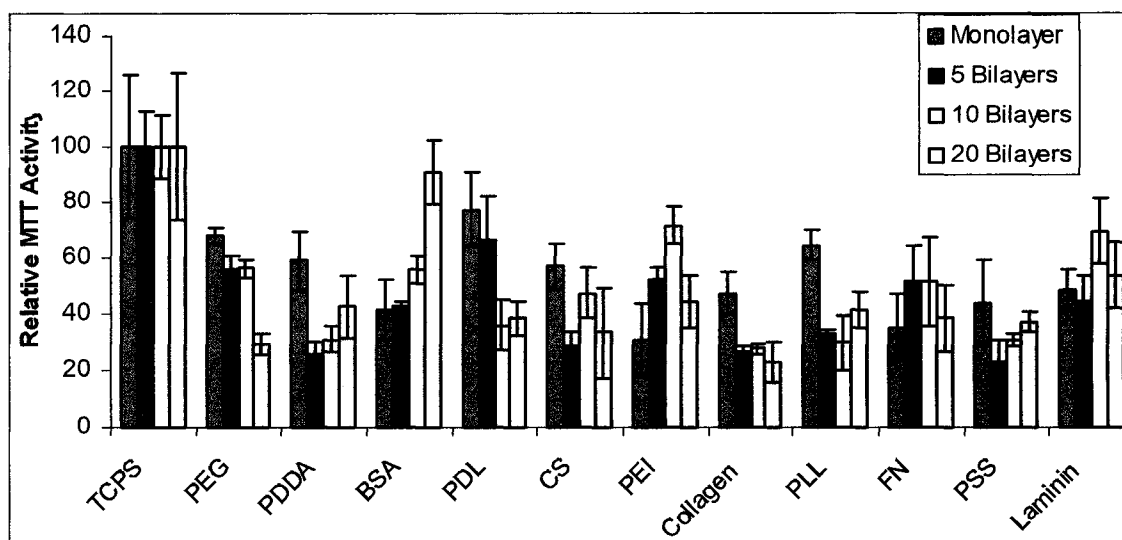


Figure 5.41 MTT assay profile of canine chondrocytes grown on monolayer, 5-, 10-, and 20-bilayers.

The cell metabolic activity of canine chondrocytes on some of the biomaterials displayed consistent and expected results. From the bar graphs in Figure 5.41, it can be clearly seen that all of the eleven biomaterials tested displayed lower relative MTT activity when compared with the control, TCPS. This indicates that canine chondrocytes exhibited decreased cell metabolic activity on all of the biomaterials. It has to be remembered however that the TCPS used in these experiments is a bare surface devoid of any attachment layer. This could have made the TCPS surface rougher resulting in increased cell metabolic activity on TCPS. But among the different biomaterials tested, BSA showed *increasing cell metabolic activity* with increasing number of layers while PEI and fibronectin showed the same up to 10-bilayers. Twenty bilayers showed a decline in cell metabolic activity for PEI and fibronectin. PDDA and PSS; these materials too displayed *increasing cell metabolic activity* but only from the 5-bilayers onwards. The monolayers of PDDA and PSS showed the highest cell metabolic activity among all the layers for these materials. PEG-amine and collagen displayed *decreasing cell*

*metabolic activity* with increasing number of layers while in PDL there was a general *decrease* in the *cell metabolic activity* with the only exception being 20-bilayers which showed slightly higher cell metabolic activity than the ten bilayers. Among the different layers of laminin, the 10-bilayers displayed the highest cell metabolic activity followed by 20-bilayers, monolayers and the 5-bilayers.

#### **5.1.14 Roughness vs. Canine Chondrocyte Cell Metabolic Activity Profiles**

To understand the relationship between the roughnesses of the surfaces of the different materials (measured using AFM) used for LbL and normalized MTT activity (NMA) better, the data were plotted in graphical form (Figures 5.42–5.52). These graphs displayed some interesting points. There is a stabilization of the roughness and the NMA in the range of 5- to 10-bilayers for most of the biomaterials. The transition from 10- to 20-bilayers for most of the materials undergoes either a decrease or increase. So this raises the question: Do the multilayer configurations have a threshold in the exhibition of their characteristics in between 5- and 10-bilayers? In a previous study with primary chondrocytes, cell adhesion was extremely low after the deposition of 10-bilayers [267]. Further studies need to be conducted to assess this question.

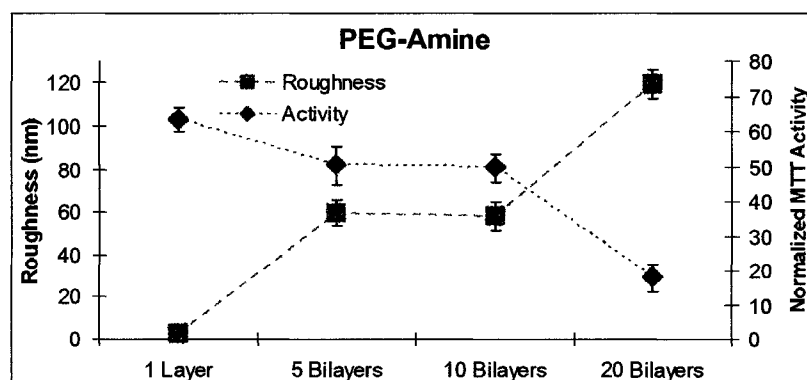


Figure 5.42 Roughness and normalized MTT activity for monolayer, 5-, 10-, and 20-bilayers of PEG-NH<sub>2</sub>.

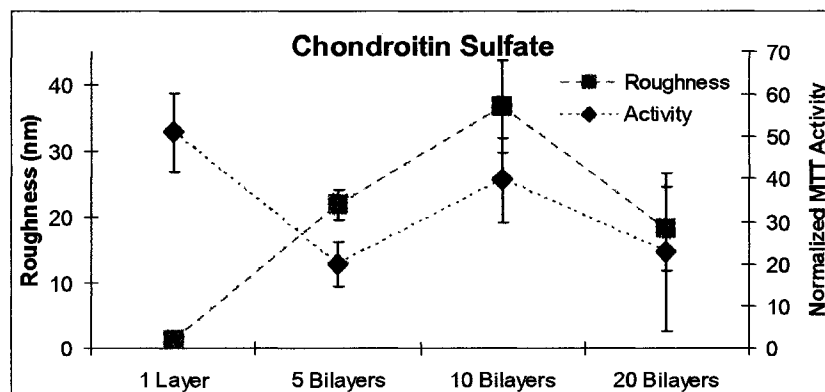


Figure 5.43 Roughness and normalized MTT activity for monolayer, 5-, 10-, and 20-bilayers of Chondroitin Sulfate.

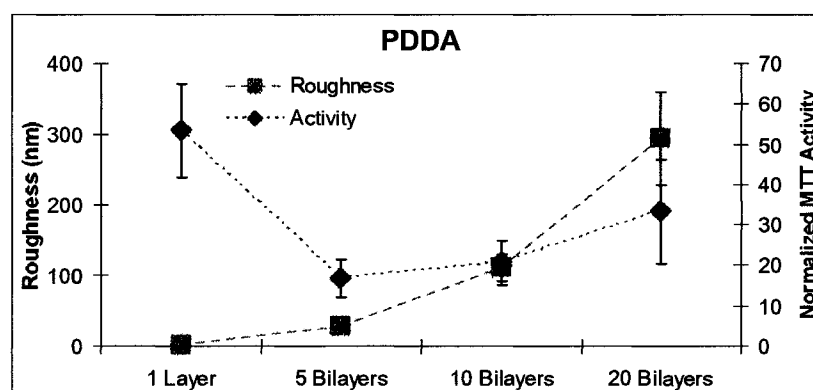


Figure 5.44 Roughness and normalized MTT activity for monolayer, 5-, 10-, and 20-bilayers of PDPA.

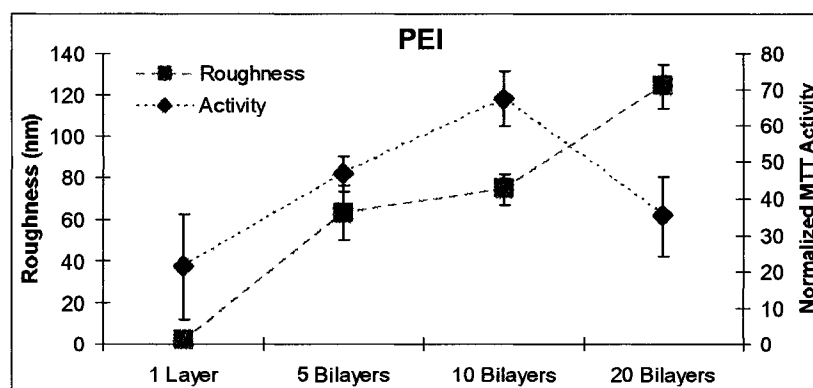


Figure 5.45 Roughness and normalized MTT activity for monolayer, 5-, 10-, and 20-bilayers of PEI.

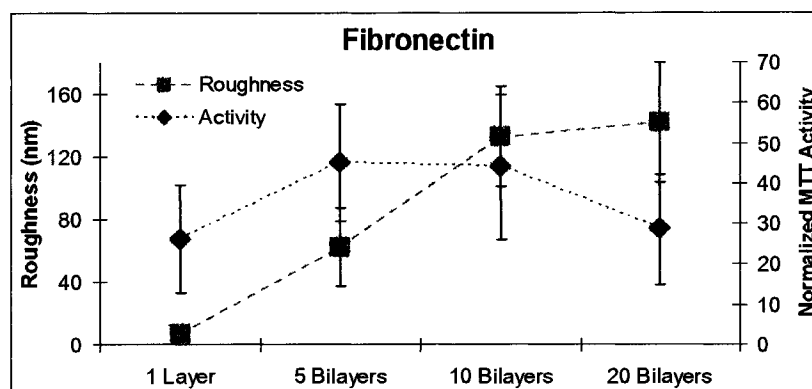


Figure 5.46 Roughness and NMA for monolayer, 5-, 10-, and 20-bilayers of Fibronectin.

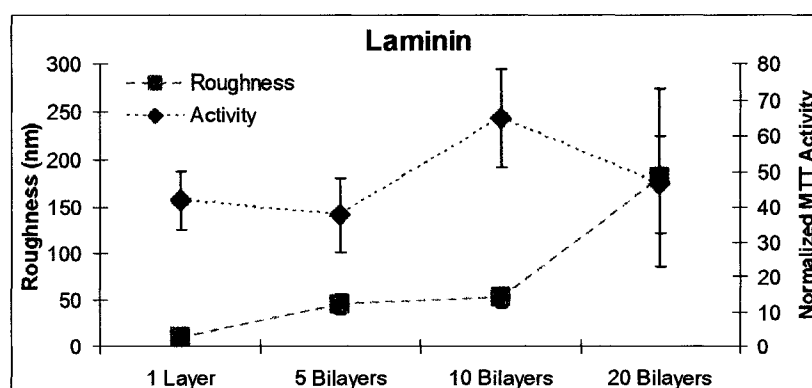


Figure 5.47 Roughness and NMA for monolayer, 5-, 10-, and 20-bilayers of Laminin.

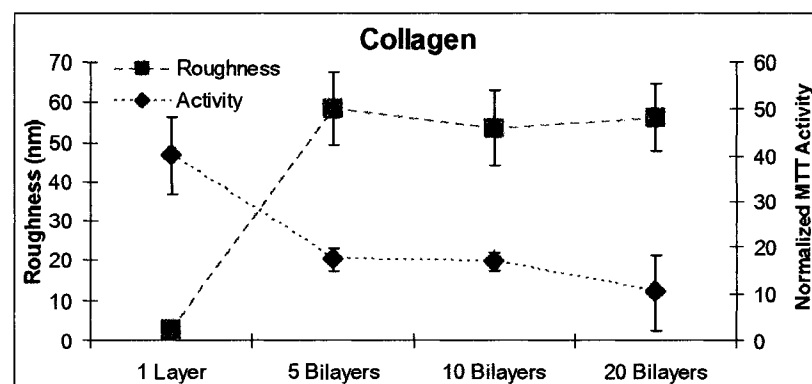


Figure 5.48 Roughness and NMA for monolayer, 5-, 10-, and 20-bilayers of Collagen.



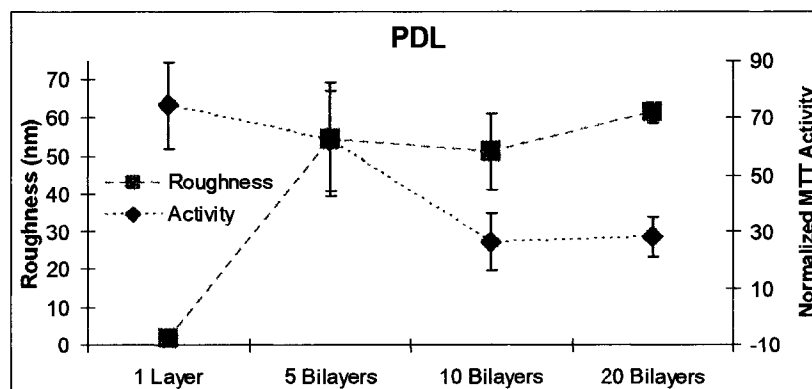


Figure 5.49 Roughness and NMA for monolayer, 5-, 10-, and 20-bilayers of PDL.

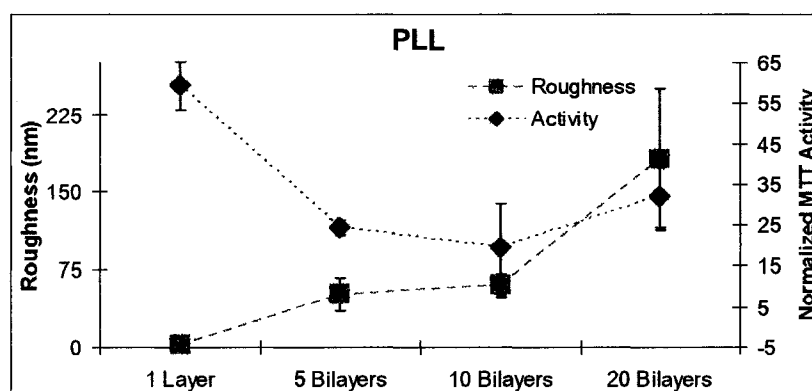


Figure 5.50 Roughness and NMA for monolayer, 5-, 10-, and 20-bilayers of PLL.

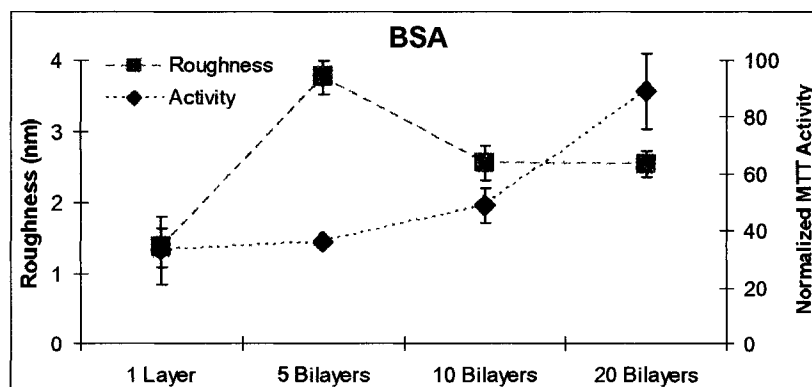


Figure 5.51 Roughness and NMA for monolayer, 5-, 10-, and 20-bilayers of BSA.

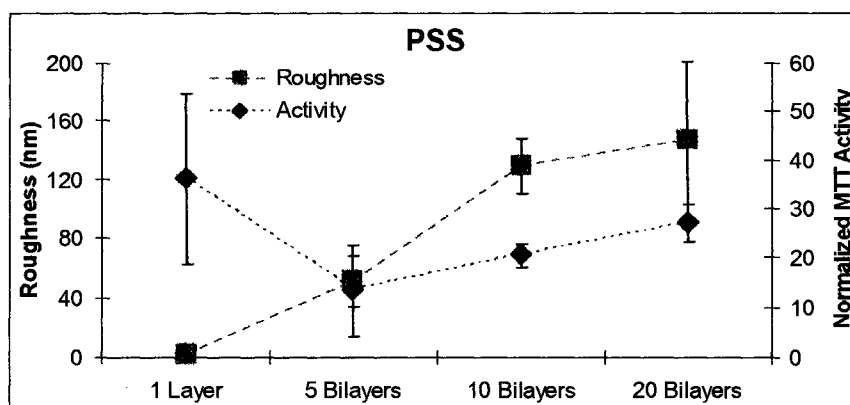


Figure 5.52 Roughness and NMA for monolayer, 5-, 10-, and 20-bilayers of PSS.

#### 5.1.14.1 PEG-NH<sub>2</sub>

The roughness and NMA exhibit a 'mirror-image' like behavior (Figure 5.42). The roughness exhibits a steep increase of 2500% from monolayer to 5-bilayers and then decreases slightly from 5- to 10-bilayers by 2.31% and again exhibits a steep increase of 105% from 10- to 20-bilayers. At the same time the NMA exhibits an opposite behavior with a slightly sharp decline of 20% from monolayer to 5-bilayers and then displays a steady level from 5- to 10-bilayers and then displays a sharp decline of 63% from 10- to 20-bilayers.

#### 5.1.14.2 Chondroitin Sulfate

There is a very sharp increase of 3000% in roughness from monolayer to 10-bilayers and then a sharp decline of 50% from 10- to 20-bilayers. At the same time there is a sharp decrease of 60% in NMA from monolayer to 5-bilayers with a subsequent increase of 98% from 5- to 10-bilayers and a subsequent decline of 42% from 10- to 20-bilayers.

#### **5.1.14.3 PDDA**

Roughness increases from monolayer to 20-bilayers steadily. As the roughness of the materials increases, there is a sharp decline of 68% in the NMA activity from monolayer to 5-bilayers, but then there is a 23% increase in the activity from 5- to 10-bilayers and a considerable increase of 61% from 10- to 20-bilayers.

#### **5.1.14.4 PEI**

For this material, both the roughness and NMA exhibit an increase from monolayer to 5-bilayers with this trend continuing up to 20-bilayers in case of roughness while the NMA shows a decline after 10-bilayers.

#### **5.1.14.5 Fibronectin**

There is a steady but sharp increase of 780% in roughness from monolayer to 10-bilayers, but then there is a subsequent small increase of 6% from 10- to 20- bilayers. At the same time, there is a steady increase of 72% in NMA from monolayer to 5-bilayers with a subsequent very slight drop of 2% from 5- to 10-bilayers and then there is a slightly sharp drop of 35% from 10- to 20-bilayers.

#### **5.1.14.6 Laminin**

This material exhibits a steady but sharp increase of 420% in roughness from monolayer to 10-bilayers with a subsequent slightly sharp incline of 241% from 10- to 20-bilayers. The NMA shows a small decline of 9% from monolayer to 5-bilayers with a subsequent sharp incline of 72 % from 5- to 10-bilayers and then a decline of 28% from 10- to 20-bilayers.

#### **5.1.14.7 Collagen**

This material displays a very sharp increase of 2000 % in roughness from monolayer to 10-bilayers with a subsequent slight decrease of 8% from 5- to 10- bilayers

and then a slight increase of 4% from 10- to 20-bilayers. On the other hand there is a sharp decline of 56% in NMA from monolayer to 5-bilayers with a nearly steady level from 5- to 10-bilayers and a subsequent slight decline of 39% from 10- to 20-bilayers. Figure 5.48 displays the relationship between the roughness and NMA for collagen.

#### **5.1.14.8 PDL**

This material exhibits a very sharp increase of 3000% in roughness from monolayer to 5 bilayers with a slight decline of 5% from 5- to 10-bilayers and then a small increase of 19% from 10- to 20-bilayers. With regard to NMA, there is a sharp decline of 64% from monolayer to 10-bilayers with a subsequent small increase of 6% from 10- to 20-bilayers.

#### **5.1.14.9 PLL**

There is a very sharp increase of 2000% in roughness from monolayer to 5-bilayers. Subsequently, there is a small increase of 15% from 5- to 10-bilayers while there is a slightly sharp incline of 200% from 10- to 20-bilayers. At the same time, the NMA shows a slightly sharp decrease of 58% from monolayer to 5-bilayers with another decline of 20% from 5 to 10 bilayers and a subsequent slightly sharp incline of 65% from 10 to 20 bilayers.

#### **5.1.14.10 BSA**

A special characteristic about roughness worth mentioning for this material is that BSA is the sole material among all the materials which exhibits a small value for monolayer while the rest of the materials exhibit even smaller values of roughness. There is a sharp increase of 175 % in the roughness from monolayer to 5-bilayers and then there is a decline of 31% from 5- to 10-bilayers with a subsequent 1% decrease in the roughness from 10 to 20 bilayers. At the same time there is a slight increase of 9% in the

NMA from monolayer to 5 bilayers, and this increases by 35% from 5 to 10 bilayers with a considerable jump of 81% in NMA from 10 to 20 bilayers.

#### **5.1.14.11 PSS**

This material exhibits a steady increase in roughness from monolayer to 20 bilayers of 10000% while in the case of NMA there is a sharp decrease of 62% from monolayer to 5-bilayers with a subsequent increase of 100% for 20 bilayers.

#### **5.1.15 Statistical Analyses**

##### **5.1.15.1 MTT Assay – Canine Chondrocytes**

The two-way ANOVA and Tukey analyses conducted on the cell metabolic activity results of canine chondrocytes using SAS show significant interactions between biomaterials and layers. Table 5.10 exhibits the results of the statistical analysis of canine chondrocytes' cell metabolic activity data.

Table 5.10 Statistical outputs for the canine chondrocytes' cell metabolic activity.

<b>2-Way ANOVA Statistic</b>	<b>Material</b>
13.50 ( $<.0001$ )	36.46 ( $<.0001$ )
<b>Layer</b>	<b>Materialx Layer</b>
13.22 ( $<.0001$ )	5.87 ( $<.0001$ )

**Note:** Each value represents the F-Statistic with the P-Value in brackets.

### 5.1.15.2 LDH-L Assay – Chondrosarcoma Cells

Three-way ANOVA and Tukey's conducted on the results obtained from the LDH-L analysis on chondrosarcoma cells revealed statistically significant differences for the type of layer. The mean of 10-bilayers (18.989) was significantly different from the mean of 5-bilayers (13.636). Table 5.11 displays the results.

Table 5.11 Statistical analysis results of LDH-L Assay conducted on PBAC.

3-Way ANOVA Statistic	Density	Material	Layer
1.28 (0.1524)	1.47 (0.2279)	0.79 (0.6504)	15.67 (0.0001)
Densityx Material	Densityx Layer	Materialx Layer	DensityxMaterialx Layer
1.15 (0.3308)	0.80 (0.3729)	0.95 (0.4942)	0.95 (0.4933)

**Note:** Each value represents the F-Statistic with the P-Value in brackets.

## 5.2 Micropatterned Surfaces

Micropatterned surfaces have been created for patterning cells using many approaches such as SAMs [87], LbL [166, 268]. These surfaces are important for developing tissue engineering, cell arrays, biosensors [268], co-culture systems [66, 269]. Different materials such as ethylene glycol (EG) [61], poly(ethylene glycol) (PEG) [113], albumin [235], of which PEG has been one of the most commonly used. PEG-amine has been used to create a cell-resistant platform [268]. A wide variety of eukaryotic cells have been grown and studied on micropatterned surfaces [84, 87, 269-272]. *In vitro* platforms are required to study the different cellular mechanisms. But with the traditional platforms, sufficient control cannot be obtained over the cellular microenvironment [87] which requires precise spatiotemporal control. Thus, micropatterned surfaces have been utilized to answer several fundamental questions in cell biology and tissue engineering.

For example, it was shown that cell function could be regulated by controlling cell shape. This fact was demonstrated by the growth of hepatocytes on micropatterned surfaces. The authors observed decreased DNA production and increased cellular apoptosis associated with a decrease in the cell adhesive surfaces [273]. Also cell shape was found to be the regulatory factor in both cell apoptosis and growth, based on the observation of increasing restriction of the size of micropatterned islands coated with different densities of ECM and growing bovine and human endothelial cells on the islands [87].

The use of LbL for creating micropatterned surfaces brings in all the advantages offered by LbL – excellent control over surface properties like thickness [268], roughness, simplicity and cost-effectiveness. LbL micropatterned surfaces help in obtaining the precise microenvironment as these surfaces can be sufficiently tuned to release the factors necessary for the growth of cells and regulate them. Based on the requirements, polyelectrolytes and proteins can be used to create either cell-resistant or cell-adhesive patterns. Different eukaryotic cells have been grown on these micropatterned surfaces demonstrating the effectiveness of these surfaces [166, 274]. In this study, micropatterned surfaces were created using LbL-LO technique [74, 90]. The most important advantage of the LbL-LO method is the spatiotemporal control and the ability to construct well-defined structures of differing functionality in close proximity [247]. In this study, Phase contrast imaging was done to characterize the micropatterned surfaces.

### **5.2.1 Phase Contrast Images of Micropatterned Substrates**

Nearly all the micropatterns with the exception of collagen had well-defined borders. Also, the 10- bilayered micropatterns appear better-formed than their 5-bilayered

counterparts, which was again expected as the increased bilayers definitely lead to better deposition of the materials in the micropatterns due to the increased thickness of the materials deposited. Depicted in figures 5.53–5.57 are the phase-contrast images of the various micropatterned substrates. The number of bilayers is shown as a subscript while the pattern sizes are mentioned in  $\mu\text{m}$ .

#### **5.2.1.1 Micropatterned Substrates with PDDA as the Outermost Layer**

From the morphological observations, the 5-bilayered micropatterned substrates appear different than their 10-bilayer counterparts. Usually, protein patterns have such an appearance as seen in the 5-bilayered PDDA micropatterns.

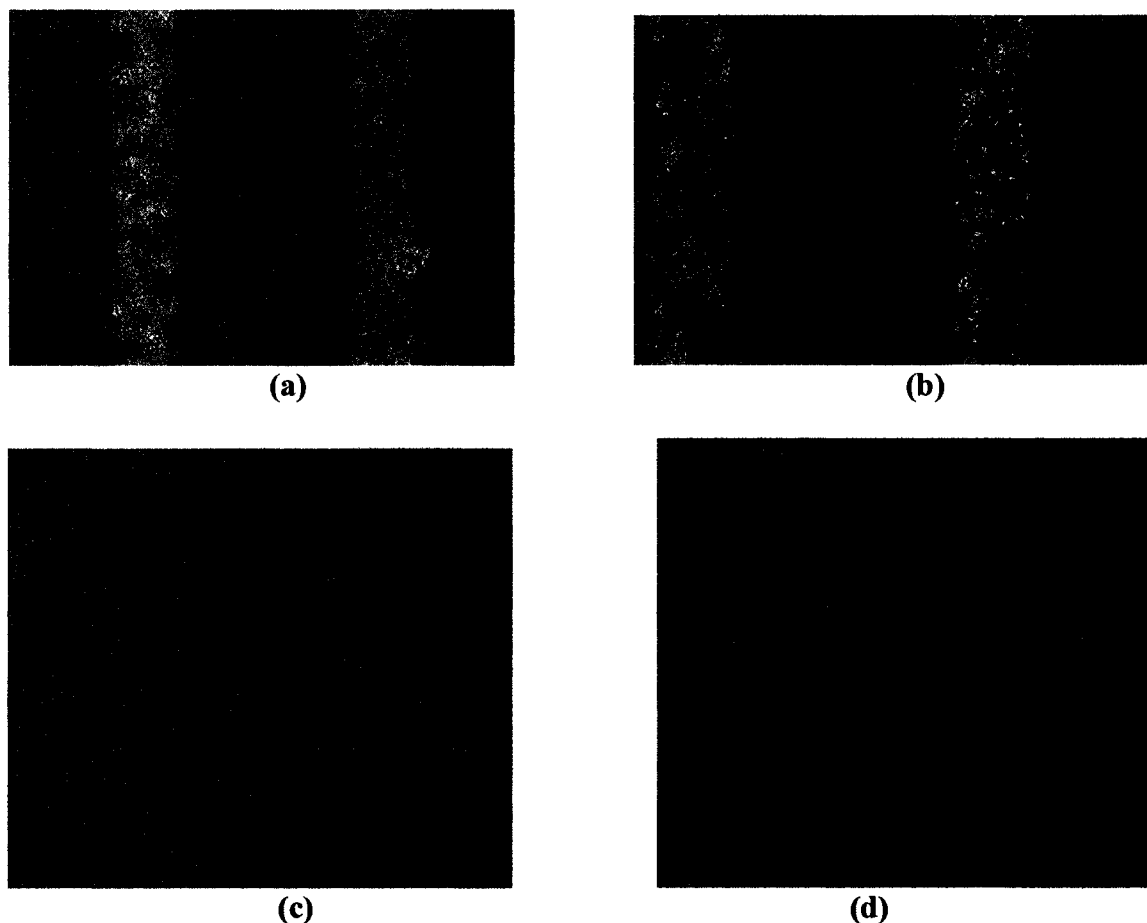


Figure 5.53 (a)  $(\text{PSS/PDDA})_5-80 \mu\text{m}$ , (b)  $(\text{PSS/PDDA})_5-100 \mu\text{m}$ , (c)  $(\text{PSS/PDDA})_{10}-80 \mu\text{m}$ , (d)  $(\text{PSS/PDDA})_{10}-100 \mu\text{m}$ .



### 5.2.1.2 Micropatterned Substrates with CS as the Outermost Layer

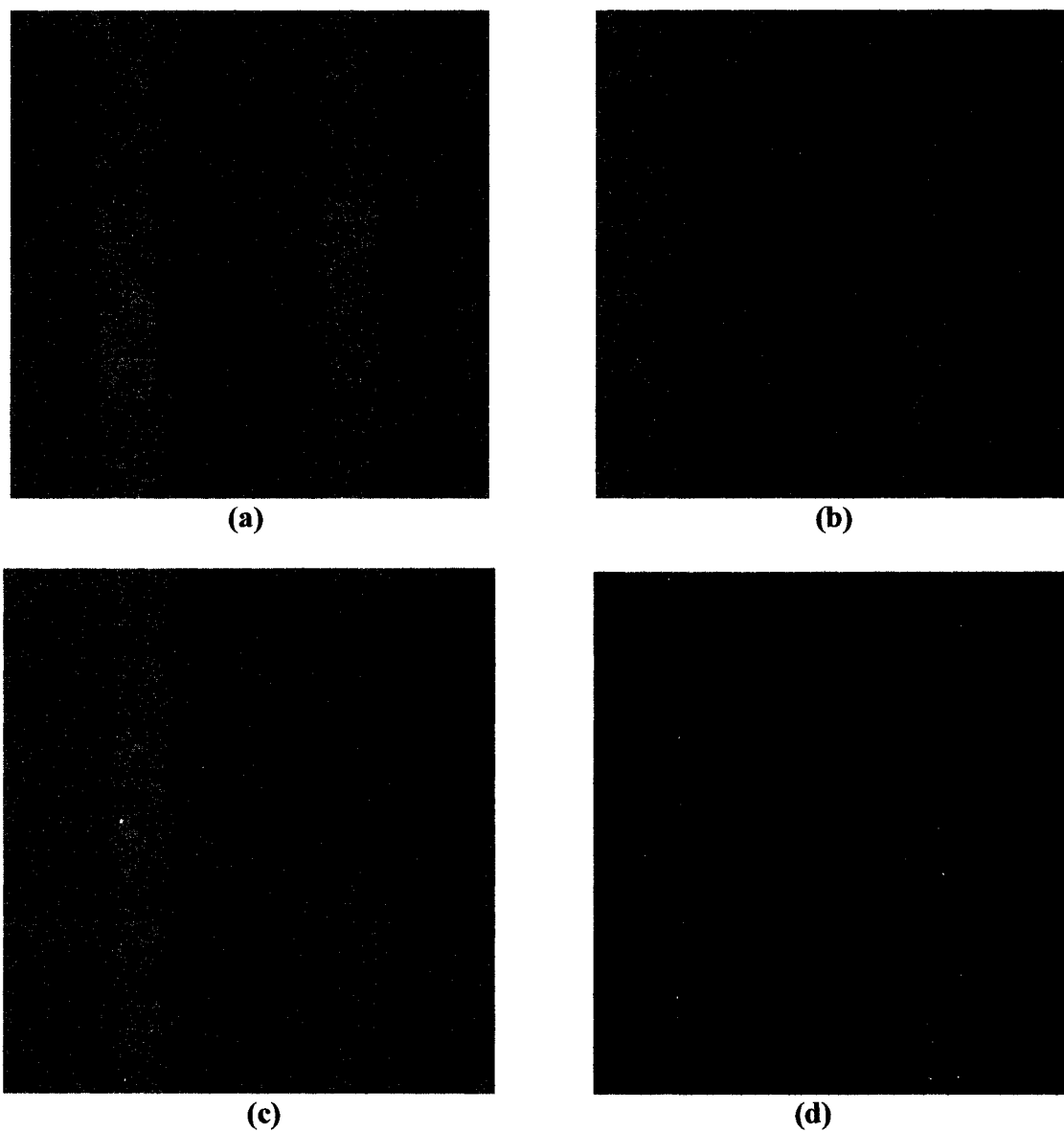


Figure 5.54 (a)  $(\text{CS/PEI})_5/\text{CS}-80 \mu\text{m}$ , (b)  $(\text{CS/PEI})_5/\text{CS}-100 \mu\text{m}$ ,  
(c)  $(\text{CS/PEI})_{10}/\text{CS}-80 \mu\text{m}$ , (d)  $(\text{CS/PEI})_{10}/\text{CS}-100 \mu\text{m}$ .

### 5.2.1.3 Micropatterned Substrates with PEI as the Outermost Layer

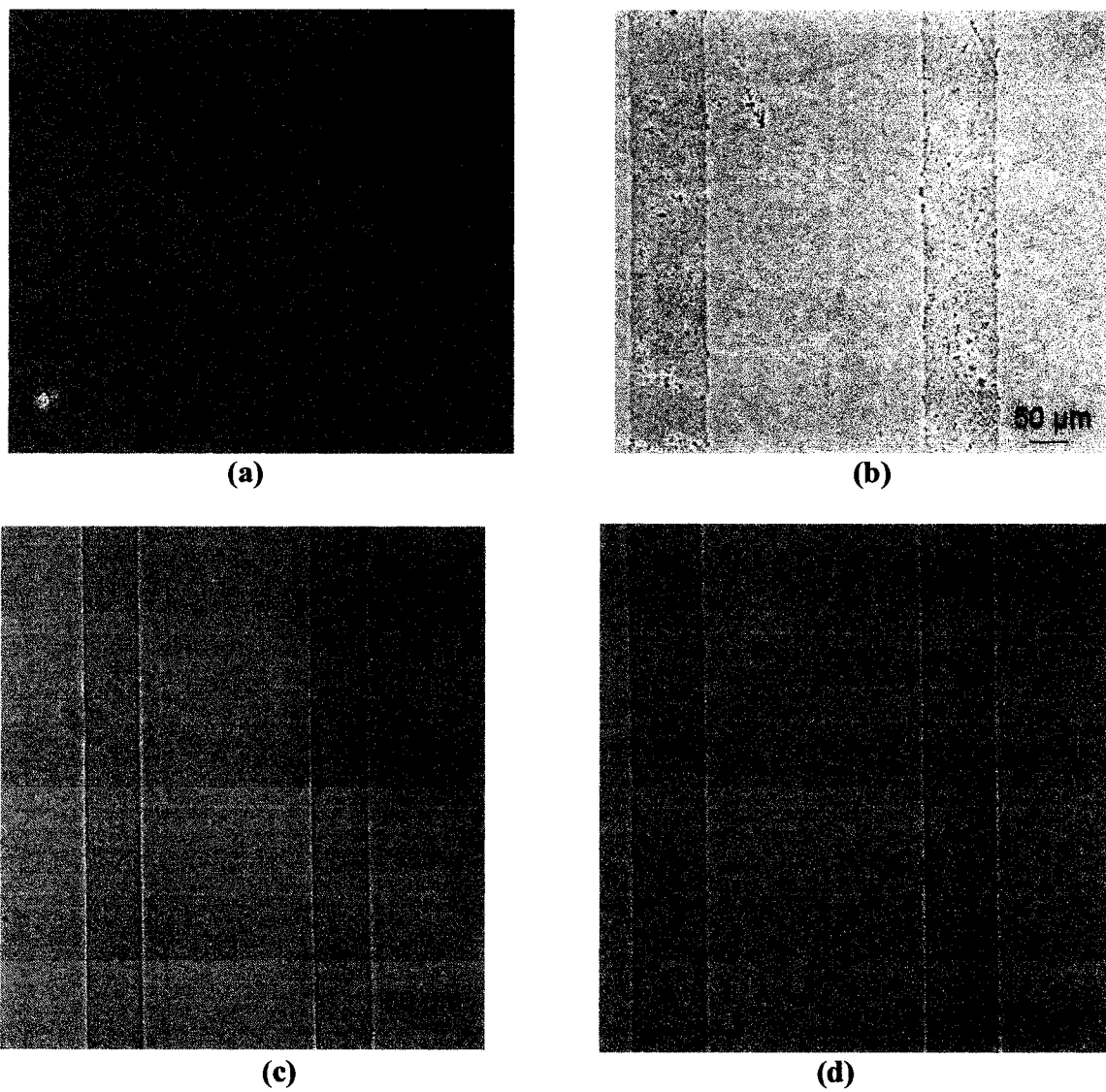


Figure 5.55 (a)  $(\text{PSS/PEI})_5$ -80 μm, (b)  $(\text{PSS/PEI})_5$ -100 μm, (c)  $(\text{PSS/PEI})_{10}$ -80 μm  
(d)  $(\text{PSS/PEI})_{10}$ -100 μm.

#### 5.2.1.4 Micropatterned Substrates with Collagen as the Outermost Layer

The slightly irregular borders of collagen were expected as collagen is a protein. The adsorption time of 30 minutes adapted for proteins like collagen might have been less, which could be another reason for the slightly irregular patterns.

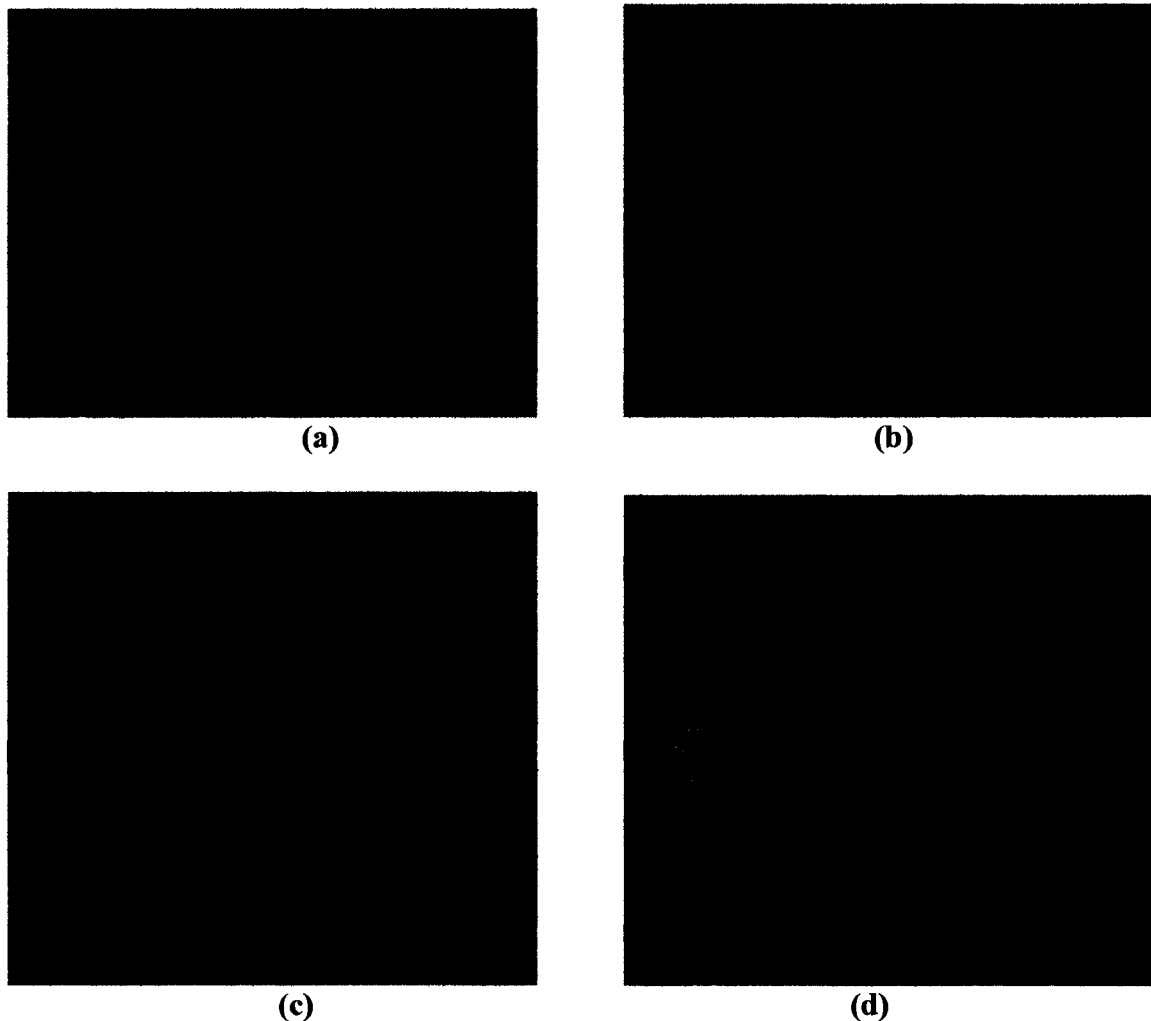


Figure 5.56 (a) (PSS/Collagen)<sub>5</sub>-80  $\mu\text{m}$ , (b) (PSS/Collagen)<sub>5</sub>-100  $\mu\text{m}$ , (c) (PSS/Collagen)<sub>10</sub>-80  $\mu\text{m}$ , (d) (PSS/Collagen)<sub>10</sub>-100  $\mu\text{m}$ .

### 5.2.1.5 Micropatterned Substrates with PSS as the Outermost Layer

The lines which appear in figure 5.57 (c and d) are a result of chromatic aberration during image-acquisition.

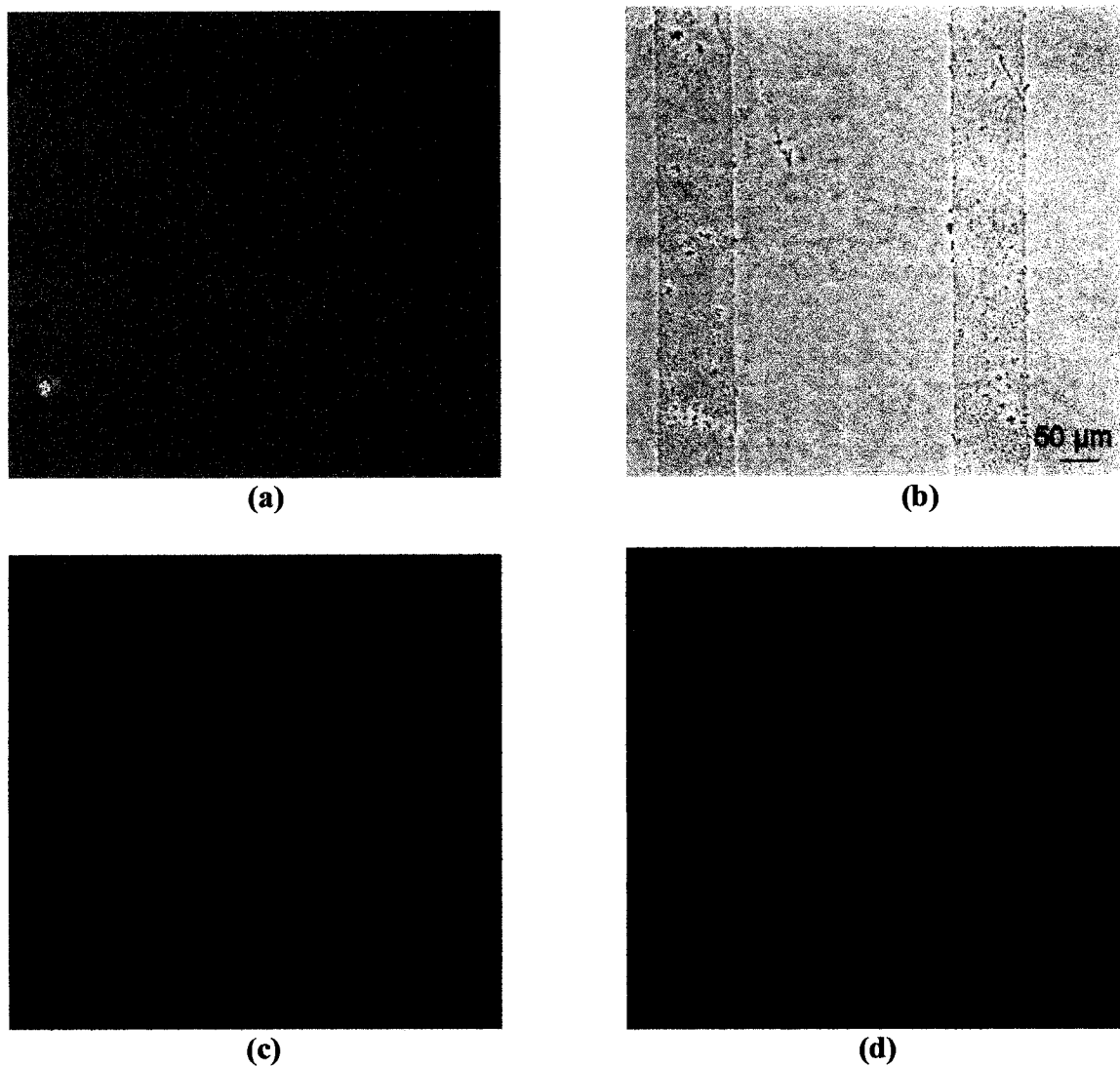


Figure 5.57 (a)  $(\text{PSS/PEI})_5/\text{PSS}$ –80  $\mu\text{m}$ , (b)  $\text{PSS/PEI})_5/\text{PSS}$ –100  $\mu\text{m}$ , (c)  $(\text{PSS/PEI})_{10}/\text{PSS}$ –80  $\mu\text{m}$ , (d)  $(\text{PSS/PEI})_{10}/\text{PSS}$ –100  $\mu\text{m}$ .

### **5.3 Micropatterned Co-Culture Platforms**

Co-cultures have served as important models and facilitators in tissue engineering for studying the interactions between cells; cells and the ECM and soluble stimuli (growth factors, cytokines). These interactions pertain to the physiology of the various organ systems in the adult and the developing embryo [66]. A wide variety of techniques has been utilized to construct these co-cultures. Some of the most common methods of building co-cultures have involved microfabrication techniques (photolithography) [275, 276], SAMs, electroactive substrates [156], microfluidic networks and patterning. Each technique has its own advantages as well as disadvantages. New methods need to be explored for the attainment of an optimal co-culture platform having maximum advantages and minimum disadvantages. In this study, co-culture scaffolds were built using the LbL-LO procedure.

Bhatia et al. were the first to use microfabrication for co-cultures of cells. They devised a modification based upon previous methods for the modification of surfaces with aminoethylaminopropyltrimethoxysilane coupled to glutaraldehyde and collagen. The differences in serum content of cell culture media too were put to advantage by Bhatia et al. The most important achievement of Bhatia et al. was the control of both homotypic and heterotypic interactions. Some of the limitations of traditional co-cultures involved the lack of variations in the local seeding density of the cells independently of the cell number [66].

Patterned proteins have been created from a variety of methods, with the most common being photolithography and soft lithography. Here, a simple approach combining photolithography, LbL self-assembly and photoresist lift-off was utilized to

create checkerboard (chessboard) patterns of antibodies on top of polyelectrolyte-protein multilayers. A spatial demarcation of five microns was achieved in between the generated patterns of anti-CD 44 rat monoclonal antibody atop vitronectin and anti-rat osteopontin (MPIIB10<sub>1</sub>) antibody atop fibronectin. Different characterization techniques like fluorescence microscopy, surface profilometry, and atomic force microscopy were used to characterize the patterns generated. These patterns have many applications including co-culture of cells, drug testing platforms and sensors.

### 5.3.1 Phase Contrast Microscopy

The single square components and double component (checker board) shown in Figure 5.58 have dimensions of  $80 \times 80 \mu\text{m}^2$  each. It can be observed that the micropatterns have clear-cut and defined borders indicating the proper replication of the photomask.

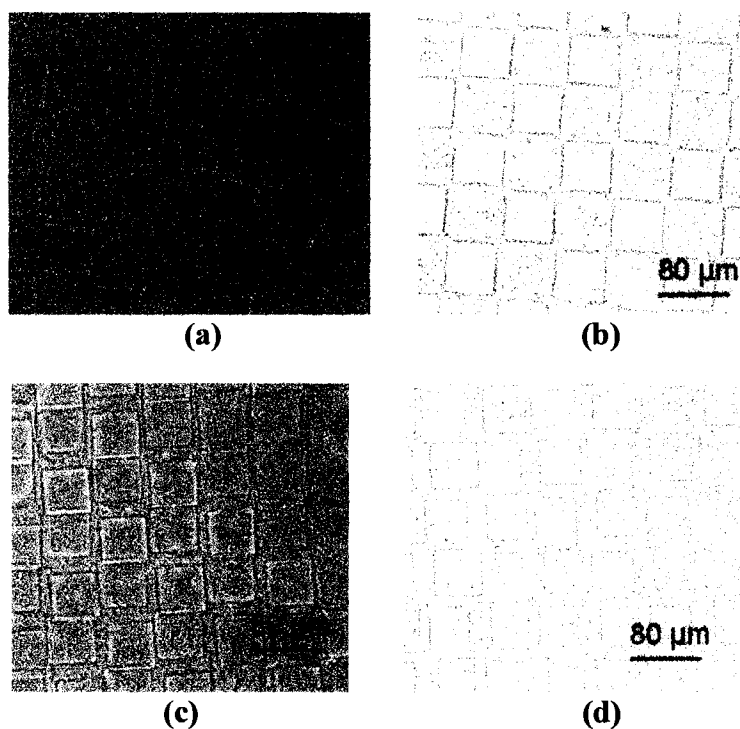


Figure 5.58 (a), (b) – Single-component micropatterns; (c), (d) – double component (checker board) patterns

The double-component checker board patterns were achieved using the LbL-LO technology [74]. The results demonstrated here in conjunction with earlier results prove that LbL-LO method is ideal for patterning applications [74, 90]. From the images it can be seen that the edges of the patterns are not very sharp. This problem can be resolved by optimizing the techniques involved in photolithography and the subsequent LbL assembly methods.

### 5.3.2 AFM Analysis

AFM scans were performed at several different positions on the co-culture patterns. The roughnesses of the patterns in the scans were determined. Six multiple measurements were made and the averages calculated ( $n=6$ ) [91]. The images obtained from the AFM analysis [Figure 5.59 (a)] confirmed the adsorption and deposition of proteins and antibodies. Figure 5.59 (b), (c) exhibit the edges of co-culture pattern tiles.

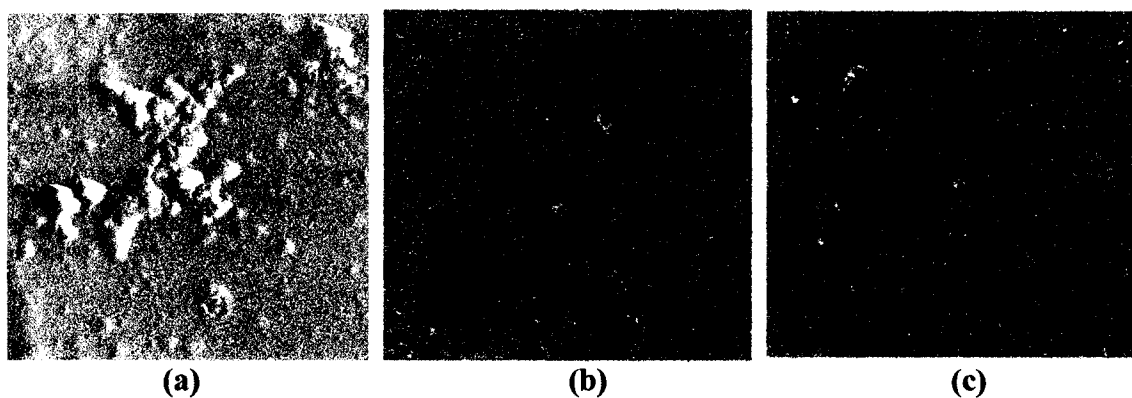


Figure 5.59 (a) AFM image of antibody deposited on the co-culture pattern; (b), (c) edges of co-culture pattern tiles.

AFM scans confirmed the differential deposition of antibodies onto the co-culture patterns. Figure 5.60 reveals the differences in the average and RMS (Root Mean Square) roughness of the two antibodies in the creation of the co-culture patterns.

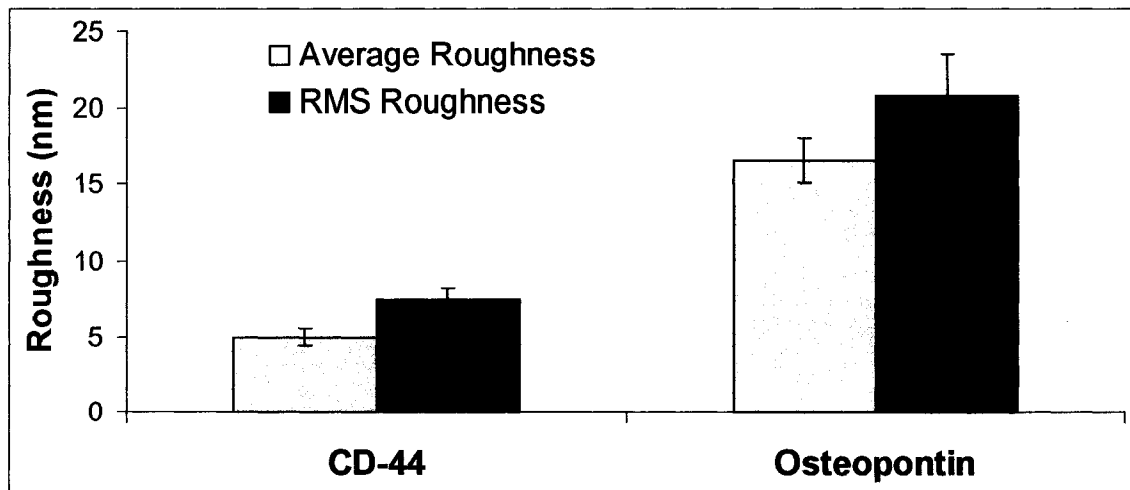


Figure 5.60 Average roughness and RMS roughness of antibodies deposited on co-culture platforms.



## CHAPTER 6

### CONCLUSIONS AND FUTURE WORK

#### 6.1 Conclusions

In this dissertation, the fledgling science of nanobiotechnology has been explored in relation to chondrocytes. The work presented here uses LbL self-assembly technique to modify surfaces with several polymers and polypeptides and examines the subsequent growth of three types of chondrocytes on these surfaces. This study's hypotheses were proved for some of the biomaterials tested, and cells on some of the materials exhibited increasing cell metabolic activity and viability with increasing number of layers.

The trend of increasing viability with increasing bilayers was the characteristic of the study on bovine articular chondrocytes. CS exhibited this tendency for cell density one (5000 cell/ml). Many materials like PEG-NH<sub>2</sub>, PDL, CS, collagen, fibronectin, PSS and laminin showed increasing viability with increasing number of layers for cell density two (15000 cell/ml). Similarly, for cell density three (25000 cell/ml), cell viability increased with the number of layers on PDDA, PDL, CS, PLL, fibronectin and PSS. This behavior can be utilized to create spatiotemporal differences in applications like tissue engineering, sensors, and co-cultures.

PBAC exhibit a SROP on mono-, bi-, and tri-layers of both polyelectrolytes and polypeptides. PEG-amine, PDL, chondroitin sulfate, PEI, PLL, fibronectin and PSS were more favorable for the growth and viability of chondrocytes than other materials used. The highest viabilities occurred on laminin, PEG-NH<sub>2</sub>, PDL, PEI, TCPS, BSA, CS and fibronectin. The highest cell metabolic activity was observed on CS, laminin, PLL, TCPS, fibronectin, PDL and BSA. Further work with increased number of bilayers needs to be done to understand the influence of multilayer architectures on PBAC. The most important observations from the live-dead morphological image analysis were that chondrocytes on bilayers of PDDA, PLL and PSS were significantly larger than cells on other layers of PDDA, PLL and PSS and that cells on bilayers of BSA were better attached when compared to the cells on other layers of BSA. This raises the question – Do cells on even-numbered bilayers behave differently than cells on odd-numbered bilayers? This question needs to be investigated further. In the present study, cells from passage three were used. Future studies can examine primary cells grown on the multilayer films right after the isolation of the cells.

The most important conclusion from the growth of human chondrosarcoma cells on 5- and 10-bilayer nanofilms was that 10-bilayer nanofilms exhibited less cytotoxicity compared than their 5-bilayer counterparts. Of all the materials tested, 10-bilayers collagen (density – 25000 cells/ml) showed the least cytotoxicity among all the materials. The difference between LDH-L activity of chondrosarcoma cells seeded at a density of 25000 cells/ml for 10-bilayer films and 5-bilayer films was statistically significant. While the comparison between 5- and 10-bilayers suggests that as the number of bilayers increases, the cytotoxicity decreases, it remains to be seen whether this tendency

continues with larger number of bilayers. However, reduced cytotoxicity was observed with increased number of bilayers in our studies of chondrocytes on nanofilms.

On BSA, cell metabolic activity increased with the number of bilayers, but for all of the biomaterials, cell metabolic activity was lower than observed on the control, bare TCPS. This result indicates that even 20-bilayers were not enough to fully enhance the cell metabolic activity. However, to see whether the trend for improved metabolic activity with number of layers continues and raises the activity above the control case, a number of bilayers larger than 20 needs to be constructed and evaluated for the effects of multilayer architecture on cell metabolic activity. MTT is not just an indicator of cell metabolic activity, it is also an indicator of viability. Further, cytotoxicity analyses need to be undertaken to evaluate the cytotoxicity of the different biomaterials.

Whereas the results indicate that cell metabolic activity increases with the number of bilayers, the results vary with the type of species of chondrocytes. Regulation of phenotype is important for tissue engineering, especially for chondrocytes which have multiple phenotypes. In this work, an attempt was made to stabilize the phenotype of chondrocytes on LbL-assembled films and there were differences among the different nanofilms. These differences were dependent upon the seeding density and the number of bilayers.

Substrates micropatterned with the LbL-LO technique may be used to engineer the phenotype of chondrocytes. Another novel aspect of this work is the demonstration of co-culture checker board patterns using LbL- LO technology. Selective deposition of the antibodies was confirmed by AFM analyses. These co-culture patterns need to be further evaluated by cell culture. LbL-LO technology can be used to deliver the necessary

growth factors, enzymes to help stabilize the phenotype of chondrocytes and other cells used.

## **6.2 Future Work**

Nanofilms with increased multilayer architectures can be built to evaluate the influence of multilayer nanofilms on cells. Nanofilms of up to 40-bilayers and beyond can be built and tested. Other species of chondrocytes and some other cell lines can be used in the studies. Is there an optimum range of bilayers (in between 5- and 10-bilayers for example) where cell functionality is the maximum? If so, what is the cause behind this? Surface roughness can be one factor involved. These questions need to be answered in future work. Influence of other factors like surface charge, elasticity of the substrate should also be taken into consideration and studied.

Cell simulation software can be used as an adjunct to traditional cell-culture work. Before starting any research, the questions can be addressed using simulation software saving valuable reagents and time. This field is advancing slowly. At present, there are a few simulation software programs available. One such program, *Virtual Cells*, is maintained by the National Resource for Cell Analysis and Modeling located at the University of Connecticut Health Center.

The spatiotemporal benefits offered by LbL-LO method can be used to create unique platforms for the differentiation of stem cells into the desired cells by constructing borders at the nanoscale in between two or more types of cells using biomaterials like PEG-amine and other mechano-chemical barriers. Also the factors required for the differentiation of stem cells can be inserted in the LbL films during the self-assembly process. These unique platforms could be used as potential scaffolds in tissue engineering

for the treatment of diseases. Innovative treatments for diseases [277] is fast becoming a tradition at Louisiana Tech and hopefully continue in the future.

## REFERENCES

- [1] F. Oberpenning, J. Meng, J. J. Yoo, and A. Atalá, "De novo reconstitution of a functional mammalian urinary bladder by tissue engineering," *Nature Biotechnology*, vol. 17, pp. 149-55, 1999.
- [2] I. V. Yannas, D. P. Orgill, J. Silver, T. V. Norregaard, N. T. Zervas, and W. C. Schoene, "Polymeric template facilitates regeneration of Sciatic Nerve across 15-mm gap," Transactions of the Annual Meeting of the Society for Biomaterials in conjunction with the Interna, San Diego, CA, USA, pp. 146, 1985.
- [3] D. P. Orgill and I. V. Yannas, "Design of an artificial skin. IV. Use of island graft to isolate organ regeneration from scar synthesis and other processes leading to skin wound closure," *Journal of Biomedical Materials Research*, vol. 39, pp. 531, 1998.
- [4] R. M. Nalbandian, R. L. Henry, K. W. Balko, D. V. Adams, and N. R. Neuman, "Pluronic F-127 gel preparation as an artificial skin in the treatment of third-degree burns in pigs," *Journal of Biomedical Materials Research*, vol. 2, pp. 35-48, 1987.
- [5] R. Matsui, K. Osaki, J. Konishi, K. Ikegami, and M. Koide, "Evaluation of an artificial dermis full-thickness skin defect model in the rat," *Biomaterials*, vol. 17, pp. 989, 1996.
- [6] I. Jones, L. James, and R. Martin, "Epidermal regeneration from disaggregated cultured keratinocytes applied beneath integra® artificial skin," Second Smith and Nephew International Symposium - Tissue Engineering 2000: Advances in Tissue Engineering, Biomaterials and Cell Signalling, York, United Kingdom, pp. 122, 2000.
- [7] J. H. De Groot, A. J. Pennings, and J. M. F. H. Coenen, "Triple-layer artificial skin: Porous 50/50 copoly (L-lactide/epsilon-caprolactone) template for neodermis regeneration," *Journal of Materials Science Letters*, vol. 16, pp. 152, 1997.
- [8] K. Ushio, M. Oka, S.-H. Hyon, T. Hayami, S. Yura, K. Matsunoura, J. Toguchida, and T. Nakamura, "Attachment of Artificial Cartilage to Underlying Bone," *Journal of Biomedical Materials Research - Part B Applied Biomaterials*, vol. 68, pp. 59, 2004.

- [9] W. Swieszkowski, D. N. Ku, H. E. N. Bersee, and K. J. Kurzydowski, "An elastic material for cartilage replacement in an arthritic shoulder joint," *Biomaterials*, vol. 27, pp. 1534, 2006.
- [10] S. U. Song, Y.-D. Cha, J.-U. Han, I.-S. Oh, K. B. Choi, Y. Yi, J.-P. Hyun, H.-Y. Lee, G. F. Chi, C.-L. Lim, J. K. Ganjei, M.-J. Noh, S.-J. Kim, D. K. Lee, and K. H. Lee, "Hyaline cartilage regeneration using mixed human chondrocytes and transforming growth factor-beta1-producing chondrocytes," *Tissue Engineering*, vol. 11, pp. 1516, 2005.
- [11] M. Oka, K. Ushio, P. Kumar, K. Ikeuchi, S. H. Hyon, T. Nakamura, and H. Fujita, "Development of artificial articular cartilage," *Proceedings of the Institution of Mechanical Engineers, Part H: Journal of Engineering in Medicine*, vol. 214, pp. 59, 2000.
- [12] O. Ike, Y. Shimizu, T. Okada, Y. Ikada, and S. Hitomi, "Experimental studies on an artificial trachea of collagen-coated poly(L-lactic acid) mesh or unwoven cloth combined with a periosteal graft," *American Society for Artificial Internal Organs Transactions*, vol. 37, pp. 24, 1991.
- [13] Z. Gu, J. Xiao, and X. Zhang, "Development of a kind of artificial articular cartilage-PVA-hydrogel," *Shengwu Yixue Gongchengxue Zazhi/Journal of Biomedical Engineering*, vol. 16, pp. 13, 1999.
- [14] M. F. Fogaca, W. L. Kao, C. A. Vacanti, and J. P. Vacanti, "Study of the immunological response to tissue engineered cartilage in vivo," *Artificial Cells, Blood Substitutes, and Immobilization Biotechnology*, vol. 22, pp. 16, 1994.
- [15] J. Shaikh Mohammed, "Multicomponent patterning of nanocomposite polymer and nanoparticle films using photolithography and layer-by-layer self-assembly," Ph.D. Dissertation, Louisiana Tech University, 2006.
- [16] W. S. Beh, I. T. Kim, D. Qin, Y. Xia, and G. M. Whitesides, "Formation of patterned microstructures of conducting polymers by soft lithography, and applications in microelectronic device fabrication," *Advanced Materials*, vol. 11, pp. 1038, 1999.
- [17] K. Bhadriraju and C. S. Chen, "Engineering cellular microenvironments to improve cell-based drug testing," *Drug Discovery Today*, vol. 7, pp. 612-620, 2002.
- [18] H. Bartos, F. Goetz, and R.-P. Peters, "Microfluidics meets Nano: Lab-on-a-Chip Devices and their Potential for Nanobiotechnology," *Nanobiotechnology: Concepts, Applications and Perspectives*, Wiley-VCH, pp. 13, 2004.
- [19] A. Folch and M. Toner, "Microengineering of cellular interactions," *Annual Review of Biomedical Engineering*, vol. 2, pp. 227-56, 2000.

- [20] F. Rosso, A. Giordano, M. Barbarisi, and A. Barbarisi. "From Cell-ECM interactions to tissue engineering," *Journal of Cellular Physiology*, vol. 199, pp. 174-180, 2004.
- [21] S. L. Voytik-Harbin, A. O. Brightman, M. R. Kraine, B. Waisner, and S. F. Badylak, "Identification of extractable growth factors from small intestinal submucosa," *Journal of Cellular Biochemistry*, vol. 67, pp. 478-491, 1997.
- [22] R. S. Kane, S. Takayama, E. Ostuni, D. E. Ingber, and G. M. Whitesides, "Patterning proteins and cells using soft lithography," *Biomaterials*, vol. 20, pp. 2363, 1999.
- [23] A. J. Engler, S. Sen, H. L. Sweeney, and D. E. Discher, "Matrix elasticity directs stem cell lineage specification," *Cell*, vol. 126, pp. 677-89, 2006.
- [24] A. J. Engler, M. A. Griffin, S. Sen, C. G. Bonnemant, H. L. Sweeney, and D. E. Discher, "Myotubes differentiate optimally on substrates with tissue-like stiffness: pathological implications for soft or stiff microenvironments," *Journal of Cell Biology*, vol. 166, pp. 877-87, 2004.
- [25] D. Schumann, R. Kujat, M. Nerlich, and P. Angele, "Mechanobiological conditioning of stem cells for cartilage tissue engineering," *Bio-Medical Materials and Engineering*, vol. 16, pp. 37-52, 2006.
- [26] C. B. Little, P. Ghosh, and C. R. Bellenger, "Topographic variation in biglycan and decorin synthesis by articular cartilage in the early stages of osteoarthritis: an experimental study in sheep," *Journal of Orthopaedic Research*, vol. 14, pp. 433, 1996.
- [27] K. W. Li, Y. H. Falcovitz, J. P. Nagraj, A. C. Chen, L. M. Lottman, J. Y. J. Shyy, and R. L. Sah, "Mechanical compression modulates proliferation of transplanted chondrocytes," *Journal of Orthopaedic Research*, vol. 18, pp. 374, 2000.
- [28] W. F. Pritchard, P. F. Davies, Z. Derafshi, D. C. Polacek, R. Tsao, R. O. Dull, S. A. Jones, and D. P. Giddens, "Effects of wall shear stress and fluid recirculation on the localization of circulating monocytes in a three-dimensional flow model," *Journal of Biomechanics*, vol. 28, pp. 1459, 1995.
- [29] S. Lossdorfer, Z. Schwartz, L. Wang, C. H. Lohmann, J. D. Turner, M. Wieland, D. L. Cochran, and B. D. Boyan, "Microrough implant surface topographies increase osteogenesis by reducing osteoclast formation and activity," *Journal of Biomedical Materials Research A*, vol. 70, pp. 361-9, 2004.
- [30] A. V. Janorkar, E. W. Fritz Jr, K. J. L. Burg, A. T. Metters, and D. E. Hirt, "Grafting amine-terminated branched architectures from polylactide film surfaces for improved cell proliferation," Annual Technical Conference - ANTEC, Conference Proceedings, Boston, MA, United States, pp. 227, 2005.



- [31] A. Curtis, "Nanofeaturing materials for specific cell responses," Materials Research Society Symposium Proceedings, Boston, MA, United States, pp. 175, 2005.
- [32] H. Zheng, M. C. Berg, M. F. Rubner, and P. T. Hammond, "Controlling cell attachment selectively onto biological polymer-colloid templates using polymer-on-polymer stamping," *Langmuir*, vol. 20, pp. 7215, 2004.
- [33] B. D. Boyan, S. Lossdorfer, L. Wang, G. Zhao, C. H. Lohmann, D. L. Cochran, and Z. Schwartz, "Osteoblasts generate an osteogenic microenvironment when grown on surfaces with rough microtopographies," *European Cells & Materials Journal*, vol. 6, pp. 22-7, 2003.
- [34] B. D. Boyan, J. Lincks, C. H. Lohmann, V. L. Sylvia, D. L. Cochran, C. R. Blanchard, D. D. Dean, and Z. Schwartz, "Effect of surface roughness and composition on costochondral chondrocytes is dependent on cell maturation state," *Journal of Orthopaedic Research*, vol. 17, pp. 446, 1999.
- [35] B. D. Boyan, L. F. Bonewald, E. P. Paschalis, C. H. Lohmann, J. Rosser, D. L. Cochran, D. D. Dean, Z. Schwartz, and A. L. Boskey, "Osteoblast-mediated mineral deposition in culture is dependent on surface microtopography," *Calcified Tissue International*, vol. 71, pp. 519-29, 2002.
- [36] A. S. G. Curtis, N. Gadegaard, M. J. Dalby, M. O. Riehle, C. D. W. Wilkinson, and G. Aitchison, "Cells React to Nanoscale Order and Symmetry in Their Surroundings," *IEEE Transactions on Nanobioscience*, vol. 3, pp. 61, 2004.
- [37] A. S. Curtis, B. Casey, J. O. Gallagher, D. Pasqui, M. A. Wood, and C. D. Wilkinson, "Substratum nanotopography and the adhesion of biological cells. Are symmetry or regularity of nanotopography important?" *Biophysical Chemistry*, vol. 94, pp. 275-83, 2001.
- [38] M. J. Dalby, S. J. Yarwood, M. O. Riehle, H. J. H. Johnstone, S. Affrossman, and A. S. G. Curtis, "Increasing Fibroblast Response to Materials Using Nanotopography: Morphological and Genetic Measurements of Cell Response to 13-nm-High Polymer Demixed Islands," *Experimental Cell Research*, vol. 276, pp. 1-9, 2002.
- [39] M. J. Dalby, S. J. Yarwood, H. J. H. Johnstone, S. Affrossman, and M. O. Riehle, "Fibroblast signaling events in response to nanotopography: a gene array study," *IEEE Transactions on NanoBioscience*, vol. 1, pp. 12-17, 2002.
- [40] R. G. Flemming, C. J. Murphy, G. A. Abrams, S. L. Goodman, and P. F. Nealey, "Effects of synthetic micro-and nano-structured surfaces on cell behavior," *Biomaterials*, vol. 20, pp. 573-88, 1999.

- [41] A. I. Teixeira, G. A. Abrams, P. J. Bertics, C. J. Murphy, and P. F. Nealey, "Epithelial contact guidance on well-defined micro-and nanostructured substrates," *Journal of Cell Science*, vol. 116, pp. 1881-1892, 2003.
- [42] S. Turner, L. Kam, M. Isaacson, H. G. Craighead, W. Shain, and J. Turner, "Cell attachment on silicon nanostructures," *Journal of Vacuum Science & Technology B: Microelectronics and Nanometer Structures*, vol. 15, pp. 2848, 1997.
- [43] A. Curtis, "Tutorial on the biology of nanotopography," *IEEE Transactions on Nanobioscience*, vol. 3, pp. 293, 2004.
- [44] D. K. Mills and J. C. Daniel, "Development of functional specializations within the maturing rabbit flexor digitorum profundus tendon," *Connective Tissue Research*, vol. 30, pp. 37-57, 1993.
- [45] S. Chien, S. Li, and J. Y. J. Shyy, "Effects of Mechanical Forces on Signal Transduction and Gene Expression in Endothelial Cells," *Hypertension*, vol. 31, pp. 162-169, 1998.
- [46] E. Tzima, M. A. Del Pozo, W. B. Kiosses, S. A. Mohamed, S. Li, S. Chien, and M. A. Schwartz, "Activation of Rac1 by shear stress in endothelial cells mediates both cytoskeletal reorganization and effects on gene expression," *The EMBO Journal*, vol. 21, pp. 6791-6800, 2002.
- [47] H. Huang, J. Sylvan, M. Jonas, R. Barresi, P. T. C. So, K. P. Campbell, and R. T. Lee, "Cell stiffness and receptors: evidence for cytoskeletal subnetworks," *American Journal of Physiology - Cell Physiology*, vol. 288, pp. C72-80, 2005.
- [48] S. B. Carter, "Principles of cell motility: the direction of cell movement and cancer invasion," *Nature*, vol. 208, pp. 1183-1187, 1965.
- [49] J. Saranak and K. W. Foster, "Rhodopsin guides fungal phototaxis," *Nature*, vol. 387, pp. 465-466, 1997.
- [50] C. M. Lo, H. B. Wang, M. Dembo, and Y. Wang, "Cell Movement Is Guided by the Rigidity of the Substrate," *Biophysical Journal*, vol. 79, pp. 144-152, 2000.
- [51] M. F. Pittenger, A. M. Mackay, S. C. Beck, R. K. Jaiswal, R. Douglas, J. D. Mosca, M. A. Moorman, D. W. Simonetti, S. Craig, and D. R. Marshak, "Multilineage potential of adult human mesenchymal stem cells," *Science*, vol. 284, pp. 143, 1999.
- [52] T. Reya, S. J. Morrison, M. F. Clarke, and I. L. Weissman, "Stem cells, cancer, and cancer stem cells," *Nature*, vol. 414, pp. 105, 2001.
- [53] C. Massard, E. Deutsch, and J. C. Soria, "Tumour stem cell-targeted treatment: elimination or differentiation," *Annals of Oncology*, vol. 17, pp. 1620-1624, 2006.

- [54] W. A. Eaton and J. Hofrichter, "Hemoglobin S gelation and sickle cell disease," *Blood*, vol. 70, pp. 1245-1266, 1987.
- [55] U. Laufs and J. K. Liao, "Targeting Rho in Cardiovascular Disease," *Circulation Research*, vol. 87, pp. 526-528, 2000.
- [56] J. C. Daniel and D. K. Mills, "Proteoglycan synthesis by cells cultured from regions of the rabbit flexor tendon," *Connective Tissue Research*, vol. 17, pp. 215-30, 1988.
- [57] T. Aigner and J. Dudhia, "Phenotypic modulation of chondrocytes as a potential therapeutic target in osteoarthritis: a hypothesis," *Annals of the Rheumatic Diseases*, vol. 56, pp. 287-291, 1997.
- [58] R. C. Thompson and T. R. Oegema, "Metabolic activity of articular cartilage in osteoarthritis. An in vitro study," *Journal of Bone and Joint Surgery*, vol. 61, pp. 407-16, 1979.
- [59] H. J. Mankin, M. E. Johnson, and L. Lippiello, "Biochemical and metabolic abnormalities in articular cartilage from osteoarthritic human hips. III. Distribution and metabolism of amino sugar-containing macromolecules," *Journal of Bone and Joint Surgery*, vol. 63, pp. 131-9, 1981.
- [60] M. B. Sweet, E. J. Thonar, A. R. Immelman, and L. Solomon, "Biochemical changes in progressive osteoarthrosis," *Annals of the Rheumatic Diseases*, vol. 36, pp. 387-398, 1977.
- [61] C. S. Chen, M. Mrksich, S. Huang, G. M. Whitesides, and D. E. Ingber, "Geometric Control of Cell Life and Death," *Science*, vol. 276, pp. 1425-1428, 1997.
- [62] G. Maheshwari, G. Brown, D. A. Lauffenburger, A. Wells, and L. G. Griffith, "Cell adhesion and motility depend on nanoscale RGD clustering," *Journal of Cell Science*, 113 (Pt 10), pp. 1677-86, 2000.
- [63] L. Y. Koo, D. J. Irvine, A. M. Mayes, D. A. Lauffenburger, and L. G. Griffith, "Co-regulation of cell adhesion by nanoscale RGD organization and mechanical stimulus," *Journal of Cell Science*, vol. 115, pp. 1423-1433, 2002.
- [64] A. J. Putnam, K. Schultz, and D. J. Mooney, "Control of microtubule assembly by extracellular matrix and externally applied strain," *American Journal of Physiology- Cell Physiology*, vol. 280, pp. 556-564, 2001.
- [65] G. Condorelli, U. Borello, L. De Angelis, M. Latronico, D. Sirabella, M. Coletta, R. Galli, G. Balconi, A. Follenzi, and G. Frati, "Cardiomyocytes induce endothelial cells to trans-differentiate into cardiac muscle: Implications for myocardium regeneration," *Proceedings of the National Academy of Sciences*, vol. 98, pp. 10733-10738, 2001.

- [66] S. N. Bhatia, M. L. Yarmush, and M. Toner, "Controlling cell interactions by micropatterning in co-cultures: hepatocytes and 3T3 fibroblasts," *Journal of Biomedical Materials Research*, vol. 34, pp. 189, 1997.
- [67] S. N. Bhatia, U. J. Balis, M. L. Yarmush, and M. Toner, "Microfabrication of Hepatocyte/Fibroblast Co-cultures: Role of Homotypic Cell Interactions," *Biotechnology Progress*, vol. 14, pp. 378-387, 1998.
- [68] R. M. Overney, E. Meyer, J. Frommer, H. J. Guentherodt, G. Decher, J. Reibel, and U. Sohling, "Comparative atomic force microscopic study of liquid crystal films: Transferred freely-suspended vs Langmuir-Blodgett. Morphology, lattice, and manipulation," *Langmuir*, vol. 9, pp. 341, 1993.
- [69] S. Y. Yang, D. Lee, R. E. Cohen, and M. F. Rubner, "Bioinert solution-cross-linked hydrogen-bonded multilayers on colloidal particles," *Langmuir*, vol. 20, pp. 5978, 2004.
- [70] L. Yan, W. T. S. Huck, and G. M. Whitesides, "Self-assembled monolayers (SAMs) and synthesis of planar micro- and nanostructures," *Journal of Macromolecular Science - Polymer Reviews*, vol. 44, pp. 175, 2004.
- [71] J. L. Wilbur, A. Kumar, H. A. Biebuyck, E. Kim, and G. M. Whitesides, "Microcontact printing of self-assembled monolayers: applications in microfabrication," *Nanotechnology*, vol. 7, pp. 452, 1996.
- [72] G. M. Whitesides, G. S. Ferguson, D. Allara, D. Scherson, L. Speaker, and A. Ulman, "Organized molecular assemblies," *Critical Reviews in Surface Chemistry*, vol. 3, pp. 49-65, 1993.
- [73] M. Li, D. K. Mills, T. Cui, and M. J. McShane, "Cellular response to gelatin- and fibronectin-coated multilayer polyelectrolyte nanofilms," *IEEE Transactions on Nanobioscience*, vol. 4, pp. 170, 2005.
- [74] M. Li, K. K. Kondabatni, T. Cui, and M. J. McShane, "Fabrication of 3-D Gelatin-Patterned Glass Substrates With Layer-by-Layer and Lift-Off (LbL-LO) Technology," *IEEE Transactions on Nanotechnology*, vol. 3, pp. 115, 2004.
- [75] X. Wen, D. Shi, and N. Zhang, "Applications of Nanotechnology in Tissue Engineering," *Handbook of Nanostructured Biomaterials and Their Applications in Nanobiotechnology*. American Scientific Publishers, pp. 1-22, 2005.
- [76] T. Niwa, H. Yokoi, T. Kinoshita, and S. Zhang, "Construction of polypeptide-based nano-template," *Polymer Journal*, vol. 36, pp. 665, 2004.
- [77] Y. Lvov, F. Essler, and G. Decher, "Combination of polycation/polyanion self-assembly and Langmuir-Blodgett transfer for the construction of superlattice films," *Journal of Physical Chemistry*, vol. 97, pp. 13773, 1993.

- [78] G. Decher and A. Ulman, "Introduction to ultrathin organic films from Langmuir-Blodgett to self-assembly," *Angewandte Chemie (International Edition in English)*, vol. 31, pp. 929, 1992.
- [79] C. D. Tidwell, S. J. Ertel, B. D. Ratner, B. J. Tarasevich, S. Atre, and D. L. Allara, "Endothelial cell growth and protein adsorption on terminally functionalized, self-assembled monolayers of alkanethiolates on gold," *Langmuir*, vol. 13, pp. 3404, 1997.
- [80] N. J. Sniadecki, R. A. Desai, S. A. Ruiz, and C. S. Chen, "Nanotechnology for cell-substrate interactions," *Annals of Biomedical Engineering*, vol. 34, pp. 59, 2006.
- [81] E. Ostuni, R. G. Chapman, M. N. Liang, G. Meluleni, G. Pier, D. E. Ingber, and G. M. Whitesides, "Self-assembled monolayers that resist the adsorption of proteins and the adhesion of bacterial and mammalian cells," *Langmuir*, vol. 17, pp. 6336, 2001.
- [82] Y. Nam, B. C. Wheeler, and G. Brewer, "*Electrical recordings with gold coated microelectrode arrays that permit the control of neuronal attachment*," Annual International Conference of the IEEE Engineering in Medicine and Biology-Proceedings, Houston, TX, United States, pp. 2125, 2002.
- [83] Y. Nam, J. C. Chang, B. C. Wheeler, and G. J. Brewer, "Gold-Coated Microelectrode Array with Thiol Linked Self-Assembled Monolayers for Engineering Neuronal Cultures," *IEEE Transactions on Biomedical Engineering*, vol. 51, pp. 158, 2004.
- [84] L. Lu, L. Kam, M. Hasenbein, K. Nyalakonda, R. Bizios, A. Gopferich, J. F. Young, and A. G. Mikos, "Retinal pigment epithelial cell function on substrates with chemically micropatterned surfaces," *Biomaterials*, vol. 20, pp. 2351, 1999.
- [85] W. S. Dillmore, M. N. Yousaf, and M. Mrksich, "A photochemical method for patterning the immobilization of ligands and cells to self-assembled monolayers," *Langmuir*, vol. 20, pp. 7223, 2004.
- [86] C. A. Scotchford, C. P. Gilmore, E. Cooper, G. J. Leggett, and S. Downes, "Protein adsorption and human osteoblast-like cell attachment and growth on alkylthiol on gold self-assembled monolayers," *Journal of Biomedical Materials Research*, vol. 59, pp. 84, 2002.
- [87] C. S. Chen, M. Mrksich, S. Huang, G. M. Whitesides, and D. E. Ingber, "Micropatterned surfaces for control of cell shape, position, and function," *Biotechnology Progress*, vol. 14, pp. 356, 1998.

- [88] J. Shaikh-Mohammed, M. Li, D. Terala, and M. J. McShane, "*Integrated Micro/Nano-Fabrication of Cell Culture Scaffolds with Selective Cell Adhesion and Fluorescent Indicators*," Proceedings of SPIE - The International Society for Optical Engineering, San Jose, CA., United States, pp. 43, 2004.
- [89] J. Shaikh-Mohammed, M. A. DeCoster, and M. J. McShane, "*Cell adhesion testing using novel testbeds containing micropatterns of complex nanoengineered multilayer films*," Annual International Conference of the IEEE Engineering in Medicine and Biology – Proceedings, San Francisco, CA, United States, pp. 2671, 2004.
- [90] J. Shaikh Mohammed, M. A. DeCoster, and M. J. McShane, "Fabrication of interdigitated micropatterns of self-assembled polymer nanofilms containing cell-adhesive materials," *Langmuir*, vol. 22, pp. 2738, 2006.
- [91] J. S. Mohammed, M. A. DeCoster, and M. J. McShane, "Micropatterning of nanoengineered surfaces to study neuronal cell attachment in vitro," *Biomacromolecules*, vol. 5, pp. 1745, 2004.
- [92] G. B. Sukhorukov, H. Moehwald, G. Decher, and Y. M. Lvov, "Assembly of polyelectrolyte multilayer films by consecutively alternating adsorption of polynucleotides and polycations," *Thin Solid Films*, vol. 284-285, pp. 220, 1996.
- [93] G. Decher and J. D. Hong, "*Buildup of ultrathin multilayer films by a self-assembly process, 1. Consecutive adsorption of anionic and cationic bipolar amphiphiles on charged surfaces*," European Conference on Organized Organic Thin Films, Mainz, Germany, pp. 321, 1991.
- [94] G. Decher and J. D. Hong, "Buildup of ultrathin multilayer films by a self-assembly process. II. Consecutive adsorption of anionic and cationic bipolar amphiphiles and polyelectrolytes on charged surfaces," *Berichte der Bunsengesellschaft fuer Physikalische Chemie*, vol. 95, pp. 1430, 1991.
- [95] K. Tsuchiya, G. Chen, T. Ushida, T. Matsuno, and T. Tateishi, "Effects of cell adhesion molecules on adhesion of chondrocytes, ligament cells and mesenchymal stem cells," *Materials Science and Engineering C*, vol. 17, pp. 79, 2001.
- [96] T. Cui, F. Hua, and Y. Lvov, "Lithographic approach to pattern multiple nanoparticle thin films prepared by layer-by-layer self-assembly for microsystems," *Sensors and Actuators, A: Physical*, vol. 114, pp. 501, 2004.
- [97] H. Thissen, Y. P. Li, L. Meagher, and W. B. Tsai, "*Surface modification of biodegradable polymers with layer-by-layer coatings*," Transactions - 7th World Biomaterials Congress, Sydney, Australia, pp. 551, 2004.

- [98] S. Yang, Y. Zhang, L. Wang, S. Hong, J. Xu, Y. Chen, and C. Li, "Composite thin film by hydrogen-bonding assembly of polymer brush and poly(vinylpyrrolidone)," *Langmuir*, vol. 22, pp 338, 2006.
- [99] Y. Zhong, B. Li, and D. T. Haynie, "Fine tuning of physical properties of designed polypeptide multilayer films by control of pH," *Biotechnology Progress*, vol. 22, pp. 126, 2006.
- [100] L. Zhang, B. Li, Z.-L. Zhi, and D. T. Haynie, "Perturbation of nanoscale structure of polypeptide multilayer thin films," *Langmuir*, vol. 21, pp. 5439, 2005.
- [101] B. Li and D. T. Haynie, "Multilayer biomimetics: Reversible covalent stabilization of a nanostructured biofilm," *Biomacromolecules*, vol. 5, pp. 1667, 2004.
- [102] L. Richert, P. Lavallo, E. Payan, X. Z. Shu, G. D. Prestwich, J.-F. Stoltz, P. Schaaf, J.-C. Voegel, and C. Picart, "Layer by Layer Buildup of Polysaccharide Films: Physical Chemistry and Cellular Adhesion Aspects," *Langmuir*, vol. 20, pp. 448, 2004.
- [103] Y. Lvov, G. Decher, H. Haas, H. Mohwald, and A. Kalachev, "X-ray analysis of ultrathin polymer films self-assembled onto substrates," *Physica B: Condensed Matter*, vol. 198, pp. 89, 1994.
- [104] Y. Lvov, G. Decher, and G. Sukhorukov, "Assembly of thin films by means of successive deposition alternate layers of DNA and poly(allylamine)," *Macromolecules*, vol. 26, pp. 5396, 1993.
- [105] C. M. Jewell, J. Zhang, N. J. Fredin, and D. M. Lynn, "Multilayered polyelectrolyte films for the localized delivery of DNA to cells," AICHE Annual Meeting, Conference Proceedings, Cincinnati, OH, United States, pp. 4532, 2005.
- [106] C. M. Jewell, J. Zhang, N. J. Fredin, and D. M. Lynn, "Multilayered polyelectrolyte films promote the direct and localized delivery of DNA to cells," *Journal of Controlled Release*, vol. 106, pp. 214, 2005.
- [107] G. Decher, F. Ebler, J. D. Hong, K. Lowack, J. Schmitt, and Y. Lvov, "Layer-by-layer adsorbed films of polyelectrolytes, proteins or DNA," *Polymer Preprints, Division of Polymer Chemistry, American Chemical Society*, vol. 34, pp. 745, 1993.
- [108] E. W. Stein and M. J. McShane, "Multilayer lactate oxidase shells on colloidal carriers as engines for nanosensors," *IEEE Transactions on Nanobioscience*, vol. 2, pp. 133, 2003.
- [109] R. Srivastava, J. Q. Brown, H. Zhu, and M. J. McShane, "Stabilization of glucose oxidase in alginate microspheres with photoreactive diazoresin nanofilm coatings," *Biotechnology and Bioengineering*, vol. 91, pp. 124, 2005.

- [110] R. Srivastava, J. Q. Brown, H. Zhu, and M. J. McShane, "Stable encapsulation of active enzyme by application of multilayer nanofilm coatings to alginate microspheres," *Macromolecular Bioscience*, vol. 5, pp. 717, 2005.
- [111] C. Picart, A. Schneider, O. Etienne, J. Mutterer, P. Schaaf, C. Egles, N. Jessel, and J.-C. Voegel, "Controlled degradability of polysaccharide multilayer films in vitro and in vivo," *Advanced Functional Materials*, vol. 15, pp. 1771, 2005.
- [112] H. Ai, M. Fang, Y. M. Lvov, D. K. Mills, and S. A. Jones, "Applications of the electrostatic layer-by-layer self-assembly technique in biomedical engineering," Annual International Conference of the IEEE Engineering in Medicine and Biology – Proceedings, Houston, TX, United States, pp. 502, 2002.
- [113] J. Lahann, M. Balcells, T. Rodon, J. Lee, I. S. Choi, K. F. Jensen, and R. Langer, "Reactive polymer coatings: A platform for patterning proteins and mammalian cells onto a broad range of materials," *Langmuir*, vol. 18, pp. 3632, 2002.
- [114] H. Ai, Y. M. Lvov, D. K. Mills, H. Meng, X. Qiao, J. S. Alexander, and S. A. Jones, "Coating bio-nanofilm on PDMS through layer-by-layer self-assembly," Annual International Conference of the IEEE Engineering in Medicine and Biology – Proceedings, Houston, TX, United States, pp. p 608, 2002.
- [115] H. Zhu, J. Ji, and J. Shen, "Osteoblast growth promotion by protein electrostatic self-assembly on biodegradable poly(lactide)," *Journal of Biomaterials Science, Polymer Edition*, vol. 16, pp. 761, 2005.
- [116] L. Richert, Y. Arntz, P. Schaaf, J.-C. Voegel, and C. Picart, "*ph dependent growth of poly(l-lysine)/poly(l-glutamic) acid multilayer films and their cell adhesion properties*," Biosurf V: Functional Polymeric Surfaces in Biotechnology, Zurich, Switzerland, pp. 13, 2004.
- [117] S. Y. Yang, J. D. Mendelsohn, and M. F. Rubner, "New class of ultrathin, highly cell-adhesion-resistant polyelectrolyte multilayers with micropatterning capabilities," *Biomacromolecules*, vol. 4, pp. 987, 2003.
- [118] P. Tryoen-Toth, D. Vautier, Y. Haikel, J.-C. Voegel, P. Schaaf, J. Chluba, and J. Ogier, "Viability, adhesion, and bone phenotype of osteoblast-like cells on polyelectrolyte multilayer films," *Journal of Biomedical Materials Research*, vol. 60, pp. 657, 2002.
- [119] L. Richert, F. Boulmedais, P. Lavalle, J. Mutterer, E. Ferreux, G. Decher, P. Schaaf, J.-C. Voegel, and C. Picart, "Improvement of stability and cell adhesion properties of polyelectrolyte multilayer films by chemical cross-linking," *Biomacromolecules*, vol. 5, pp. 284, 2004.



- [120] C. Picart, R. Elkaim, L. Richert, F. Audoin, Y. Arntz, M. D. S. Cardoso, P. Schaaf, J.-C. Voegel, and B. Frisch, "Primary cell adhesion on RGD-functionalized and covalently crosslinked thin polyelectrolyte multilayer films," *Advanced Functional Materials*, vol. 15, pp. 83, 2005.
- [121] M. R. Kreke, A. S. Badami, J. B. Brady, R. Michael Akers, and A. S. Goldstein, "Modulation of protein adsorption and cell adhesion by poly(allylamine hydrochloride) heparin films," *Biomaterials*, vol. 26, pp. 2975-2981, 2005.
- [122] M. C. Berg, J. D. Mendelsohn, S. Y. Yang, P. T. Hammond, and M. F. Rubner, "Controlling cell adhesion on polyelectrolyte multilayers through micropatterning," Abstracts of Papers, 223rd ACS National Meeting, Orlando, FL, United States, pp. Coll-158, 2002.
- [123] C. Vodouhe, M. Schmittbuhl, F. Boulmedais, D. Bagnard, D. Vautier, P. Schaaf, C. Egles, J.-C. Voegel, and J. Ogier, "Effect of functionalization of multilayered polyelectrolyte films on motoneuron growth," *Biomaterials*, vol. 26, pp. 545, 2005.
- [124] D. Vautier, V. Karsten, C. Egles, J. Chluba, P. Schaaf, J.-C. Voegel, and J. Ogier, "Polyelectrolyte multilayer films modulate cytoskeletal organization in chondrosarcoma cells," *Journal of Biomaterials Science, Polymer Edition*, vol. 13, pp. 713-732, 2002.
- [125] K. Cai, A. Rechtenbach, J. Hao, J. Bossert, and K. D. Jandt, "Polysaccharide-protein surface modification of titanium via a layer-by-layer technique: Characterization and cell behaviour aspects," *Biomaterials*, vol. 26, pp. 5960, 2005.
- [126] L. Mhamdi, C. Picart, C. Lagneau, A. Othmane, B. Grosgeat, N. Jaffrezic-Renault, and L. Ponsonnet, "Study of the polyelectrolyte multilayer thin films' properties and correlation with the behavior of the human gingival fibroblasts," *Materials Science and Engineering C*, vol. 26, pp. 273, 2006.
- [127] C. Boura, S. Muller, D. Vautier, D. Dumas, P. Schaaf, J. C. Voegel, J. F. Stoltz, and P. Menu, "Endothelial cell - Interactions with polyelectrolyte multilayer films," *Biomaterials*, vol. 26, pp. 4568, 2005.
- [128] N. Benkirane-Jessel, P. Lavalle, F. Meyer, F. Audouin, B. Frisch, P. Schaaf, J. Ogier, G. Decher, and J.-C. Voegel, "Control of monocyte morphology on and response to model surfaces for implants equipped with anti-inflammatory agents," *Advanced Materials*, vol. 16, pp. 1507, 2004.
- [129] L. Richert, A. J. Engler, D. E. Discher, and C. Picart, "Elasticity of native and cross-linked polyelectrolyte multilayer films," *Biomacromolecules*, vol. 5, pp. 1908, 2004.

- [130] D. L. Elbert, C. B. Herbert, and J. A. Hubbell, "Thin polymer layers formed by polyelectrolyte multilayer techniques on biological surfaces," *Langmuir*, vol. 15, pp. 5355, 1999.
- [131] Y. Zhu, C. Gao, Y. Liu, and J. Shen, "Endothelial cell functions in vitro cultured on poly(L-lactic acid) membranes modified with different methods," *Journal of Biomedical Materials Research - Part A*, vol. 69, pp. 436, 2004.
- [132] Y. Zhu, C. Gao, T. He, X. Liu, and J. Shen, "Layer-by-layer assembly to modify poly(L-lactic acid) surface toward improving its cytocompatibility to human endothelial cells," *Biomacromolecules*, vol. 4, pp. 446, 2003.
- [133] H. Zhu, J. Ji, Q. Tan, J. Shen, and M. A. Barbosa, "Surface engineering of poly(DL-lactide) via electrostatic self-assembly of extracellular matrix-like molecules," *Biomacromolecules*, vol. 4, pp. 378, 2003.
- [134] H. Zhu, J. Ji, and J. Shen, "Construction of multilayer coating onto poly-(DL-lactide) to promote cytocompatibility," *Biomaterials*, vol. 25, pp. 109, 2004.
- [135] L. Zhang, G. Feng, J. Chen, X. Li, Y. Gao, and M. Shen, "Nonlinear gain coefficient experienced by non-paraxial perturbations under small signal approximation," Proceedings of SPIE - The International Society for Optical Engineering, San Diego, CA, United States, pp. 1, 2005.
- [136] P. D. Benya and J. D. Shaffer, "Dedifferentiated chondrocytes reexpress the differentiated collagen phenotype when cultured in agarose gels," *Cell*, vol. 30, pp. 215, 1982.
- [137] S. Kidambi, I. Lee, and C. Chan, "Patterns of aptamers on polyelectrolyte multilayers," AIChE Annual Meeting, Conference Proceedings, Cincinnati, OH, United States, pp. 4296, 2005.
- [138] J. J. J. P. Van Den Beucken, M. R. J. Vos, P. C. Thune, T. Hayakawa, T. Fukushima, Y. Okahata, X. F. Walboomers, N. A. J. M. Sommerdijk, R. J. M. Nolte, and J. A. Jansen, "Fabrication, characterization, and biological assessment of multilayered DNA-coatings for biomaterial purposes," *Biomaterials*, vol. 27, pp. 691, 2006.
- [139] S. H. Kim, S.-Y. Kwak, B.-H. Sohn, and T. H. Park, "Design of TiO<sub>2</sub> nanoparticle self-assembled aromatic polyamide thin-film-composite (TFC) membrane as an approach to solve biofouling problem," *Journal of Membrane Science*, vol. 211, pp. 157, 2003.
- [140] D. Kommireddy, J. Shi, X. Yan, H. Ji, and Y. Lvov, "Electrostatic layer-by-layer nano-assembly: Films, cantilevers, micropatterns and nanocapsules," Proceedings of SPIE - The International Society for Optical Engineering, Philadelphia, PA, United States, pp. 120, 2005.

- [141] C. Picart, P. Lavalle, P. Hubert, F. J. G. Cuisinier, G. Decher, P. Schaaf, and J. C. Voegel, "Buildup mechanism for poly(L-lysine)/hyaluronic acid films onto a solid surface," *Langmuir*, vol. 17, pp. 7414, 2001.
- [142] P. Lavalle, C. Gergely, F. J. G. Cuisinier, G. Decher, P. Schaaf, J. C. Voegel, and C. Picart, "Comparison of the structure of polyelectrolyte multilayer films exhibiting a linear and an exponential growth regime: An in situ atomic force microscopy study," *Macromolecules*, vol. 35, pp. 4458, 2002.
- [143] F. Boulmedais, V. Ball, P. Schwinte, B. Frisch, P. Schaaf, and J.-C. Voegel, "Buildup of exponentially growing multilayer polypeptide films with internal secondary structure," *Langmuir*, vol. 19, pp. 440, 2003.
- [144] E. M. Liston, L. Martinu, and M. R. Wertheimer, "Plasma surface modification of polymers for improved adhesion: a critical review," *Journal of adhesion science and technology*, vol. 7, pp. 1091-1127, 1993.
- [145] M. Mrksich, "A surface chemistry approach to studying cell adhesion," *Chemical Society Reviews*, vol. 29, pp. 267-273, 2000.
- [146] R. G. Nuzzo and D. L. Allara, "Adsorption of bifunctional organic disulfides on gold surfaces," *Journal of the American Chemical Society*, vol. 105, pp. 4481-4483, 1983.
- [147] Y. Xia and G. M. Whitesides, "Soft lithography," *Annual Review of Materials Science: Annual Reviews Inc*, Palo Alto, CA, USA, vol. 28, pp. 153, 1998.
- [148] A. Ulman, "Formation and Structure of Self-Assembled Monolayers," *Chemical Reviews*, vol. 96, pp. 1533-1554, 1996.
- [149] O. M. Magnussen, B. M. Ocko, M. Deutsch, M. J. Regan, P. S. Pershan, D. Abernathy, G. Grübel, and J. F. Legrand, "Self-assembly of organic films on a liquid metal," *Nature*, vol. 384, pp. 250-252, 1996.
- [150] G. K. Jennings and P. E. Laibinis, "Self-Assembled n-Alkanethiolate Monolayers on Underpotentially Deposited Adlayers of Silver and Copper on Gold," *Journal of the American Chemical Society*, vol. 119, pp. 5208-5214, 1997.
- [151] D. P. Dowling, K. Donnelly, M. L. McConnell, R. Eloy, and M. N. Arnaud, "Deposition of anti-bacterial silver coatings on polymeric substrates," *Thin Solid Films*, vol. 398, pp. 602-606, 2001.
- [152] M. Kato and M. Mrksich, "Rewiring cell adhesion," *Journal of the American Chemical Society*, vol. 126, pp. 6504, 2004.

- [153] L. T. Minassian-Saraga, "*Thin Films Including Layers: Terminology In Relation To Their Preparation And Characterization*," Pure And Applied Chemistry, International Union Of Pure And Applied Chemistry, vol. 66, pp. 1667-1738, 1994.
- [154] Y.-Y. Luk, M. Kato, and M. Mrksich, "Self-assembled monolayers of alkanethiolates presenting mannitol groups are inert to protein adsorption and cell attachment," *Langmuir*, vol. 16, pp. 9604, 2000.
- [155] J. C. Love, L. A. Estroff, J. K. Kriebel, R. G. Nuzzo, and G. M. Whitesides, "Self-assembled monolayers of thiolates on metals as a form of nanotechnology," *Chemical Reviews*, vol. 105, pp. 1103, 2005.
- [156] M. N. Yousaf, B. T. Houseman, and M. Mrksich, "Using electroactive substrates to pattern the attachment of two different cell populations," *Proceedings of the National Academy of Sciences*, vol. 98, pp. 5992-5996, 2001.
- [157] M. N. Yousaf, "*New surface chemistries for dynamic substrates*," 208th Meeting of The Electrochemical Society, Los Angeles, CA, United States, pp. 752, 2005.
- [158] T. Serizawa, Y. Arikawa, K.-I. Hamada, H. Yamashita, T. Fujiwara, Y. Kimura, and M. Akashi, "Alkaline hydrolysis of enantiomeric poly(lactide)s stereocomplex deposited on solid substrates," *Macromolecules*, vol. 36, pp. 1762, 2003.
- [159] V. Kozlovskaya, S. Ok, A. Sousa, M. Libera, and S. A. Sukhishvili, "Hydrogen-bonded polymer capsules formed by layer-by-layer self-assembly," *Macromolecules*, vol. 36, pp. 8590-8592, 2003.
- [160] H. Sakaguchi, T. Serizawa, and M. Akashi, "*Nano-coated hydrogels with naturally-occurring polymer films for controlled release application*," Polymer Preprints-Japan, Yamagata, Japan, pp. 4729, 2005.
- [161] C. R. Wittmer, J. A. Phelps, W. M. Saltzman, and P. R. Van Tassel, "Fibronectin terminated multilayer films: Protein adsorption and cell attachment studies," *Biomaterials*, vol. 28, pp. 851, 2007.
- [162] M. Li, H. Ai, D. K. Mills, Y. M. Lvov, B. K. Gale, and M. J. McShane, "*Culturing smooth muscle cells on modified PDMS substrates*," Annual International Conference of the IEEE Engineering in Medicine and Biology – Proceedings, Houston, TX, United States, pp. 388, 2002.
- [163] D. S. Kommireddy, S. M. Sriram, Y. M. Lvov, and D. K. Mills, "Stem cell attachment to layer-by-layer assembled TiO<sub>2</sub> nanoparticle thin films," *Biomaterials*, vol. 27, pp. 4296, 2006.

- [164] K. Glinel, A. Moussa, A. M. Jonas, and A. Laschewsky, "Influence of Polyelectrolyte Charge Density on the Formation of Multilayers of Strong Polyelectrolytes at Low Ionic Strength," *Langmuir*, vol. 18, pp. 1408-1412, 2002.
- [165] R. Steitz, W. Jaeger, and R. v. Klitzing, "Influence of Charge Density and Ionic Strength on the Multilayer Formation of Strong Polyelectrolytes," *Langmuir*, vol. 17, pp. 4471-4474, 2001.
- [166] J. D. Mendelsohn, S. Y. Yang, J. A. Hiller, A. I. Hochbaum, and M. F. Rubner, "Rational design of cytophilic and cytophobic polyelectrolyte multilayer thin films," *Biomacromolecules*, vol. 4, pp. 96, 2003.
- [167] J. Chluba, J. C. Voegel, G. Decher, P. Erbacher, P. Schaaf, and J. Ogier, "Peptide hormone covalently bound to polyelectrolytes and embedded into multilayer architectures conserving full biological activity," *Biomacromolecules*, vol. 2, pp. 800-805, 2001.
- [168] D. R. Reyes, E. M. Perruccio, S. P. Becerra, L. E. Locascio, and M. Gaitan, "Micropatterning neuronal cells on polyelectrolyte multilayers," *Langmuir*, vol. 20, pp. 8805, 2004.
- [169] Z. P. Yang and A. Chilkoti, "*Light-activated affinity micropatterning of proteins*," Annual International Conference of the IEEE Engineering in Medicine and Biology - Proceedings, Atlanta, GA, USA, pp. 738, 1999.
- [170] S. Y. Yang, J. D. Mendelsohn, and M. F. Rubner, "*Patternable, cell-resistant surfaces prepared with H-bonded polyelectrolyte multilayers*," Abstracts of Papers, 224th ACS National Meeting, Boston, MA, United States, pp. POLY-397, 2002.
- [171] Y. C. Wang and C. C. Ho, "Micropatterning of proteins and mammalian cells on biomaterials," *The FASEB Journal*, vol. 18, pp. 525-7, 2004.
- [172] J. L. Tan, W. Liu, C. M. Nelson, S. Raghavan, and C. S. Chen, "Simple approach to micropattern cells on common culture substrates by tuning substrate wettability," *Tissue Engineering*, vol. 10, pp. 865-72, 2004.
- [173] S. A. Park, I. A. Kim, Y. J. Lee, J. W. Shin, C. R. Kim, J. K. Kim, Y. I. Yang, and J. W. Shin, "Biological responses of ligament fibroblasts and gene expression profiling on micropatterned silicone substrates subjected to mechanical stimuli," *Journal of Bioscience and Bioengineering*, vol. 102, pp. 402-12, 2006.
- [174] K. Kurpinski, J. Chu, C. Hashi, and S. Li, "Anisotropic mechanosensing by mesenchymal stem cells," *Proceedings of the National Academy of Sciences U S A*, vol. 103, pp. 16095-100, 2006.

- [175] T. A. Desai, J. Deutsch, D. Motlagh, W. Tan, and B. Russell, "Microtextured Cell Culture Platforms: Biomimetic Substrates for the Growth of Cardiac Myocytes and Fibroblasts," *Biomedical Microdevices*, vol. 2, pp. 123-129, 1999.
- [176] M. Morra and C. Cassinelli, "Cell Adhesion Micropatterning by Plasma Treatment of Alginate Coated Surfaces," *Plasmas and Polymers*, vol. 7, pp. 89, 2002.
- [177] Z. Ma and S. Ramakrishna, "Nanostructured Extracellular Matrix," *Encyclopedia of Nanoscience and Nanotechnology*, Vol. 7, American Scientific Publishers. pp. 641-655, 1998.
- [178] S. N. Bhatia, U. J. Balis, M. L. Yarmush, and M. Toner, "Effect of cell-cell interactions in preservation of cellular phenotype: cocultivation of hepatocytes and nonparenchymal cells," *The FASEB Journal*, vol. 13, pp. 1883-1900, 1999.
- [179] J. Tan, S. N. Bhatia, W. E. Jastromb, C. S. Chen, and J. Y. Tien, "Methods of patterning protein and cell adhesivity." Patent 20020182633, United States, 2002.
- [180] A. R. Derubeis and R. Cancedda, "Bone marrow stromal cells (BMSCs) in bone engineering: Limitations and recent advances," *Annals of Biomedical Engineering*, vol. 32, pp. 160, 2004.
- [181] R. Bellamkonda, J. P. Ranieri, N. Bouche, and P. Aebischer, "Hydrogel-based three-dimensional matrix for neural cells," *Journal of Biomedical Materials Research*, vol. 29, pp. 663-671, 1995.
- [182] E. Cukierman, R. Pankov, D. R. Stevens, and K. M. Yamada, "Taking Cell-Matrix Adhesions to the Third Dimension," *Science*, vol. 294, pp. 1708-1712, 2001.
- [183] K. M. Yamada, R. Pankov, and E. Cukierman, "Dimensions and dynamics in integrin function," *Brazilian Journal of Medical and Biological Research*, vol. 36, pp. 959-966, 2003.
- [184] J. P. Stegemann and R. M. Nerem, "Altered response of vascular smooth muscle cells to exogenous biochemical stimulation in two- and three-dimensional culture," *Experimental Cell Research*, vol. 283, pp. 146-55, 2003.
- [185] S. Shortkroff, J. Garcia, J. H. Yu, J. Lowery, T. S. Thornhill, and G. C. Rutledge, "Nanofibrous/microfibrous scaffolds: Effect of seeding techniques on chondrocyte adhesion," *Transactions - 7th World Biomaterials Congress, Sydney, Australia*, pp. 1613, 2004.
- [186] W.-J. Li, C. T. Laurencin, E. J. Caterson, R. S. Tuan, and F. K. Ko, "Electrospun nanofibrous structure: A novel scaffold for tissue engineering," *Journal of Biomedical Materials Research*, vol. 60, pp. 613, 2002.

- [187] E. Ruoslahti and M. D. Pierschbacher, "New perspectives in cell adhesion: RGD and integrins," *Science*, vol. 238, pp. 491-497, 1987.
- [188] B. M. Gumbiner, "Cell adhesion: the molecular basis of tissue architecture and morphogenesis," *Cell*, vol. 84, pp. 345-57, 1996.
- [189] H. Robson, T. Siebler, D. A. Stevens, S. M. Shalet, and G. R. Williams, "Thyroid Hormone Acts Directly on Growth Plate Chondrocytes to Promote Hypertrophic Differentiation and Inhibit Clonal Expansion and Cell Proliferation," *Endocrinology*, vol. 141, pp. 3887-3897, 2000.
- [190] F. Lupu, J. D. Terwilliger, K. Lee, G. V. Segre, and A. Efstratiadis, "Roles of Growth Hormone and Insulin-like Growth Factor 1 in Mouse Postnatal Growth," *Developmental Biology*, vol. 229, pp. 141-162, 2001.
- [191] F. P. Luyten, Y. M. Yu, M. Yanagishita, S. Vukicevic, R. G. Hammonds, and A. H. Reddi, "Natural bovine osteogenin and recombinant human bone morphogenetic protein-2B are equipotent in the maintenance of proteoglycans in bovine articular cartilage explant cultures," *Journal of Biological Chemistry*, vol. 267, pp. 3691, 1992.
- [192] F. P. Luyten, P. Chen, V. Paralkar, and A. H. Reddi, "Recombinant bone morphogenetic protein-4, transforming growth factor-beta 1, and activin A enhance the cartilage phenotype of articular chondrocytes in vitro," *Experimental Cell Research*, vol. 210, pp. 224-9, 1994.
- [193] E. Kolettas, H. I. Muir, J. C. Barrett, and T. E. Hardingham, "Chondrocyte phenotype and cell survival are regulated by culture conditions and by specific cytokines through the expression of Sox-9 transcription factor," *Rheumatology*, vol. 40, pp. 1146, 2001.
- [194] R. Yasuhara, Y. Miyamoto, T. Akaike, T. Akuta, M. Nakamura, M. Takami, N. Morimura, K. Yasu, and R. Kamijo, "Interleukin-1beta induces death in chondrocyte-like ATDC5 cells through mitochondrial dysfunction and energy depletion in a reactive nitrogen and oxygen species-dependent manner," *Biochemical Journal*, vol. 389, pp. 315, 2005.
- [195] J.-H. Ryu and J.-S. Chun, "Opposing roles of WNT-5A and WNT-11 in interleukin-1beta regulation of type II collagen expression in articular chondrocytes," *Journal of Biological Chemistry*, vol. 281, pp. 22039, 2006.
- [196] J. H. Ryu, S. J. Kim, S. H. Kim, C. D. Oh, S. G. Hwang, C. H. Chun, S. H. Oh, J. K. Seong, T. L. Huh, and J. S. Chun, "Regulation of the chondrocyte phenotype by beta-catenin," *Development*, vol. 29, pp. 5541-5550, 2002..
- [197] R. Langer, H. Brem, and D. Tapper, "Biocompatibility of Polymeric Delivery Systems for Macromolecules," *Journal of Biomedical Materials Research*, vol. 15, pp. 267, 1981.

- [198] R. Langer, "*Macromolecular Delivery Systems for Therapeutic Applications of Controlled Drug Release*," Contemporary Biomaterials: Material and Host Response, Clinical Applications, New Technology, and Legal Aspects: Noyes Publications, Park Ridge, NJ, USA, pp. 560-572, 1984.
- [199] A. J. Khopade and F. Caruso, "Surface-modification of polyelectrolyte multilayer-coated particles for biological applications," *Langmuir*, vol. 19, pp. 6219, 2003.
- [200] M. K. McHale, L. A. Setton, and A. Chilkoti, "Synthesis and in vitro evaluation of enzymatically cross-linked elastin-like polypeptide gels for cartilaginous tissue repair," *Tissue Engineering*, vol. 11, pp. 1768, 2005.
- [201] T. Masuko, N. Iwasaki, S. Yamane, T. Funakoshi, T. Majima, A. Minami, N. Ohsuga, T. Ohta, and S.-I. Nishimura, "Chitosan-RGDSGGC conjugate as a scaffold material for musculoskeletal tissue engineering," *Biomaterials*, vol. 26, pp. 5339, 2005.
- [202] D. L. Elbert and J. A. Hubbell, "Conjugant addition and free-radical crosslinking to produce cell-adhesive materials," *American Chemical Society, Polymer Preprints, Division of Polymer Chemistry*, vol. 41, pp. 991, 2000.
- [203] D. L. Elbert and J. A. Hubbell, "Surface treatments of polymers for biocompatibility," *Polymers*, vol. 26, *Annual Review of Materials Science: Annual Reviews Inc, Palo Alto, CA, USA*, pp. 365, 1996.
- [204] A. J. Engler, L. Richert, J. Y. Wong, C. Picart, and D. E. Discher, "*Surface probe measurements of the elasticity of sectioned tissue, thin gels and polyelectrolyte multilayer films: Correlations between substrate stiffness and cell adhesion*," BIOSURF V: Functional Polymeric Surfaces in Biotechnology, Zurich, Switzerland, pp. 142-154, 2004.
- [205] J. B. Recknor, J. C. Recknor, D. S. Sakaguchi, and S. K. Mallapragada, "Oriented astroglial cell growth on micropatterned polystyrene substrates," *Biomaterials*, vol. 25, pp. 2753-2767, 2004.
- [206] I. M. Shapiro, K. D. Mansfield, S. M. Evans, E. M. Lord, and C. J. Koch, "Chondrocytes in the endochondral growth cartilage are not hypoxic," *American Journal of Physiology- Cell Physiology*, vol. 272, pp. 1134-1143, 1997.
- [207] A. Hall, "Rho GTPases and the Actin Cytoskeleton," *Science*, vol. 279, pp. 509-514, 1998.
- [208] L. A. Durrant, C. W. Archer, M. Benjamin, and J. R. Ralphs, "Organisation of the chondrocyte cytoskeleton and its response to changing mechanical conditions in organ culture," *Journal of Anatomy*, vol. 194, pp. 343-353, 2000.



- [209] W. R. Trickey, G. M. Lee, and F. Guilak, "Viscoelastic properties of chondrocytes from normal and osteoarthritic human cartilage," *Journal of Orthopaedic Research*, vol. 18, pp. 891, 2000.
- [210] W. R. Trickey, F. P. T. Baaijens, T. A. Laursen, L. G. Alexopoulos, and F. Guilak, "Determination of the Poisson's ratio of the cell: Recovery properties of chondrocytes after release from complete micropipette aspiration," *Journal of Biomechanics*, vol. 39, pp. 78, 2006.
- [211] J. L. Guan, J. E. Trevithick, and R. O. Hynes, "Fibronectin/integrin interaction induces tyrosine phosphorylation of a 120-kDa protein," *Cell Regulation*, vol. 2, pp. 951, 1991.
- [212] L. Kornberg, H. S. Earp, J. T. Parsons, M. Schaller, and R. L. Juliano, "Cell adhesion or integrin clustering increases phosphorylation of a focal adhesion-associated tyrosine kinase," *Journal of Biological Chemistry*, vol. 267, pp. 23439-23442, 1992.
- [213] K. Burridge, C. E. Turner, L. H. Romer, "Tyrosine phosphorylation of paxillin and pp125FAK accompanies cell adhesion to extracellular matrix: a role in cytoskeletal assembly," *The Journal of Cell Biology*, vol. 119, pp. 893-903, 1992.
- [214] K. Burridge, K. Fath, T. Kelly, G. Nuckolls, and C. Turner, "Focal Adhesions: Transmembrane Junctions Between the Extracellular Matrix and the Cytoskeleton," *Annual Review of Cell Biology*, vol. 4, pp. 487-525, 1988.
- [215] A. Richardson and J. T. Parsons, "Signal transduction through integrins: A central role for focal adhesion kinase?" *BioEssays*, vol. 17, pp. 229-236, 1995.
- [216] K. M. Yamada and B. Geiger, "Molecular interactions in cell adhesion complexes," *Current Opinion in Cell Biology*, vol. 9, pp. 76-85, 1997.
- [217] B. Geiger, S. Yehuda-Levenberg, and A. D. Bershadsky, "Molecular interactions in the submembrane plaque of cell-cell and cell-matrix adhesions," *Acta Anatomica (Basel)*, vol. 154, pp. 46-62, 1995.
- [218] N. Q. Balaban, U. S. Schwarz, D. Riveline, P. Goichberg, G. Tzur, I. Sabanay, D. Mahalu, S. Safran, A. Bershadsky, and L. Addadi, "Force and focal adhesion assembly: a close relationship studied using elastic micropatterned substrates," *Nature Cell Biology*, vol. 3, pp. 466-472, 2001.
- [219] F. G. Giancotti and E. Ruoslahti, "Integrin Signaling," *Science*, vol. 285, pp. 1028-1033, 1999.
- [220] D. Segat, R. Comai, E. Di Marco, A. Strangio, R. Cancedda, A. T. Franzini, and C. Tacchetti, "Integrins alpha(6A)beta 1 and alpha(6B)beta 1 promote different stages of chondrogenic cell differentiation," *Journal of Biological Chemistry*, vol. 277, pp. 31612, 2002.

- [221] D. L. Reid, M. B. Aydelotte, and J. Mollenhauer, "Cell attachment, collagen binding, and receptor analysis on bovine articular chondrocytes," *Journal of Orthopaedic Research*, vol. 18, pp. 364, 2000.
- [222] S. J. Millward-Sadler and D. M. Salter, "Integrin-dependent signal cascades in chondrocyte mechanotransduction," *Annals of Biomedical Engineering*, vol. 32, pp. 435, 2004.
- [223] R. F. Loeser, C. S. Carlson, and M. P. McGee, "Expression of beta 1 integrins by cultured articular chondrocytes and in osteoarthritic cartilage," *Experimental Cell Research*, vol. 217, pp. 248-57, 1995.
- [224] R. F. Loeser, "Integrin-mediated attachment of articular chondrocytes to extracellular matrix proteins," *Arthritis & Rheumatism*, , vol. 36, pp. 1103-10, 1993.
- [225] R. F. Loeser, "Modulation of integrin-mediated attachment of chondrocytes to extracellular matrix proteins by cations, retinoic acid, and transforming growth factor beta," *Experimental Cell Research*, vol. 211, pp. 17-23, 1994.
- [226] M. S. Kurtis, B. P. Tu, O. A. Gaya, J. Mollenhauer, W. Knudson, R. F. Loeser, C. B. Knudson, and R. L. Sah, "Mechanisms of chondrocyte adhesion to cartilage: Role of beta1-integrins, CD44, and annexin V," *Journal of Orthopaedic Research*, vol. 19, pp. 1122, 2001.
- [227] S. J. Kim, E. J. Kim, Y. H. Kim, S. B. Hahn, and J. W. Lee, "The modulation of integrin expression by the extracellular matrix in articular chondrocytes," *Yonsei Medical Journal*, vol. 44, pp. 493-501, 2003.
- [228] T. T. Chowdhury, R. N. Appleby, D. M. Salter, D. A. Bader, and D. A. Lee, "Integrin-mediated mechanotransduction in IL-1beta stimulated chondrocytes," *Biomechanics and Modeling in Mechanobiology*, vol. 5, pp. 192, 2006.
- [229] F. H. Chen, A. O. Thomas, J. T. Hecht, M. B. Goldring, and J. Lawler, "Cartilage oligomeric matrix protein/thrombospondin 5 supports chondrocyte attachment through interaction with integrins," *Journal of Biological Chemistry*, vol. 280, pp. 32655, 2005.
- [230] H. D. Inerowicz, S. Howell, F. E. Regnier, and R. Reifenger, "Multiprotein Immunoassay Arrays Fabricated by Microcontact Printing," *Langmuir*, vol. 18, pp. 5263-5268, 2002.
- [231] X. P. Jiang, S. L. Clark, and P. T. Hammond, "Side-by-Side Directed Multilayer Patterning Using Surface Templates," *Advanced Materials*, vol. 13, pp. 1669, 2001.

- [232] X. Jiang, H. Zheng, S. Gourdin, and P. T. Hammond, "Polymer-on-Polymer Stamping: Universal Approaches to Chemically Patterned Surfaces," *Langmuir*, vol. 18, pp. 2607-2615, 2002.
- [233] L. Yan, X.-M. Zhao, and G. M. Whitesides, "Patterning a preformed, reactive SAM using microcontact printing," *Journal of the American Chemical Society*, vol. 120, pp. 6179, 1998.
- [234] Y. Xia and G. M. Whitesides, "Reduction in the size of features of patterned SAMs generated by microcontact printing with mechanical compression of the stamp," *Advanced Materials*, vol. 7, pp. 471, 1995.
- [235] E. Ostuni, R. Kane, C. S. Chen, D. E. Ingber, and G. M. Whitesides, "Patterning mammalian cells using elastomeric membranes," *Langmuir*, vol. 16, pp. 7811, 2000.
- [236] A. Folch, B.-H. Jo, B.-H. Hurtado, D. J. Beebe, O. Hurtado, and M. Toner, "Microfabricated elastomeric stencils for micropatterning cell cultures," *Journal of Biomedical Materials Research*, vol. 52, pp. 346, 2000.
- [237] J. Park and P. T. Hammond, "Multilayer Transfer Printing for Polyelectrolyte Multilayer Patterning: Direct Transfer of Layer-by-Layer Assembled Micropatterned Thin Films," *Advanced Materials*, vol. 16, pp. 520-525, 2004.
- [238] J. Park, L. D. Fouche, and P. T. Hammond, "Multicomponent patterning of layer-by-layer assembled polyelectrolyte/nanoparticle composite thin films with controlled alignment," *Advanced materials*, vol. 17, pp. 2575-2579, 2005.
- [239] S. K. Sia and G. M. Whitesides, "Microfluidic devices fabricated in Poly (dimethylsiloxane) for biological studies," *Electrophoresis*, vol. 24, pp. 3563-3576, 2003.
- [240] A. S. Blawas and W. M. Reichert, "Review Protein Patterning," *Biomaterials*, vol. 19, pp. 595-609, 1998.
- [241] Y. Ito, "Surface micropatterning to regulate cell functions," *Biomaterials*, vol. 20, pp. 2333-42, 1999.
- [242] H. Sorribas, C. Padeste, and L. Tiefenauer, "Photolithographic generation of protein micropatterns for neuron culture applications," *Biomaterials*, vol. 23, pp. 893-900, 2002.
- [243] C. S. Lee, S. H. Lee, S. S. Park, Y. K. Kim, and B. G. Kim, "Protein patterning on silicon-based surface using background hydrophobic thin film," *Biosensors and Bioelectronics*, vol. 18, pp. 437-444, 2003.

- [244] A. Douvas, P. Argitis, C. D. Diakoumakos, K. Misiakos, D. Dimotikali, and S. E. Kakabakos, "Photolithographic patterning of proteins with photoresists processable under biocompatible conditions," *Journal of Vacuum Science & Technology B: Microelectronics and Nanometer Structures*, vol. 19, pp. 2820, 2001.
- [245] C. D. Diakoumakos, A. Douvas, I. Raptis, S. Kakabakos, D. Dimotikalli, G. Terzoudi, and P. Argitis, "Dilute aqueous base developable resists for environmentally friendly and biocompatible processes," *Microelectronic Engineering*, vol. 61, pp. 819-827, 2002.
- [246] J. M. Havard, N. Vladimirov, J. M. J. Frechet, S. Yamada, C. G. Willson, and J. D. Byers, "Photoresists with reduced environmental impact: Water-soluble resists based on photo-cross-linking of a sugar-containing polymethacrylate," *Macromolecules*, vol. 32, pp. 86-94, 1999.
- [247] F. Hua, Y. Lvov, and T. Cui, "Spatial Patterning of Colloidal Nanoparticle-Based Thin Film by a Combinative Technique of Layer-by-Layer Self-Assembly and Lithography," *Journal of Nanoscience and Nanotechnology*, vol. 2, pp. 357-361, 2002.
- [248] H. G. Abdelhady, S. Allen, S. J. Ebbens, C. Madden, N. Patel, C. J. Roberts, and J. Zhang, "Towards nanoscale metrology for biomolecular imaging by atomic force microscopy," *Nanotechnology*, vol. 16, pp. 966, 2005.
- [249] Y. Deng, K. Zhao, X.-f. Zhang, P. Hu, and G.-Q. Chen, "Study on the three-dimensional proliferation of rabbit articular cartilage-derived chondrocytes on polyhydroxyalkanoate scaffolds," *Biomaterials*, vol. 23, pp. 4049, 2002.
- [250] Invitrogen, "*LIVE/DEAD* ® *Viability/Cytotoxicity Kit \*for mammalian cells\**," The Handbook, Web Edition, Assays for Cell Viability, Proliferation and Function: Invitrogen Corporation, pp. 732, 2005.
- [251] T. Serizawa, N. Kawanishi, and M. Akashi, "Layer-by-layer assembly between poly(vinylamine hydrochloride-co-N-vinylformamide) with variable primary amine content and poly(sodium styrenesulfonate)," *Macromolecules*, vol. 36, pp. 1967, 2003.
- [252] Y. Liu, T. He, and C. Gao, "Surface modification of poly(ethylene terephthalate) via hydrolysis and layer-by-layer assembly of chitosan and chondroitin sulfate to construct cytocompatible layer for human endothelial cells," *Colloids and Surfaces B: Biointerfaces*, vol. 46, pp. 117, 2005.
- [253] A. D. Stroock, R. S. Kane, M. Weck, S. J. Metallo, and G. M. Whitesides, "Synthesis of free-standing quasi-two-dimensional polymers," *Langmuir*, vol. 19, pp. 2466, 2003.

- [254] J. D. Hong, K. Lowack, J. Schmitt, and G. Decher, "Layer-by-layer deposited multilayer assemblies of polyelectrolytes and proteins: from ultra thin films to protein arrays," Proceedings of the 6th European Colloid and Interface Society (ECIS) Conference, vol. 93, Progress in Colloid & Polymer Science. Graz, Austria, pp. 98, 1992.
- [255] H. Zhu and M. J. McShane, "Macromolecule encapsulation in diazoresin-based hollow polyelectrolyte microcapsules," *Langmuir*, vol. 21, pp. 424, 2005.
- [256] B. Thierry, F. M. Winnik, Y. Merhi, J. Silver, and M. Tabrizian, "Bioactive coatings of endovascular stents based on polyelectrolyte multilayers," *Biomacromolecules*, vol. 4, pp. 1564, 2003.
- [257] J. L. Van Susante, P. Buma, G. J. van Osch, D. Versleyen, P. M. van der Kraan, W. B. van der Berg, and G. N. Homminga, "Culture of chondrocytes in alginate and collagen carrier gels," *Acta Orthopaedica Scandinavica*, vol. 66, pp. 549-56, 1995.
- [258] L. Schuman, P. Buma, D. Versleyen, B. de Man, P. M. van der Kraan, W. B. van den Berg, and G. N. Homminga, "Chondrocyte behaviour within different types of collagen gel in vitro," *Biomaterials*, vol. 16, pp. 809, 1995.
- [259] K. Chaipinyo, B. W. Oakes, and M.-P. van Damme, "Effects of growth factors on cell proliferation and matrix synthesis of low-density, primary bovine chondrocytes cultured in collagen I gels," *Journal of Orthopaedic Research*, vol. 20, pp. 1070, 2002.
- [260] I. Galois, S. Hutasse, D. Cortial, C. F. Rousseau, L. Grossin, M.-C. Ronziere, D. Herbage, and A.-M. Freyria, "Bovine chondrocyte behaviour in three-dimensional type I collagen gel in terms of gel contraction, proliferation and gene expression," *Biomaterials*, vol. 27, pp. 79, 2006.
- [261] D. Kuila, M. Tien, Y. Lvov, M. McShane, R. Aithal, S. Singh, A. Potluri, S. Kaul, D. Patel, and G. Krishna, "Nanoassembly of immobilized ligninolytic enzymes for biocatalysis, bioremediation and biosensing," Proceedings of SPIE - The International Society for Optical Engineering, Philadelphia, PA, United States, pp. 267, 2004.
- [262] K. Iida, H. Matsuno, K. Kurita, and T. Serizawa, "Enzymatic degradation of ultrathin multilayer films composed of polysaccharides," Polymer Preprints-Japan, Yokohama, Japan, pp. 2009, 2005.
- [263] J. Zhang, B. Senger, D. Vautier, C. Picart, P. Schaaf, J.-C. Voegel, and P. Lavalley, "Natural polyelectrolyte films based on layer-by layer deposition of collagen and hyaluronic acid," *Biomaterials*, vol. 26, pp. 3353, 2005.

- [264] L. Richert, P. Lavalle, D. Vautier, B. Senger, J. F. Stoltz, P. Schaaf, J. C. Voegel, and C. Picart, "Cell Interactions with Polyelectrolyte Multilayer Films," *Biomacromolecules*, vol. 3, pp. 1170-1178, 2002.
- [265] H. Ai, H. Meng, I. Ichinose, S. A. Jones, D. K. Mills, Y. M. Lvov, and X. Qiao, "Biocompatibility of layer-by-layer self-assembled nanofilm on silicone rubber for neurons," *Journal of Neuroscience Methods*, vol. 128, pp. 1-8, 2003.
- [266] P. Lonu, A. Srinivas, M. Overstreet, M. Hungerford, and C. G. Frondoza, "Cell death induced by prosthetic metal ions in human chondrocytes," Transactions - 7th World Biomaterials Congress, Sydney, Australia, pp. 1316, 2004.
- [267] C. M. Isacke and H. Yarwood, "The hyaluronan receptor, CD44," *International Journal of Biochemistry and Cell Biology*, vol. 34, pp. 718-21, 2002.
- [268] M. C. Berg, S. Y. Yang, P. T. Hammond, and M. F. Rubner, "Controlling Mammalian Cell Interactions on Patterned Polyelectrolyte Multilayer Surfaces," *Langmuir*, vol. 20, pp. 1362, 2004.
- [269] Y. S. Zinchenko, L. W. Schrum, M. Clemens, and R. N. Cogger, "Hepatocyte and Kupffer Cells Co-cultured on Micropatterned Surfaces to Optimize Hepatocyte Function," *Tissue Engineering*, vol. 12, pp. 751-761, 2006.
- [270] J. Tan and W. M. Saltzman, "Topographical control of human neutrophil motility on micropatterned materials with various surface chemistry," *Biomaterials*, vol. 23, pp. 3215, 2002.
- [271] S. G. Olenych, M. D. Moussallem, D. S. Salloum, J. B. Schlenoff, and T. C. S. Keller, "Fibronectin and cell attachment to cell and protein resistant polyelectrolyte surfaces," *Biomacromolecules*, vol. 6, pp. 3252-3258, 2005.
- [272] J. T. Groves, L. K. Mahal, and C. R. Bertozzi, "Control of cell adhesion and growth with micropatterned supported lipid membranes," *Langmuir*, vol. 17, pp. 5129, 2001.
- [273] R. Singhvi, A. Kumar, G. P. Lopez, G. N. Stephanopoulos, D. I. Wang, G. M. Whitesides, and D. E. Ingber, "Engineering cell shape and function," *Science*, vol. 264, pp. 696, 1994.
- [274] M. C. Berg, S. Y. Yang, J. D. Mendelsohn, P. T. Hammond, and M. F. Rubner, "Controlling mammalian cell adhesion on patterned weak polyelectrolyte multilayers," Abstracts of Papers, 225th ACS National Meeting, New Orleans, LA, United States, pp. PMSE-026, 2003.
- [275] A. Folch and M. Toner, "Cellular micropatterns on biocompatible materials," *Biotechnology Progress*, vol. 14, pp. 388, 1998.

- [276] A. Revzin, P. Rajagopalan, A. W. Tilles, F. Berthiaume, M. L. Yarmush, and M. Toner, "Designing a Hepatocellular Microenvironment with Protein Microarraying and Poly(ethylene glycol) Photolithography," *Langmuir*, vol. 20, pp. 2999, 2004.
- [277] R. Patwardhan, M. Fasiuddin, and W. Besio, "*Medical Devices for the detection, prevention and/or treatment of neurological disorders, and methods related thereto*," Patent 20060173510, United States, 2006.